1250012
[0064822H]

RPP-CALC-60345, Rev. 0

Heterogeneous Media Model for Waste Management Area C Performance Assessment

Author Name:
K. Gordon, A. Mayenna. A K. Wahi – INTERA, Inc.
M. P. Bergeron – Washington River Protection Solutions, LLC
Richland, WA 99352
U.S. Department of Energy Contract DE-AC27-08RV14800

RECEIVED
AUG 29 2018
EDMC

EDT/ECN: DRCF UC: N/A
Cost Center: N/A Charge Code: N/A
B&R Code: N/A Total Pages: 124

Key Words: Performance Assessment, Waste Management Area C, PA, WMA C, single-shell tank, STOMP, process-level model, modeling codes, vadose zone, groundwater, unsaturated flow, vadose zone flow, groundwater flow, contaminant transport, heterogeneity, DOE Order 435.1, Washington Administrative Code, RCRA, tank farm closure

Abstract: The report is an environmental modeling calculation file focused for the development and application of the three-dimensional heterogeneous flow and transport model based on Subsurface Transport Over Multiple Phases (STOMP) computer code used in the Waste Management Area C Performance Assessment and Resource Conservation and Recovery Act of 1976 (RCRA) Closure Analysis.

TRADEMARK DISCLAIMER. Reference herein to any specific commercial product, process, or service by trade name, trademark, manufacturer, or otherwise, does not necessarily constitute or imply its endorsement, recommendation, or favoring by the United States Government or any agency thereof or its contractors or subcontractors.

DATE:
Oct 03, 2016
HANFORD RELEASE

APPROVED
By Julia Raymer at 4:05 pm, Oct 03, 2016

Release Approval Date Release Stamp

Approved For Public Release

WMA-C

118

Supporting Information for

Environmental Modeling Calculational File (RPP-CALC-60345)

1. Identification of Need for EMCF RPP-CALC-60345:

This EMCF is needed to document the basis for the development and implementation of the heterogeneous flow and contaminant transport model(s) based on STOMP found in:

- RPP-ENV-58782, Performance Assessment of Waste Management Area C at the Hanford Site, Southeast Washington, Rev. 0
- RPP-ENV-58806, RCRA Closure Analysis of Waste Management Area C at the Hanford Site, Southeast Washington, Rev. 0

2. Identification of Originator, Checker, and Subject Matter Expert (SME)/Senior Reviewer (SR)

Originator:

Kimberly Gordon, INTERA, Inc.

B.S., Geosystems Engineering and Hydrogeology, University of Texas at Austin

Ms. Gordon is a qualified individual to originate the geostatistical model calculations documented for the heterogeneous case for WMA C performance assessment in this EMCF. She has received specific training from the authors of the GSLIB code for its use and application in geostatistical modeling, and has received training on the WRPS procedures for this environmental model work. She has more than seventeen years of experience constructing three-dimensional geostatistical models using GSLIB and other methods for various hydrogeologic and geologic applications.

Amena Mayenna, INTERA, Inc.

P.E (Washington State)
M.S., Environmental Engineering, Washington State University
B.S., Civil Engineering, University of Engineering & Technology, Bangladesh

Ms. Mayenna is a qualified individual to help originate the documentation of the development and implementation of heterogeneous flow and transport model simulations based on STOMP provided in this EMCF. She has a solid background in vadose zone and groundwater hydrology, is a qualified STOMP User at the Hanford and has received training on the WRPS procedures for this environmental model work. She has over eight years of experience performing numerical modeling using STOMP and MODFLOW in the saturated and unsaturated zones, including model calibration and sensitivity analysis, geostatistical analysis, and Geographic Information System (GIS).

Arun K. Wahi, INTERA, Inc.

MS, Hydrology, University of Arizona
BS, Chemical Engineering, Carnegie Mellon University

Mr. Wahi is a qualified individual to originate the documentation of the development and implementation of heterogeneous flow and transport model simulations based on STOMP provided in this EMCF. He has a strong background in vadose zone and groundwater hydrology, is a qualified STOMP user at the Hanford Site and has completed training in STOMP and in WRPS quality assurance procedures. He has 13 years of consulting and research experience in the fields of hydrology, hydrogeology, and chemistry. At INTERA, Inc., he has two years of experience using STOMP to perform numerical modeling of contaminant fate and transport in the saturated and unsaturated zones.

Checker:

Ali Ali, INTERA, Inc.
M.S., Environmental Engineering, Washington State University
B.S., Civil Engineering, University of Al-Mustansiriyah

Mr. Ali is a qualified individual to check the modeling work performed for WMA C PA documented in the EMCF. He has over two years of experience in performing groundwater and vadose zones modeling tasks related to Hanford projects and has received training on the WRPS procedures for this environmental model work.

Travis Hammond, INTERA, Inc.
M.S., Geology, Central Washington University
B.S., Medical Technology, University of South Alabama

Mr. Hammond is a qualified individual to assist Mr. Ali in the checking of the STOMP-based model calculations documented in this EMCF. He is a qualified STOMP User at Hanford and has received STOMP training and training on the WRPS procedures for environmental modeling work. He is a registered Professional Geologist in the State of Washington (license #2994) with over 8 years of experience in the field of geology and hydrogeology.

Subject Matter Expert/Senior Reviewer

Raziuddin Khaleel, INTERA, Inc.

Ph.D., Soil and Water Engineering, Texas A&M University
M.S., Water Science and Engineering, Asian University of Technology
B.S., Civil Engineering, Bangladesh University of Engineering and Technology

Dr. Hasan is a qualified individual for performing the senior review of the development and implementation of the heterogeneous flow and contaminant transport model(s) based on STOMP documented in this EMCF. He has a strong background in vadose zone and groundwater hydrology and has received training on the WRPS procedures for this environmental model work. He has over 25 years of experience in groundwater hydrology and numerical simulations

of subsurface flow and transport. He was a key contributor to the Hanford Site Performance Assessment for the Disposal of Low-Level Waste in the 200 West Area Burial Grounds, the Performance Assessment for the Disposal of Low-Level Waste in the 200 East Area Burial Grounds, and the Hanford Immobilized Low-Activity Tank Waste Performance Assessment, particularly in the area of conceptual model development, direction of modeling, and in writing the document.

Responsible WRPS Manager:

Marcel P. Bergeron

Technical Lead, Waste Management Area C Performance Assessment

Senior Scientist, Closure and Interim Measures Technical Group
Chief Technology Office
Washington River Protection Solutions

Marcel P. Bergeron 8/17/16

Marcel P. Bergeron Date

Heterogeneous Media Model for Waste Management Area C Performance Assessment

Prepared by:

K. Gordon
A. Mayenna
A. K. Wahi
INTERA, Inc.

Prepared for:
Washington River Protection Solutions, LLC

Date:
August 2016

Approved for public release; distribution unlimited

Version History

Version	Date	Author	Change Description
Draft A	09-Dec-2015	K. Gordon, A. Mayenna, A. K. Wahi	Initial Draft for DOE-ORP Review
Draft B	12-Feb-2016	K. Gordon, A. Mayenna, A. K. Wahi	Text updates to address comments from DOE-ORP review
Rev. 0	1-May-2016	K. Gordon, A. Mayenna, A. K. Wahi	Includes STOMP Options Analysis and Checker Log for Process Models

RPP-CALC-60345, Rev. 0

ENVIRONMENTAL MODEL CALCULATION COVER PAGE

Section 1: Completed by Responsible Manager

RELEASE/ISSUE

Project: Waste Management Area C Performance Assessment

Date: 07/14/2016

Calculation Title & Description: Heterogeneous Media Model for Waste Management Area C Performance Assessment

Section 2: Completed by Preparer

Calculation No.: RPP-CALC-60345 Revision No.: 0

Revision History

Revision No.	Description	Date	Affected Pages
0	Initial issue	07/14/2016	All

Section 3: Completed by Responsible Manager

Document Control

1. Is document intended to be controlled within SmartPlant? ☒ Yes ☐ No
2. Does document contain scientific and technical information intended for public use? ☒ Yes ☐ No
3. Does document contain controlled-use information? ☐ Yes ☒ No

Section 4: Training and Software Installation Approval (Completed Prior to Performing Calculation)

Modeler-Required Training Completed:

Ghada Saad
Project Associate, INTERA — Ghada Saad — 7/14/16
Training Coordinator (Name/Position) — Signature — Date

Software Installation and Checkout Certified:

William Nichols
Principal Engineer, INTERA — 19 JUL 2016
Integration Lead (Name/Position) — Signature — Date

Section 5: Document Review & Approval

K. Gordon, A. Mayenna, Arun Wahi, INTERA — Arun K. Wahi — 7/14/16
Preparer (Name/Position) — Signature — Date

AH Ali
Environmental Engineer, INTERA — 7/19/16
Checker (Name/Position) — Signature — Date

R Khaleel
Senior Hydrogeologist, INTERA — 7/14/16
Senior Reviewer (Name/Position) — Signature — Date

MP Bergeron
Senior Scientist, WRPS — 7/15/16
Responsible Manager (Name/Position) — Signature — Date

CHECKER LOG FOR PROCESS MODELS

EMCF CHECK LOG: MODEL PARAMETERIZATION (SPECIFY UNITS IN EACH COLUMN)

Model Parameter Type	(1) Input Documented in the EMCF?	(2) Values Checked Against Parameter Source?	(3) Input in EMCF Matches Model Input File(s)?
Simulation duration: historic	TH	N/A	AA
Simulation duration: predictive	TH	N/A	AA
Boundary conditions: recharge	TH	AA	AA
Boundary conditions: river	N/A	N/A	N/A
Boundary conditions: head dependent	TH	AA	AA
Boundary conditions: specified flux	TH	AA	AA
Initial conditions: hydraulic	TH	N/A	AA
Initial conditions: contaminant	TH	N/A	AA
Sources & sinks: aqueous mass	N/A	N/A	N/A
Sources & sinks: contaminant mass	TH	N/A	AA
Hydraulic properties: conductivity	TH	TH	AA
Hydraulic properties: porosity	TH (saturated moisture content for vadose zone)	TH	AA
Hydraulic properties: water retention (vadose only)	TH	TH	AA
Hydraulic properties: formation density	TH	TH	AA
Transport properties: diffusion	TH	TH	AA
Transport properties: dispersivity	TH	TH	AA
Transport properties: sorption (typically K_d)	TH	TH	AA
Transport properties: radioactive decay rate	TH	TH	AA

EMCF CHECK LOG: FURTHER CHECKS

Additional checks performed and results:

Checked output vadose zone moisture content and matric potentials and saturated zone Tc-99 concentrations. No discrepancies. -- AA

AA = Ali H. Ali, Environmental Engineer, INTERA, Inc.
TH = Travis Hammond, Hydrogeologist, INTERA, Inc. (checking coordinated with Ali Ali)

Quality Assurance Checklist for RPP-CALC-60345

Item	Checked By	Date	Discrepancies/Comments	Resolution
General				
Review draft text, tables, and figures	AA	10/13/2015	Mislabeled STOMP index of cross-section on plan view figure.	Figure corrected.
Data Compilation/Reduction				
Step 1 through 7 Microsoft Access queries for data compilation/reduction checked	AA	10/7/2015	none	n/a
KT3D				
Check input (variograms and datasets in *.par files for the base case)	AA	10/14/2015	none	n/a
Run KT3D and check kriged output for the base case	AA	10/14/2015	none	n/a
STOMP				
Check STOMP input for heterogeneous Cross-Section 1, 2, and 3 with recharge 3.5 mm/yr	AA	10/8/2015	none	n/a
Check output vadose moisture content and matric potentials and Tc-99 groundwater concentrations	AA	10/9/2015	none	n/a
TecPlot				
Reproduced Tc-99 breakthrough curves for Cross-Section 1, 2, and 3	AA	10/9/2015	none	n/a
Reproduced Cross-Section 1, 2, and 3 rock/soil zonation for heterogeneous and base case	AA	10/9/2015	none	n/a

AA = Ali Ali, Environmental Engineer, INTERA, Inc., Richland Washington
n/a = not applicable

This page intentionally left blank.

CONTENTS

1 PURPOSE 1-1

2 BACKGROUND 2-1

2.1 WASTE MANAGEMENT AREA C PERFORMANCE ASSESSMENT MODEL DOMAIN 2-1

2.2 STUDY AREA HYDROGEOLOGY AND HYDROSTRATIGRAPHIC UNITS 2-2

2.3 DATA COLLECTION 2-5

2.3.1 Overview of Compiled Moisture Content Dataset 2-5

2.3.2 Hanford Environmental Information System Geophysical Logs Moisture Content Dataset 2-5

2.3.3 Handheld Moisture Gauges Dataset 2-6

2.3.4 Moisture Content Dataset from Development of RPP-CALC-60450 2-7

2.4 GEOSTATISTICAL ESTIMATION 2-8

2.4.1 Variogram/Correlogram Analysis 2-8

2.4.2 Data Interpolation 2-10

3 METHODOLOGY 3-1

4 ASSUMPTIONS AND INPUTS 4-1

4.1 DATA COMPILATION AND ANALYSES 4-1

4.2 VARIOGRAM ANALYSES 4-6

4.3 GEOSTATISTICAL ESTIMATION 4-6

4.3.1 Sensitivity Analyses 4-7

4.4 VADOSE ZONE HYDRAULIC PROPERTIES 4-10

5 SOFTWARE APPLICATIONS 5-1

5.1 EXEMPT SOFTWARE 5-1

5.2 APPROVED SOFTWARE 5-1

5.2.1 GSLIB – KT3D 5-1

5.2.2 Subsurface Transport Over Multiple Phases 5-2

6 CALCULATIONS 6-1

6.1 COMPILATION OF DATA 6-1

6.1.1 Data Reduction and Conditioning 6-1

6.2 DATASET STATISTICS 6-2

6.3 VARIOGRAM/CORRELOGRAM ANALYSIS 6-3

6.4 GEOSTATISTICAL ESTIMATION 6-4

6.5 SENSITIVITY ANALYSES 6-4

6.6 DEVELOPMENT OF TWO-DIMENSIONAL SUBSURFACE TRANSPORT OVER MULTIPLE PHASES MODELS 6-8

6.6.1 Base Case Two-Dimensional Models 6-8

6.6.2 Heterogeneous Case Two-Dimensional Models 6-18

6.6.3 Boundary and Initial Conditions 6-29

6.6.4 Contaminant Source and Model Output Point of Calculation 6-29

7 RESULTS AND DISCUSSION 7-1

7.1 SUMMARY STATISTICS FOR MOISTURE CONTENT DATASETS 7-1

7.2 MOISTURE CONTENT INTERPOLATION 7-3

7.3 SIMULATION OF MOISTURE CONTENT 7-5

7.4 SIMULATION OF MATRIC POTENTIAL 7-7

7.5 SIMULATION OF TECHNETIUM-99 CONCENTRATION 7-8

8 SUMMARY AND CONCLUSIONS 8-1

9 REFERENCES 9-1

ATTACHMENTS

1 – Listing of Microsoft Access® and Excel® Files Containing Moisture Content Data Analyzed in This Environmental Model Calculation File Att-1-i

2 – Software Installation and Checkout Att-2-i

3 – STOMP Options Analysis Att-3-i

FIGURES

Figure 1-1. Waste Management Area C Basemap with Moisture Content (vol %) Data Locations. 1-2

Figure 2-1. Hydrogeologic Interpretation for Wellbore C4124. 2-3

Figure 2-2. Hydrostratigraphic Units in the Three-Dimensional Waste Management Area C Performance Assessment Model. 2-4

Figure 2-3. Semivariogram Components Including Sill, Range, and Nugget. 2-11

Figure 4-1. Time Series of Drywell Moisture at 10-foot Intervals Showing Reduced Variability at Depth. 4-2

Figure 4-2. Consistent Vertical Profile of Neutron Moisture Measurements over Time in a Drywell from Multiple Logs in 2003 and Un-calibrated Data from 1976. 4-3

Figure 4-3. Comparison of Neutron Moisture Logging System and Handheld Instrument Logs of Neutron Moisture Profile in Drywell A6696 (30-06-10). 4-4

Figure 4-4. Comparison of Neutron Moisture Logging System and Handheld Instrument Logs of Neutron Moisture Profile in Drywell A6698 (30-06-04). 4-5

Figure 4-5. Histograms for Moisture Content (vol %) Datasets. 4-8

Figure 4-6. Cross-Section D-D' with Continuous Contours for Moisture Content (vol %) Interpolation. 4-9

Figure 4-7. Moisture Retention Curves and Unsaturated Hydraulic Conductivity Curves for 44 Integrated Disposal Facility Samples. 4-11

Figure 6-1. Horizontal and Vertical Variograms for Moisture Content Datasets with Model Variograms Fit to Empirical Variograms Using Indicated Values of Range. 6-5

Figure 6-2. Horizontal and Vertical Correlograms for Waste Management Area C Moisture Content Datasets. 6-9

Figure 6-3. Cross-Section A-A' with Continuous Contours for Moisture Content (vol %) Interpolation. 6-12

Figure 6-4. Cross-Section A-A' with Binned Contours for Moisture Content (vol %) Interpolation. 6-12

Figure 6-5. Cross-Section B-B' with Continuous Contours for Moisture Content (vol %) Interpolation. 6-13

Figure 6-6. Cross-Section B-B' with Binned Contours for Moisture Content (vol %) Interpolation. 6-13

Figure 6-7. Cross-Section C-C' with Continuous Contours for Moisture Content (vol %) Interpolation. 6-14

Figure 6-8. Cross-Section C-C' with Binned Contours for Moisture Content (vol %) Interpolation. 6-15

Figure 6-9. Cross-Section D-D' with Binned Contours for Moisture Content (vol %) Interpolation. 6-16

Figure 6-10. Fence Diagram with Moisture Content (vol %) Data Interpolation Showing Approximate Elevations of Hydrogeologic Contacts. 6-17

Figure 6-11. Moisture Content (vol %) Interpolations Using Base Case Ranges (Middle Figures) Compared to Minimum (Upper Figures) and Maximum (Lower Figures) Ranges (Cross-Section C-C'). 6-19

Figure 6-12. Moisture Content (vol %) Interpolations Showing Sensitivity to Range (Cross-Section A-A'). 6-21

Figure 6-13. Base Case versus Exclusion of Handheld Data (Cross-Section C-C'). 6-23

Figure 6-14. Base Case versus Samples from H2 Interval Only (Cross-Section C-C'). 6-25

Figure 6-15. Location of Selected Cross-Sections for the Two-Dimensional Models. 6-27

Figure 6-16. (a) Unsaturated Hydraulic Conductivity and (b) Moisture Retention Curves Selected for Moisture Content-Based Rock/Soil Zones. 6-28

Figure 6-17. Cross-Section 1 (Northwest to Southeast). 6-31

Figure 6-18. Cross-Section 2 (Northwest to Southeast). 6-32

Figure 6-19. Cross-Section 3 (Southwest to Northeast). 6-33

Figure 6-20. Location of Contaminant Source and Point of Calculation. 6-34

Figure 7-1. Comparison of Measured (C4297) and Simulated Moisture Contents for Base Case and Heterogeneous Case for Cross-Section 1. 7-6

Figure 7-2. Comparison of Measured Moisture Contents at 299-E27-22 and Simulated Moisture Contents near C4297 for Base Case and Heterogeneous Case for Cross-Section 1. 7-7

Figure 7-3. Location of Well C4297 and 299-E27-22. 7-9

Figure 7-4. Technetium-99 Breakthrough Curves for Cross-Section 1 for Arbitrary Source Term. 7-10

Figure 7-5. Technetium-99 Breakthrough Curves for Cross-Section 2 for Arbitrary Source Term. 7-11

Figure 7-6. Technetium-99 Breakthrough Curves for Cross-Section 3 for Arbitrary Source Term. 7-12

TABLES

Table 4-1. Vadose Zone Hydraulic Properties for Waste Management Area C Hydrostratigraphic Units. 4-10

Table 6-1. Summary Statistics for the Moisture Content (volume %) Dataset at Waste Management Area C. 6-3

Table 6-2. Empirical Variogram Parameters for Different Datasets. 6-7

Table 6-3. Correlation Lengths for Different Moisture Content Datasets. 6-11

Table 6-4. Model Variogram Parameters for Different Moisture Datasets. 6-11

Table 6-5. Vadose Zone Hydraulic Properties for Moisture Content-Based Rock/Soil Zones. 6-27

Table 7-1. Mean Moisture Content and Matric Potential from Simulations and Borehole Samples. 7-8

Table 7-2. Summary of Technetium-99 Transport Model Results. 7-12

TERMS

Am	Americium
Be	Beryllium
CHPRC	CH2M HILL Plateau Remediation Company
cm	centimeter (note negative values of matric potential are reported in –cm)
DOE	U.S. Department of Energy
EHM	equivalent homogeneous medium
EMCF	environmental model calculation file
EMMA	Environmental Model Management Archive maintained by INTERA, Inc. and backed up to a server location managed by WRPS
ft	Foot
FY	fiscal year
g/cm^3	grams per cubic centimeter
GPL	geophysical logs
GSLIB	Geostatistical Software Library
HEIS	Hanford Environmental Information System
HISI	Hanford Information System Inventory
IDF	Integrated Disposal Facility
L	Liter
m	Meter
mCi	millicurie
MPa	megapascal
NMLS	Neutron Moisture Logging System
NQA	Nuclear Quality Assurance
PA	performance assessment
pCi	picocurie
PNG	Pacific Northwest Geophysics
PNNL	Pacific Northwest National Laboratory
RCRA	Resource Conservation and Recovery Act of 1976
s	second
S&L	Sisson and Lu
SST	Single Shell Tank
Stoller	S.M. Stoller Corporation
STOMP	Subsurface Transport Over Multiple Phases (computer code)
TRS	Three Rivers Scientific
UPR	unplanned release
WMA	Waste Management Area
WRPS	Washington River Protection Solutions, LLC

1 PURPOSE

Geologic media is heterogeneous at a variety of scales. The purpose of this environmental model calculation file (EMCF) is to characterize the heterogeneous media at Waste Management Area (WMA) C located within the Hanford Site's Central Plateau (Figure 1-1) using the field-measured moisture content data obtained under essentially non-transient conditions. Contaminant transport models are then developed for the heterogeneous media using soil moisture as a proxy for soil texture, and simulated contaminant breakthrough curves are compared with those for the base case model for the WMA C Performance Assessment (PA).

The groundwater pathway analysis is an important aspect of the WMA C PA. For WMA C PA base case vadose zone modeling, hydraulic properties developed from small-scale laboratory measurements are used to predict the large, field-scale flow behavior (RPP-RPT-58949, "Model Package Report Flow and Contaminant Transport Numerical Model used in WMA C Performance Assessment and RCRA Closure Analysis," Appendix B). Each heterogeneous geologic unit is replaced by an equivalent homogeneous medium (EHM) with macroscopic flow properties. Each heterogeneous unit is assigned its upscaled or effective hydraulic properties; the simulated flow fields predict the bulk or mean flow behavior at the field scale. Upscaling, in effect, accounts for differences in scale between small, core-scale measurements and large, field-scale modeling.

The EHM model is the base case for PA modeling, whereas this work considers an alternate vadose zone model. The premise of the alternate vadose model development is the hypothesis that for the porous media at WMA C, the baseline soil moisture distribution can be used as an indicator of sediment texture. Field-measured moisture contents can then be used as "soft" data from which estimates of soil hydraulic properties can be inferred.

For any subsurface conditions, uncertainty exists in the geology and depositional history for sediments. For the 200 Area at the Hanford Site, previous studies have indicated that moisture content may be an indicator of sediment type and may impact subsurface transport ("Conditional simulation and upscaling of soil hydraulic properties" [Rockhold et al. 1999], "A Markov chain model for characterizing medium heterogeneity and sediment layering structure" [Ye and Khaleel 2008]). In the absence of transient changes in recharge (e.g., anthropogenic discharges), *in situ* moisture content observations would be anticipated to broadly correlate with sediment texture (i.e., higher moisture contents are associated with fine-textured sediments and lower moisture contents are associated with coarse-textured sediments). Also, except during transient changes in recharge, *in situ* moisture contents are in equilibrium with the long-term recharge rate. These inferences, as applied to a geostatistical analysis of the moisture content database, are used to identify and select the hydraulic properties for the heterogeneous media model.

Figure 1-1. Waste Management Area C Basemap with Moisture Content (vol %) Data Locations.

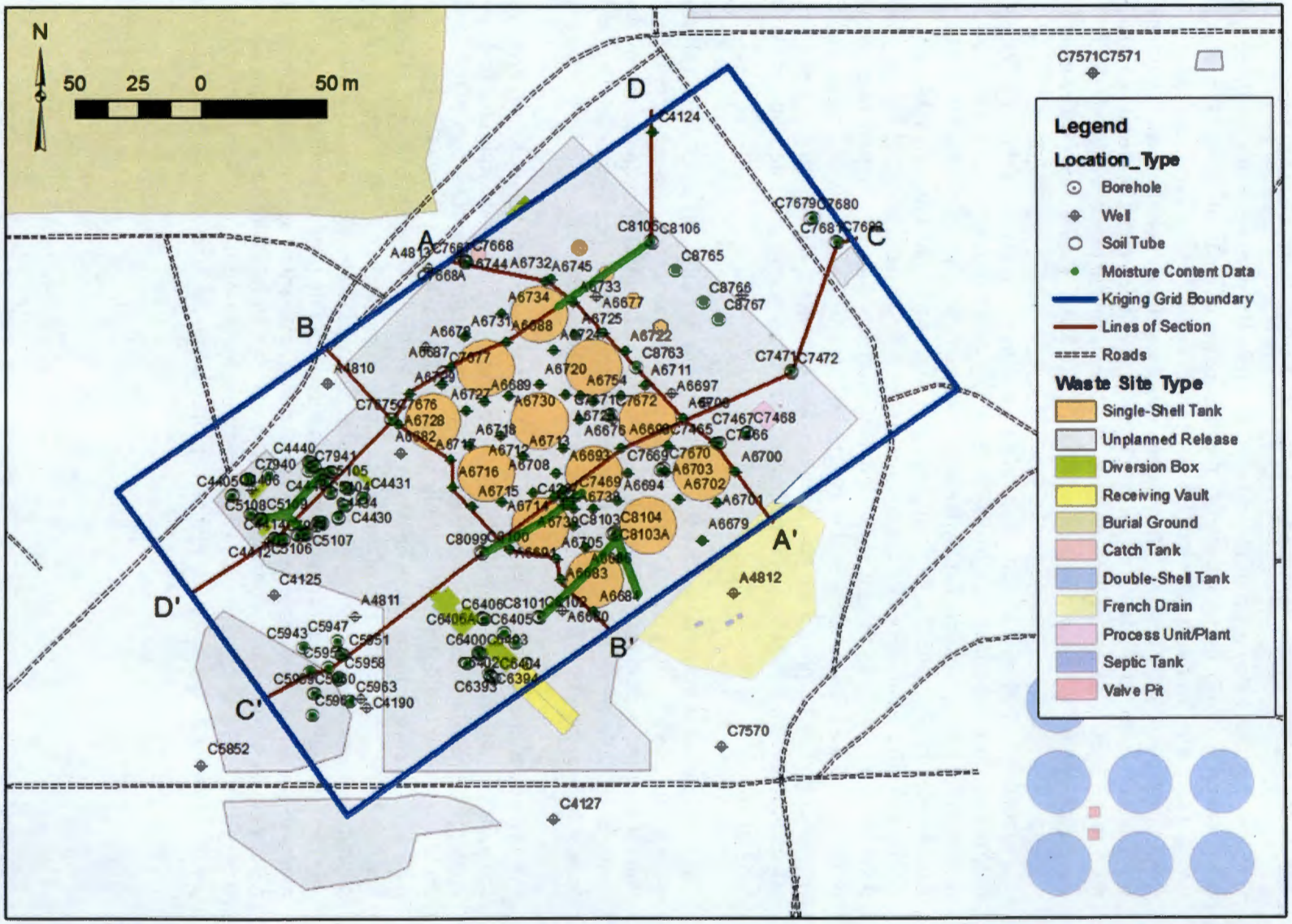

A three-dimensional model of the moisture content distribution was developed using geostatistical estimation including variography and kriging to assess local heterogeneity. A base case estimation and alternative estimations were determined for the moisture content distribution. Alternative estimations were developed based on variations in the horizontal and vertical variogram ranges determined for the dataset. Another alternative estimation limited the moisture dataset considered based on lithologic intervals determined from the WMA C PA Alternative Geologic Model II as implemented in the Subsurface Transport Over Multiple Phases (STOMP)©[1]-based model (RPP-RPT-58949). STOMP© is the code with which the PA models are developed and is described in Section 5 and in PNNL-15782, "STOMP Subsurface Transport Over Multiple Phases Version 4.0 User's Guide."

From the WMA C PA three-dimensional base case model based on the STOMP© software, three cross-sections were selected to develop two-dimensional STOMP©-based models for both the EHM base case model and the heterogeneous case model to efficiently simulate and compare results to test the impact of the interpreted heterogeneity in model predictions of contaminant breakthrough in groundwater.

[1] Subsurface Transport Over Multiple Phases (STOMP)© is copyrighted by Battelle Memorial Institute, 1996.

This page intentionally left blank.

2 BACKGROUND

WMA C is located in the 200 East Area of the Hanford Site; it includes 16 underground storage tanks, called single-shell tanks, associated ancillary equipment such as vaults, boxes, and piping, and soil contaminated by releases from these structures (Figure 1-1). The WMA C tank area was constructed between 1943 and 1944 and began operations in 1946 storing and transferring waste that extended into the mid-1980s. As a result of the long operational history, WMA C received waste generated by essentially the entire Hanford Site major chemical processing operations.

The PA modeling currently associated with WMA C is being conducted in accordance with U.S. Department of Energy (DOE) implementation guidelines for DOE M 435.1-1, Radioactive Waste Management Manual. Existing regulations express compliance in terms of comparisons of single "base case" values to the performance objectives as a means to demonstrate that the closed facility adequately protects the environment and the public from exposure to radiation from radioactive materials per the requirements contained in DOE O 5400.1, General Environmental Protection Program and DOE O 5400.5, Radiation Protection of the Public and the Environment. The modeling includes a detailed evaluation of the groundwater concentrations and radionuclide arrival times during the 1,000-year compliance and 10,000-year sensitivity-uncertainty periods per DOE O 435.1, Radioactive Waste Management. Hazardous chemical impacts are also being considered under the requirements of Appendix I of the Hanford Federal Facility Agreement and Consent Order (Ecology et al. 1989).

The WMA C PA analysis of tank waste residuals after closure does not consider contaminant release during WMA C operations, but only the post-closure impacts to the environment of the radionuclides and non-radiological contaminants remaining in the residual waste. Although suspected tank leaks and unplanned releases are believed to have impacted groundwater, the evaluation of their impacts to groundwater is outside the scope of the WMA C PA but will be evaluated in fiscal year (FY) 2016.

2.1 WASTE MANAGEMENT AREA C PERFORMANCE ASSESSMENT MODEL DOMAIN

The STOMP© three-dimensional model domain for the WMA C PA is a rectangular prism running southwest to northeast. Details of the PA base case model can be found in RPP-RPT-58949. The horizontal dimensions of the model domain are 737.9 m (2,421 ft) northwest to southeast by 795.3 m (2,609 ft) southwest to northeast. The vertical domain is 116 m (381 ft), extending from the current land surface to about 12 m (49 ft) below the water table. The southwestern and northwestern corners of the model are at (574656.09 m, 136454.41 m), and (575218.45 m, 137016.78 m), respectively (Lambert Coordinate system easting, NOAA Manual NOS NGS 5, "State Plane Coordinate System of 1983"). The southeastern and northeastern corners are at (575177.86 m, 135932.64 m), and (575740.22 m, 136495.00 m), respectively. The vertical base elevation of the model is nominally 95 m ("North American Vertical Datum of 1988" [NAVD88]).

2.2 STUDY AREA HYDROGEOLOGY AND HYDROSTRATIGRAPHIC UNITS

Within the WMA C study area, recent deposits and the Hanford formation make up the majority of the vadose zone sediments. RPP-23748, "Geology, Hydrogeology, Geochemistry, and Mineralogy Data Package for the Single-Shell Tank Waste Management Areas at the Hanford Site" describes the general hydrogeology for each of the 200 Area tank farms. Figure 2-1 from RPP-23748 shows representative geologic units for the site based on wellbore C4124 located in the northeastern section of the study area. Unconsolidated deposits overlie basalt bedrock of the Columbia River Basalt Group. Locally, within WMA C, the Hanford formation overlies Ringold Formation deposits (including the undifferentiated Cold Creek unit) that were below the water table and therefore not considered in this vadose zone analysis. The WMA C PA model treats the deposits comprising the aquifer as a single hydrostratigraphic unit (RPP-RPT-58949). The mostly unconsolidated Hanford formation in the study area is greater than 70 m thick and is divided into three informal units: the H1, H2, and H3 units.

The following hydrostratigraphic units are included in Alternative Geologic Model I used in the WMA C PA base case numerical model (RPP-RPT-58949):

- Backfill (Hdb – Holocene gravel-dominated backfill material, ~10 m thick)
- Hanford formation unit H1 – Gravel-dominated sequence (Hf1 unit) (~10 m to 30 m thick)
- Hanford formation unit H2 – Sand-dominated sequence (H2 unit) (~45 m to 70 m thick)
- Hanford formation unit H3 – Gravel-dominated sequence (Hf3 unit) (~0 m to 20 m thick)
- Aquifer.

Figure 2-2 (after RPP-RPT-58949) presents a cutaway section of hydrostratigraphic units in the three-dimensional STOMP© WMA C PA base case model.

Particle sizes of sediments at Hanford are reported in many documents without explicit reference to a formal classification scheme, but descriptions in RPP-RPT-58949 that summarize past investigations conform to the Folk-Wentworth scheme, as described, for example, in PNNL-15503, "Characterization of Vadose Zone Sediments Below the C Tank Farm: Borehole C4297 and RCRA Borehole 299-E27-22." The main divisions are as follows. Mud-sized particles include silt and clay particles with diameters less than 1/16 mm. Silts are coarser than clays, whose individual particles are not visible to the naked eye. Sand-sized particles range from 1/16 mm to 2 mm. Gravel-sized particles range from pebbles greater than 2 mm to boulders greater than 256 mm (10 in. or larger).

Figure 2-1. Hydrogeologic Interpretation for Wellbore C4124.

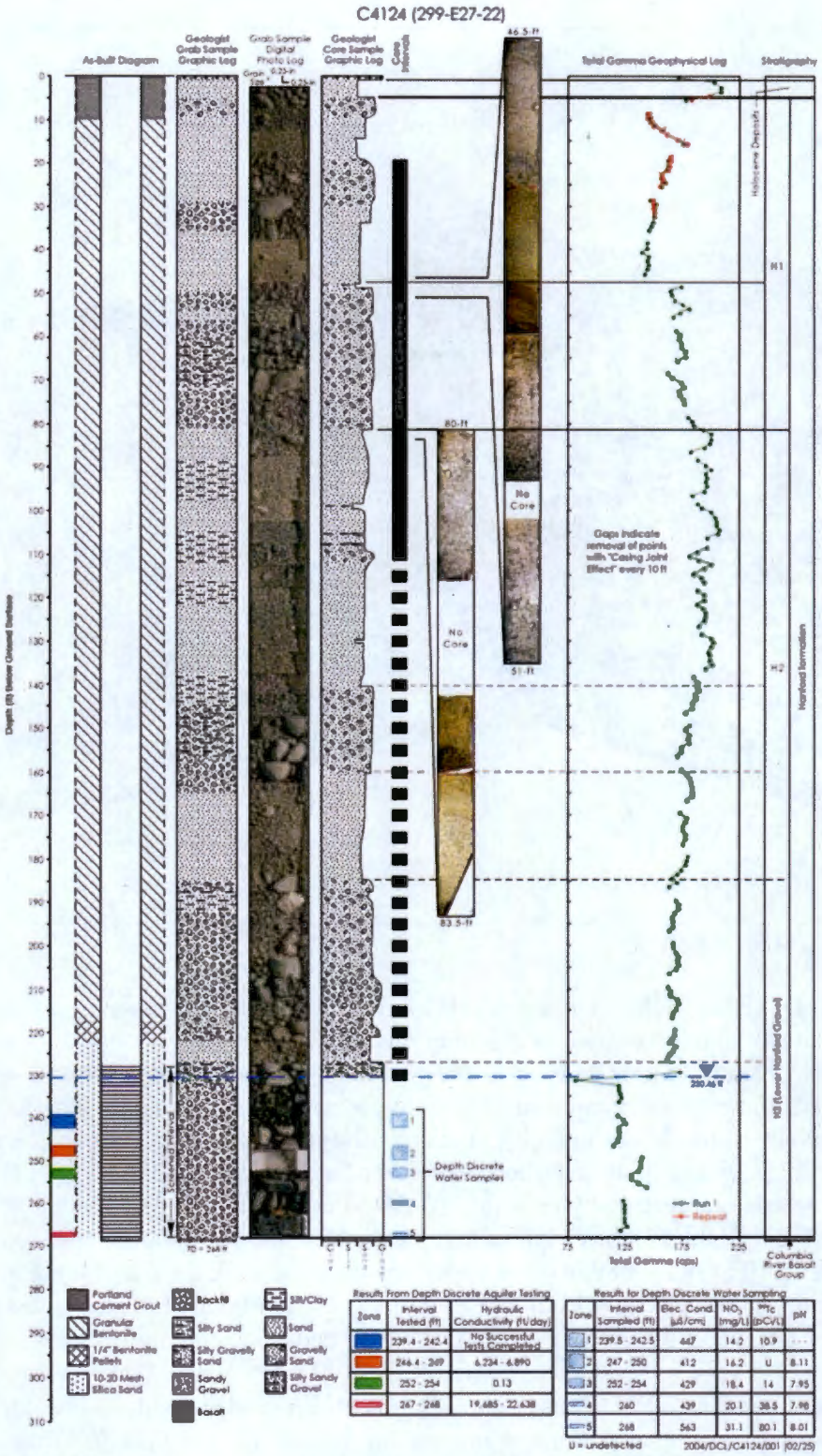

Source: RPP-23748, "Geology, Hydrogeology, Geochemistry, and Mineralogy Data Package for the Single-Shell Tank Waste Management Areas at the Hanford Site."

Figure 2-2. Hydrostratigraphic Units in the Three-Dimensional Waste Management Area C Performance Assessment Model.

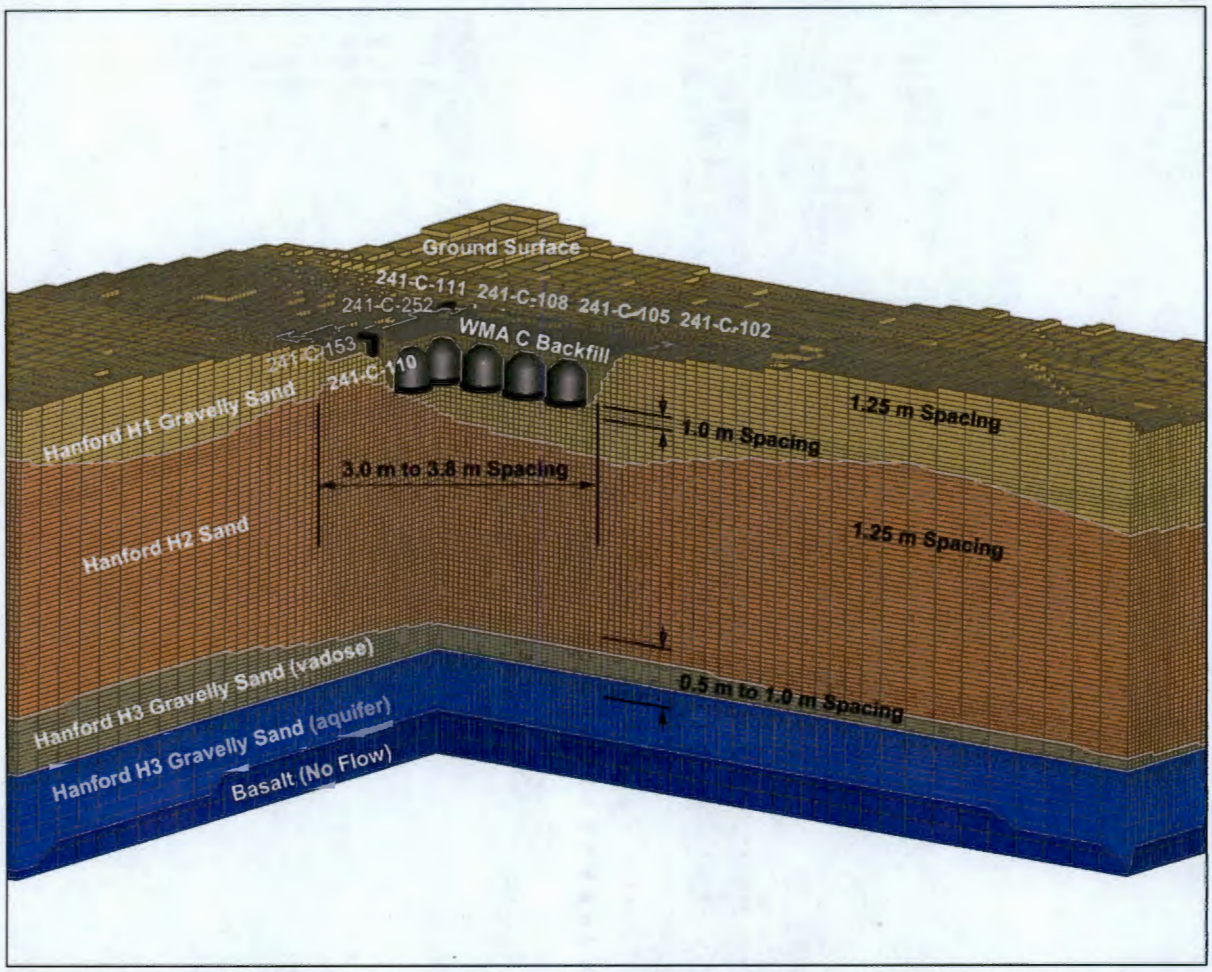

WMA = Waste Management Area

Predominantly gravel facies comprise the H3 unit that consists of clast-supported, sandy, pebble to boulder gravel to matrix-supported pebbly sand. The H2 sand sequence overlies the H3 unit and consists of a sand-dominated facies and generally thickens to the south and west across the study area. Sediments are comprised of fine- to coarse-grained sand with lenses of silty sand to slightly gravelly sand. Minor gravelly sand and sandy gravel beds occur occasionally within the H2 unit. Silt lenses and thinly interbedded zones of silt and sand (generally < 1 ft [0.3 m] in thickness) are also represented within the H2 unit. For the vadose zone modeling of Alternative Geologic Model II, the unit has been further subdivided into continuous sand, coarse sand, and fine sand units (RPP-RPT-58949). An upper gravel sequence known as the H1 unit overlies the H2 unit sand sequence. The H1 unit consists of loose, sandy gravel to gravelly sand with minor instances of interbedded sand to silty sand. Coarser beds may contain boulder-sized materials.

Recent deposits in the WMA C study area include eolian sand and silt, and backfill material. The eolian sand and silt consist of fine to medium sand to silty sand derived from flood sediments deposited approximately 13,000 years before present. Within the immediate vicinity

of the tank farm operations, most of the eolian deposits have been removed and replaced with backfill. Backfill materials consist of unstructured, poorly-sorted mixtures of gravel, sand, and silt removed during tank excavation, and then later used as fill around the tanks. Backfill materials extend to depths of 50 ft within the tank farm.

2.3 DATA COLLECTION

A dataset of soil moisture measurements collected between 2003 and 2013 from 124 borings and wells in or near WMA C that had moisture-versus-depth profiles was compiled from multiple sources. Subsections herein describe each source dataset in more detail.

2.3.1 Overview of Compiled Moisture Content Dataset

Neutron moisture data for 52 borings and 2 drywells were retrieved from the Hanford Environmental Information System (HEIS) Geophysical Logs (GPL) dataset in October 2014. Neutron moisture data collected from 57 drywells using handheld neutron moisture instruments were provided by Washington River Protection Solutions, LLC (WRPS) in spreadsheets last modified in 2012 to 2013 (EMDT-OB-0009, "WMA C Vadose Zone Moisture Content from Handheld Neutron Moisture Gauges," archived in the Environmental Model Management Archive [EMMA]). Moisture data for an additional 13 locations were obtained from a dataset compiled from original data for use in the preparation of RPP-CALC-60450, "Process for Determining the Volumetric Moisture Content for the Vadose Zone Geologic Units Underlying Waste Management Area C," and provided in January 2015, including several angled boreholes and vertical boreholes with neutron moisture logs similar to those in HEIS, and two locations with gravimetric moisture data that had been converted to a volumetric basis. WRPS provided data for more locations than counted in these totals. Locations were excluded from the totals if their data were duplicated between sources, could not be reliably converted to a basis consistent with the rest of the dataset (e.g., neutron moisture counts per second measured without calibration to a volumetric moisture content basis), were not available in electronic format at the time of the calculation, or were reserved for validation of the geostatistical estimation.

2.3.2 Hanford Environmental Information System Geophysical Logs Moisture Content Dataset

Data from HEIS GPL were collected using vehicle-mounted instruments to record moisture along with precise depth measurements nominally every 3 in. (0.0762 m). Most of these boreholes were associated with investigations of unplanned releases or with risk assessment activities. The contractors who generated the data were Pacific Northwest Geophysics (PNG), Three Rivers Scientific (TRS), and S.M. Stoller Corporation (Stoller). It appears that the type of neutron source used with all detectors, including those used in the handheld moisture gauges and RPP-CALC-60450 datasets, was a 50 mCi ^{241}Am/Be neutron source (RPP-22393, "241-C-102, 241-C-104, 241-C-107, 241-C-108 and 241-C-112 Tanks Waste Retrieval Work Plan," Section 4.2.1.1; "Hanford Geophysical Logging Project DOE-RL Annual Report for FY 2005" [Stoller 2006], Attachment 1; RPP-32130, "Summary of Direct Push Exploration at 241-C-152 Diversion Box in 241-C Tank Farm," Appendix F). RPP-32130, Appendix F (reporting a

portion of the data in the RPP-CALC-60450 dataset) describes some of the same detectors that were used for PNG/TRS data in HEIS GPL as thermal-neutron detectors. Attachment 1 to Stoller (2006) more specifically indicated a ^{3}He detector was used with the Neutron Moisture Logging System (NMLS). Count times, where indicated, ranged from 10 to 20 seconds with 15 seconds by far the most common (the mode). Stoller's count times for data collected from 2003 to 2004 using the NMLS were not recorded in HEIS, but as of 2005, Stoller's list of logging capabilities indicated the NMLS was "Generally run in continuous mode with 1 ft/min logging speed and 15-sec count time" (Stoller 2006, Attachment 1).

As of early 2015, moisture data collected near unplanned release UPR-82 were incorrectly coded in HEIS GPL as "Percent moisture (wet sample)," implying gravimetric measurements of percent moisture by mass, whereas other HEIS GPL data were identified as "Percent moisture by volume." Comparison of the affected values to published plots in units of percent by volume (RPP-32130, Appendix F) confirmed they were actually volumetric. Both parameter names were queried to obtain a complete HEIS GPL moisture dataset.

2.3.3 Handheld Moisture Gauges Dataset

Handheld neutron moisture gauge data were provided in a separate spreadsheet for each drywell, and copies of the spreadsheets as provided are archived with EMDT-OB-0009 in the file Handheld_Moisture_Data.zip. Data from the handheld moisture gauges were recorded at nominal 1-ft (0.3048-m) intervals in pre-prepared tables and subsequently adjusted by subtracting 1.6 ft (0.4877 m) to account for the depth stop on the instrument. The provided Microsoft Excel®[2] spreadsheets converted neutron counts (N) to volumetric moisture content (Θ_w) using calibration constants (A and B) according to the equation:

$$\theta_w(vol\%) = e^A \times N^B \tag{1}$$

RPP-22393, Section 4.2.1.1 describes the general use of both handheld and vehicle-mounted neutron moisture instruments at WMA C, indicating similarities between the different instruments and their operation. For example, RPP-22393 states, "The neutron moisture logging system uses a similar source-detector relationship as the handheld moisture gauge." It appears that the type of neutron source used with all detectors was a 50 mCi ^{241}Am/Be neutron source (RPP-32130, Appendix F; RPP-22393, Section 4.2.1.1; Stoller 2006, Attachment 1), and in some cases the serial numbers indicate the same individual source was used with both handheld and vehicle-mounted instruments.

RPP-22393, Section 4.2.1.1 indicates that the handheld neutron moisture gauges used were CPN International model 503DR HYDROPROBE®[3] units and states, "The handheld moisture gauge will be deployed by qualified personnel in accordance with TO-320-022, *Operate Model 503DR M1 HP-2 or M1 HP-3 Hydroprobe Neutron Moisture Gauge* or TO-320-060, *Operate Model 503DR M1 HP-4 Hydroprobe Neutron Moisture Gauge*." The quoted procedures both specify a 16-second logging time. Meter (instrument) numbers M1-HP-1, M1-HP-2, and M1-HP-3 were indicated in the spreadsheets depending on the location and date, along with the neutron source

[2] Excel® is a registered trademark of Microsoft Corporation in the U.S. and other countries.

[3] 503DR HYDROPROBE® is a registered trademark of CPN International, Inc., Concord, California.

serial number and the name of the operator on each date. Each spreadsheet included a copy of a master table of calibration factors with periodic recalibrations of the meters over time.

Drywells are identified in the provided data by their "tank farm names" which consist of three numbers separated by dashes. The first number is 30 in WMA C, the second is usually the last two digits of the nearest tank number, and the third is a counting number usually indicating the position in a circle around the tank. Analyses of data were done after translating each tank farm name to a HEIS WELL_ID beginning with *A*; however, some discussion herein may retain usage of tank farm names for drywells that arose from working with data as organized by those who generated it. Excel® file Locations.xlsx can be used to cross-reference WELL_ID with other naming conventions.

2.3.4 Moisture Content Dataset from Development of RPP-CALC-60450

Moisture content data collected from other direct push and borehole characterization efforts at WMA C have been previously reported and were also used in this analysis. This dataset was used in the development of RPP-CALC-60450. This dataset included neutron moisture data collected from angled direct push boreholes reported in RPP-32130; RPP-RPT-49956, "Completion Report for the 241-C Tank Farm, C-104 Angle Direct Push Characterization"; RPP-RPT-50581, "Completion Report for the 241-C Tank Farm, C-101 Angle Direct Push Characterization"; and RPP-RPT-51384, "Completion Report for the 241-C Tank Farm C-203 Angle Direct Push Characterization." This dataset also included gravimetric moisture data (already converted to a volumetric basis as provided) for two boreholes that were reported along with corresponding matric potential measurements in PNNL-15503.

Gravimetric data in the RPP-CALC-60450 dataset included only the deeper portions of the boreholes attributed to the Hanford H2 unit. Exceptions were one data point from each borehole tabulated at 0 or -0.0001 ft depth and rejected due to apparently spurious moisture measurements which would have received undue weight without intervening measurements above the H2. Gravimetric moisture data had been converted to a volumetric basis by assuming a soil bulk density of 1.8 g/cm^3, as discussed in the last bulleted item in Section 4.1, and as verified against the original data in PNNL-15503 Tables 4.1 and 4.15. One location with gravimetric data, borehole C4297, was near to other data locations and was included to extend the depth coverage locally. Neutron moisture data had been collected for C4297 but were not calibrated for the casing configuration (PNNL-15503, Section 2.3.1.1). The other location, well C4124 (299-E27-22), was at the margin of the domain defined by the neutron moisture data and was included to minimize extrapolation around the margin. PNNL-15503 (Executive Summary pp. ii) recommended against "holistically" using C4124 data as background values for uncontaminated sediment, stating, "the [chemical] data strongly suggest the sediment has been contacted by a non-radiological waste stream." Notwithstanding that cautionary statement about background values from C4124 in general, because moisture values in the deep portion of C4124 were lower than in the nearest boreholes, there was no clear evidence that contact with a waste stream had caused any difference from background moisture. Moreover, the lower moisture values represent a significant constraint for the interpolation of higher moisture levels in the northeast area of the tank farm. Therefore, it was assumed that including the data would produce

an interpolation more representative of field conditions than if the data were excluded, and so no further changes or rejections of C4124 data were made.

The dataset used to support the development of RPP-CALC-60450 also includes moisture data for drywells and other locations that were already included from the HEIS GPL dataset described in Section 2.3.2, and the duplicated data within the RPP-CALC-60450 dataset were excluded from the final dataset used in this analysis. Due to repeat logging of the drywells and other replicate measurements, the RPP-CALC-60450 dataset had averaged data for each location by depth. Because data were only included from locations not already covered by HEIS GPL, there was no influence of the averaging on the retained dataset.

In the case of angled boreholes, depths in the provided dataset reflected linear distances along the boreholes, whereas elevations reflected vertical locations. Therefore, the elevations were used for any further analyses requiring vertical depths or elevations. Lateral coordinates for each measurement included in the RPP-CALC-60450 dataset were provided as part of the data compilation.

2.4 GEOSTATISTICAL ESTIMATION

The combined datasets (HEIS GPL, handheld, and the RPP-CALC-60450 dataset) are used to develop a three-dimensional representation of moisture content in the subsurface of the WMA C tank farm using geostatistical interpolation. Geostatistical estimation is a two-step process, as follows.

1) Variogram Analysis – establishes the predictability of data from place to place. The variogram models the difference between a value at one location and the value at another location according to the distance and direction between them. When using borehole and geophysical log data, the vertical direction is typically well informed and the horizontal direction is typically less well informed. In order to establish horizontal correlations between data (borehole) locations, geologic knowledge is applied to develop an empirical (experimental) variogram based on the data.

2) Data Estimation – estimation at locations that have not been sampled. Kriging uses a weighted average of neighboring samples to estimate the "unknown" value at a given location. The weights are optimized using the variogram model, the location of the samples, and the relative distance between sampling locations.

2.4.1 Variogram/Correlogram Analysis

Variograms and correlograms describe the spatial continuity of the data. Variogram analysis consists of calculating an empirical variogram from the data and fitting a variogram model to the data. Empirical variograms are discrete functions calculated using a measure of variability, usually the semivariance, $\gamma(h)$, between pairs of data separated by a specified distance, h, known

as the lag distance. As shown in Figure 2-3, typical semivariograms can be described using the following three parameters.

1) Nugget Effect – represents micro-scale variation or measurement error. It is estimated from the empirical variogram $\gamma(h)$ at $h = 0$.

2) Range – the distance (if any) at which the variogram reaches a plateau, i.e., the distance at which data are no longer correlated.

3) Sill – the variance of the dataset, disregarding the spatial structure. It is the magnitude of the plateau the variogram reaches at the range γ(range).

Some datasets exhibit anisotropy where the spatial correlations are stronger or more persistent in some directions than others. Spatial correlations that depend only on the distance (and not on the direction) of separation between the data pairs are said to be isotropic.

Both vertical and horizontal empirical variograms were used for the characterization of the moisture content data using the following expressions:

- Vertical semivariogram

$$\gamma(h) = \frac{1}{2N(h)} \sum_{i=1}^{N(h)} (x_i - y_i)^2 \tag{2}$$

- Horizontal pairwise relative semivariogram

$$\gamma_{PR}(h) = \frac{1}{2N(h)} \sum_{i=1}^{N(h)} \frac{(x_i - y_i)^2}{\left(\frac{(x_i + y_i)}{2}\right)^2} \tag{3}$$

In the horizontal direction, the most continuous correlation in the empirical data was observed using a pair-wise relative semivariogram. Pair-wise relative semivariograms can be used to correct erratic variogram behavior by adjusting the squared mean of the head and tail values of data pairs. This method is resistant to data sparsity and outliers, and can reveal structure and anisotropy that otherwise could not be detected (GSLIB: Geostatistical Software Library and User's Guide [Deutsch and Journel 1998]).

Because kriging algorithms need to access semivariogram values for lag distances other than those used in the empirical semivariogram, the empirical semivariogram needs to be replaced with an acceptable semivariogram model. The semivariogram models used in the kriging process also need to obey certain numerical properties in order for the kriging equations to be solvable. Mathematically, the semivariogram model needs to be non-negative definite, in order for the system of kriging equations to be non-singular. Most frequently, one or more of five types of model variograms are selected: spherical, exponential, Gaussian, power, or hole-effect model (see Deutsch and Journel [1998] for a complete description of each). Based on the moisture content data correlations developed for the empirical semivariograms, the exponential model semivariograms were chosen as the best fit for the interpolation of the three-dimensional model using kriging. Using "h" to represent lag distance, "a" to represent

(practical) range, and "c" to represent sill, the exponential model is defined by Equation II.16 in Deutsch and Journel (1998):

$$\gamma(h) = c \cdot exp\left(\frac{h}{a}\right) = c \cdot \left[1 - exp\left(-\frac{3h}{a}\right)\right] \quad (4)$$

It can be shown that the right-hand side of Equation 4 is equivalent to the simpler exponential function in the left-hand side, but the derivation is omitted here as in Deutsch and Journel (1998). Graphically, the exponential variogram is linear near the origin and curves asymptotically toward the sill value.

Correlograms plot autocorrelation rather than variance, so they resemble mirror images of variograms for the same datasets. Equation III.4 from Deutsch and Journel (1998) is used to prepare empirical correlograms. For empirical variograms described by an exponential model, the corresponding correlogram is likewise described by an exponential model as given by Equation 13 from "Hydrogeological Decision Analysis: 1. A Framework" (Freeze et al. 1990).

2.4.2 Data Interpolation

Once a model of spatial dependence has been established, attribute values can be estimated at unsampled locations. Interpolation is the estimation of a variable at an unsampled location based on information from surrounding sampled locations. Kriging is used to estimate unknown values based on the regression against observed values of the surrounding data. Kriging methods use weighted coefficients based on observed patterns in the data developed using the empirical and model variograms. Based on the discussion provided by Geostatistics for Natural Resources Evaluation (Goovaerts 1997), kriging is a variation of the basic linear regression estimator $Z^*(\mathbf{u})$ as described by:

$$Z^*(\mathbf{u}) - m(\mathbf{u}) = \sum_{\alpha=1}^{n(\mathbf{u})} \lambda_\alpha [Z(\mathbf{u}_\alpha) - m(\mathbf{u}_\alpha)] \quad (5)$$

Where

$\mathbf{u}$, $\mathbf{u}_\alpha$	=	location vectors for a point to be estimated and one of the neighboring data points indexed by α, respectively
$n(\mathbf{u})$	=	number of data points
$m(\mathbf{u})$, $m(\mathbf{u}_\alpha)$	=	means of $Z(\mathbf{u})$ and $Z(\mathbf{u}_\alpha)$, respectively
$\lambda(\mathbf{u})$	=	kriging weight assigned data point $z(\mathbf{u}_\alpha)$ for estimation at location $\mathbf{u}$.

The objective of kriging is to minimize the variance $\sigma_E^2(\mathbf{u})$ of the estimator at the estimation locations as given by:

$$\sigma_E^2(\mathbf{u}) = Var\{Z^*(\mathbf{u}) - Z(\mathbf{u})\} \quad (6)$$

subject to the unbiasedness constraint that the expected value of the estimation error $E\{Z^*(\mathbf{u}) - Z(\mathbf{u})\} = 0$ where the expected value of a discrete random variable is the probability-weighted average of all possible values.

Figure 2-3. Semivariogram Components Including Sill, Range, and Nugget.

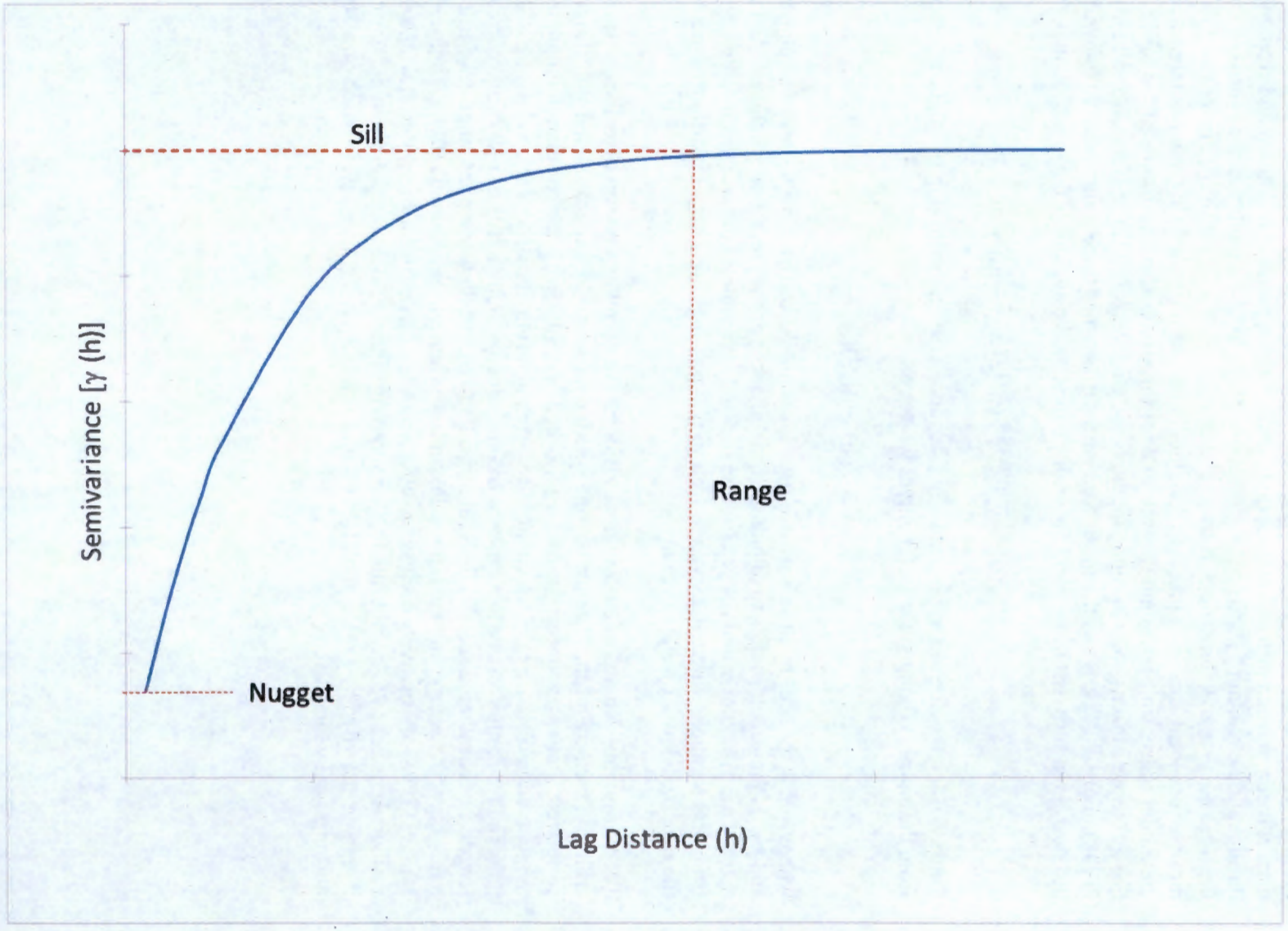

Three commonly used variations of kriging are simple kriging, ordinary kriging, and universal kriging. The primary difference between each kriging type is the treatment of the model for the dataset mean or trend m(**u**). Simple kriging considers the mean to be known and constant throughout the domain. Ordinary kriging accounts for local variability in the mean, and limits the local mean to a defined area. Universal kriging applies a smooth variation or trend in the mean across local areas. To preserve the global mean of the dataset in the unsampled areas of the model space, simple kriging was selected for this exercise and is discussed further below. For a complete discussion of kriging methods see Goovaerts (1997) or Deutsch and Journel (1998). For simple kriging, the mean component is assumed to be a constant and known across the study area such that m(**u**) = m. This allows the linear estimator (Equation 5) to be written as

$$Z^*_{SK}(\mathbf{u}) = \sum_{\alpha=1}^{n(\mathbf{u})} \lambda_\alpha^{SK}(\mathbf{u})[Z(\mathbf{u}_\alpha) - m] + m \tag{7}$$

Further, using the derivation presented by Goovaerts (1997), the kriging weights are determined from the simple kriging system of matrices written as

$$\boldsymbol{\lambda}_{SK}(\mathbf{u}) = \mathbf{K}_{SK}^{-1}\mathbf{k}_{SK} \tag{8}$$

where $\mathbf{K}_{SK}$ is the n(**u**) by n(**u**) matrix of data covariances, $\boldsymbol{\lambda}_{SK}(\mathbf{u})$ is the vector of kriging weights, and $\mathbf{k}_{SK}$ is the vector of data to of unknown covariances at the prediction locations. Assuming that the mean is known and constant across the study area allows the weights to decrease away from data locations where the stationary mean will dominate. Points with distances greater than the range will have a weight of zero.

The "correlation length" of an empirical variogram or correlogram is an objective, albeit arbitrary, measure of the distance beyond which data are no longer considered significantly correlated. For an exponential model, Freeze et al. (1990) define the correlation length to mean the separation distance over which the autocorrelation function decays to a value of e^{-1}. There is potential for confusion due to a practice among some geostatisticians of ascribing "correlation length" or "correlation scale" a definition similar to that of the variogram range or of using the terms interchangeably, and the term is absent from Deutsch and Journel (1998). Deutsch and Journel (1998) alternatively discuss the effective range, a, defined as the value at which the variogram reaches 95% of the sill, c. For purposes of this EMCF, the definition of "correlation length" is that used by Freeze et al. (1990), and a model variogram range is based on visual fit to the empirical variogram.

3 METHODOLOGY

The following steps were performed in the geostatistical estimation of the WMA C moisture content data and the development and execution of the heterogeneous case model.

1. Data compilation, reduction, and conditioning

    - Compiled adjusted moisture content (volume %) dataset from HEIS GPL, handheld, and RPP-CALC-60450 datasets.

    - Rejected non-physical values and performed other quality assurance steps as reported in EMDT-OB-0009.

    - Re-sampled dataset to 1-ft vertical intervals taking maximum volumetric moisture content on each interval and posting at the interval center.

2. Calculation of summary statistics

    - Histograms for each dataset were developed in the preprocessor and visualization tool for the datasets and interpolation results.

    - Calculated mean, minimum, maximum, and standard deviation for the following datasets:

        i. "Combined Adjusted" (the complete dataset, including measurements from different hydrostratigraphic units and from different instruments)

        ii. "Handheld Only" (subset of the handheld gauge measurements)

        iii. "Combined Adjusted Dataset without Handheld" (subset of everything other than handheld gauge measurements)

        iv. "H2 Unit Only" (subset of data collected from the horizon attributed to the H2 unit).

3. Variogram/correlogram analysis

    - Horizontal pair-wise relative semivariograms were constructed using Equation 3.

    - Vertical semivariograms were constructed using Equation 2.

    - Correlograms were constructed using Equation III.4 from Deutsch and Journel (1998). Correlation lengths as defined in Freeze et al. (1990) were estimated from linear interpolation of points on the correlograms.

- Model variograms were selected based on a visual fit to the empirical (experimental) variograms.

4. Interpolation

- Interpolation was performed with the software routine in the KT3D kriging software package provided with Geostatistical Software Library (GSLIB)[4] that used Equations 5 through 8 as a basis. A more complete description of the calculation method can be found in Deutsch and Journel (1998) and Goovaerts (1997).

5. Sensitivity analysis

- Endpoint ranges for the model variograms were determined from the empirical variograms while maintaining visual fit to the data. Alternative interpolations were prepared for combinations of the central and endpoint ranges of the horizontal and vertical model variograms.

- An alternative variogram analysis and interpolation was prepared for "Combined Adjusted Dataset without Handheld".

- An alternative variogram analysis and interpolation was prepared for the "H2 Unit Only" dataset. The combined dataset was trimmed to include only the H2 interval based on the STOMP© implementation of Alternative Geologic Model II. Kriging model grid elevations were adjusted to correspond to the trimmed dataset.

6. Development and execution of heterogeneous case model

- Three cross-sections were selected from the three-dimensional WMA C PA base case STOMP© model to develop two-dimensional STOMP© models. One set of two-dimensional models was extracted without any alteration to provide a comparison of the base case EHM approach. The heterogeneous case is developed by mapping the base case moisture interpolation onto the three-dimensional PA base case model grid, and then extracting another set of the same two-dimensional cross-sections, and redefining the rock/soil zonation for grid blocks according to the interpolated moisture values.

- Bands of moisture values are specified to group the continuous range of interpolated moisture values into a discrete set used to declare new rock/soil zones. Hydraulic parameters for these new zones are selected from analyses of Hanford formation sediment samples meeting the condition that at a unit gradient condition the sample hydraulic parameters yield moisture contents within the specified bands.

---

[4] GSLIB is an acronym for Geostatistical Software LIBrary and was originally used for a collection of geostatistical programs developed at Stanford University, Stanford, California.

- For each cross-section, a historical simulation is run to obtain a steady-state flow field to set initial conditions, then a predictive simulation is run in which an arbitrary concentration of technetium-99 (^{99}Tc) is instantly injected at calendar year 2020 at a location near the base of the backfill. Output concentrations are observed at a point of calculation 100 m downgradient from the source location.

This page intentionally left blank.

4 ASSUMPTIONS AND INPUTS

A description of the assumptions and inputs for the calculations is provided below.

4.1 DATA COMPILATION AND ANALYSES

The moisture content data from all three sources (HEIS GPL, handheld, and RPP-CALC-60450) were imported into tables in the Microsoft Access®[5] 2013 database, WMAC_Moisture.accdb, that have been archived in EMMA. Copies of the tables are also archived in EMMA as Microsoft Excel® 2013 format (extension .xlsx). A listing of these files and their descriptions are provided in Attachment 1. The table in the database titled "Locations" includes the surface coordinates of locations from all datasets and the multiple names used for each location by different sources. Location names were matched to the WELL_ID field in the Locations table to avoid duplication and ensure unique names for reporting results herein. The table in the database titled "Angled_boreholes" summarizes directional data as applicable. The table "Freestone_data" includes moisture measurements with x-, y-, and z-coordinates as provided in the RPP-CALC-60450 dataset for the angled boreholes and the other selected locations. HEIS GPL data with a reduced number of fields were imported into the table "HEIS_GPL_data". Handheld neutron moisture gauge data were provided in a separate spreadsheet for each drywell, and copies of the spreadsheets as provided are also archived in EMDT-OB-0009. Following selection and quality assurance of handheld neutron moisture gauge data by methods discussed in EMDT-OB-0009, the resulting dataset was imported to the table HandheldDataCorrected.

Assumptions for the data compilation are provided below.

- Selected profiles were assumed to be representative of steady-state moisture conditions. This assumption is justified because the shape of moisture profiles are consistent over time (Figures 4-1 to 4-4). Selecting the maximum of the measurements provided representative values despite using a high bias to emphasize the strongest departures from the mode. That is, given the consistency over time, the strongest departures from the mode are similar to smaller departures at other times. In general, the analysis in this EMCF tests for correlation of relatively high moisture measurements with heterogeneity in both lateral and vertical dimensions, so when alternative methods of data reduction have potential to introduce bias, the method that errs on the side of retaining elevated moisture measurements is selected.

- Selecting maximum values over 1-ft (0.3048-m) vertical intervals and using 1-ft vertical intervals for kriging preserved vertical variability at the scale of interest, with a high bias to emphasize the strongest departures from the mode. Note the probable range of neutron detection was larger than the nominal sampling increment of 3 in., from somewhat less than 1 ft for the most saturated regions up to about 2 ft for the driest regions. Also note the smallest vertical interval in the STOMP® model gridding was 1 m, so the kriging interval provided higher resolution than was ultimately used in the models.

[5] Access® is a registered trademark of Microsoft Corporation in the U.S. and other countries.

Figure 4-1. Time Series of Drywell Moisture at 10-foot Intervals Showing Reduced Variability at Depth.

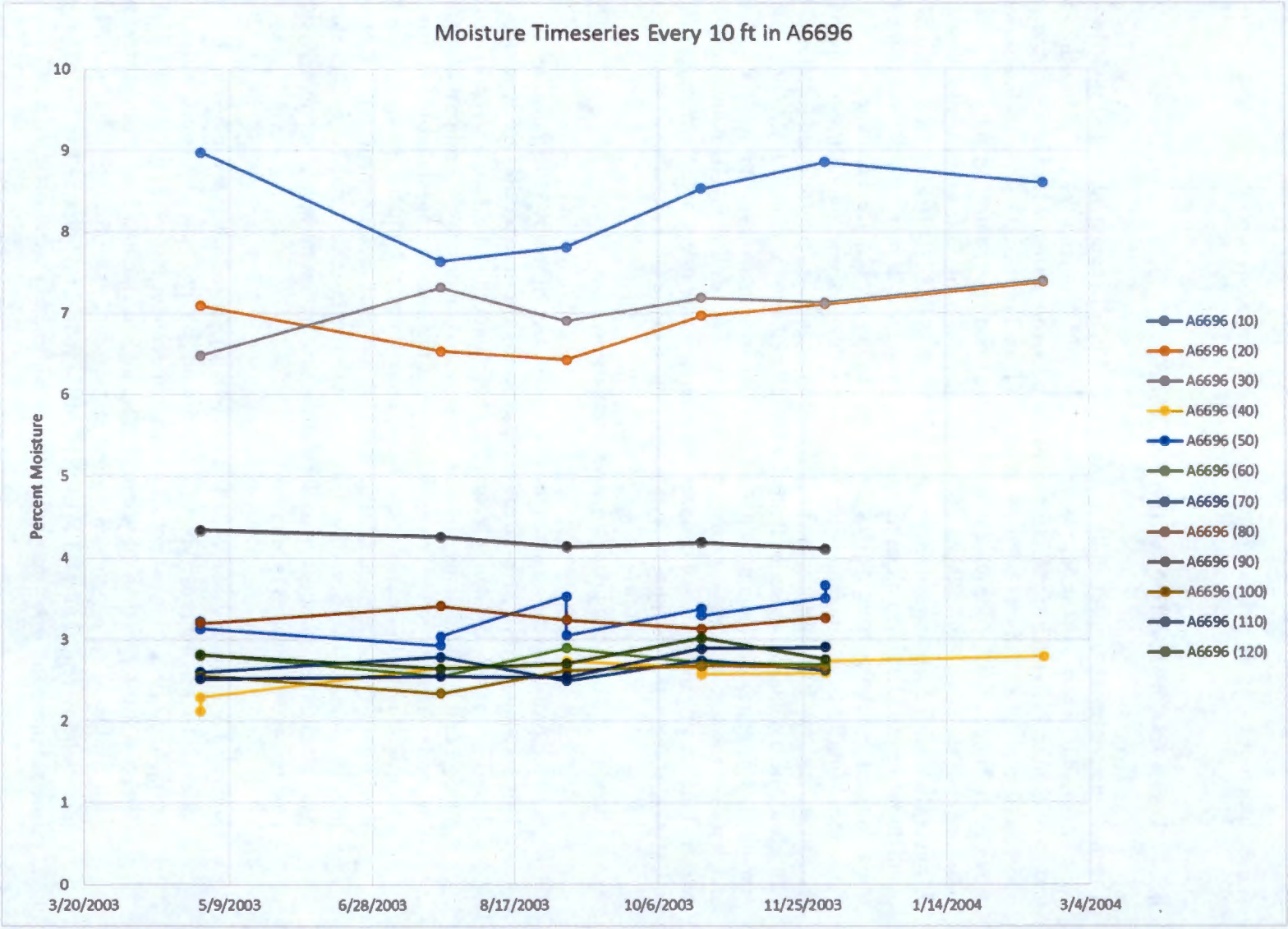

Figure 4-2. Consistent Vertical Profile of Neutron Moisture Measurements over Time in a Drywell from Multiple Logs in 2003 and Un-calibrated Data from 1976.

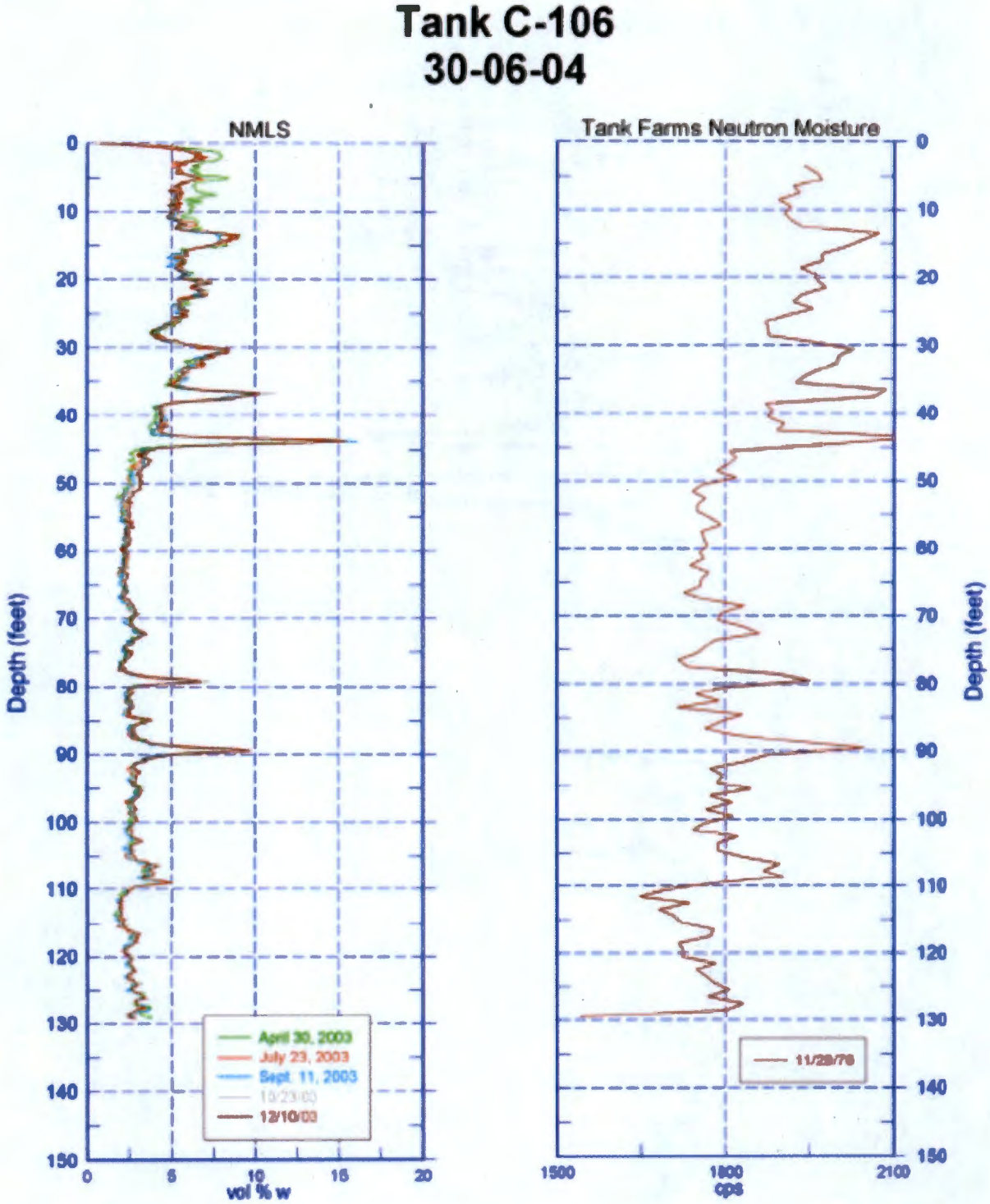

Figure 4-3. Comparison of Neutron Moisture Logging System and Handheld Instrument Logs of Neutron Moisture Profile in Drywell A6696 (30-06-10).

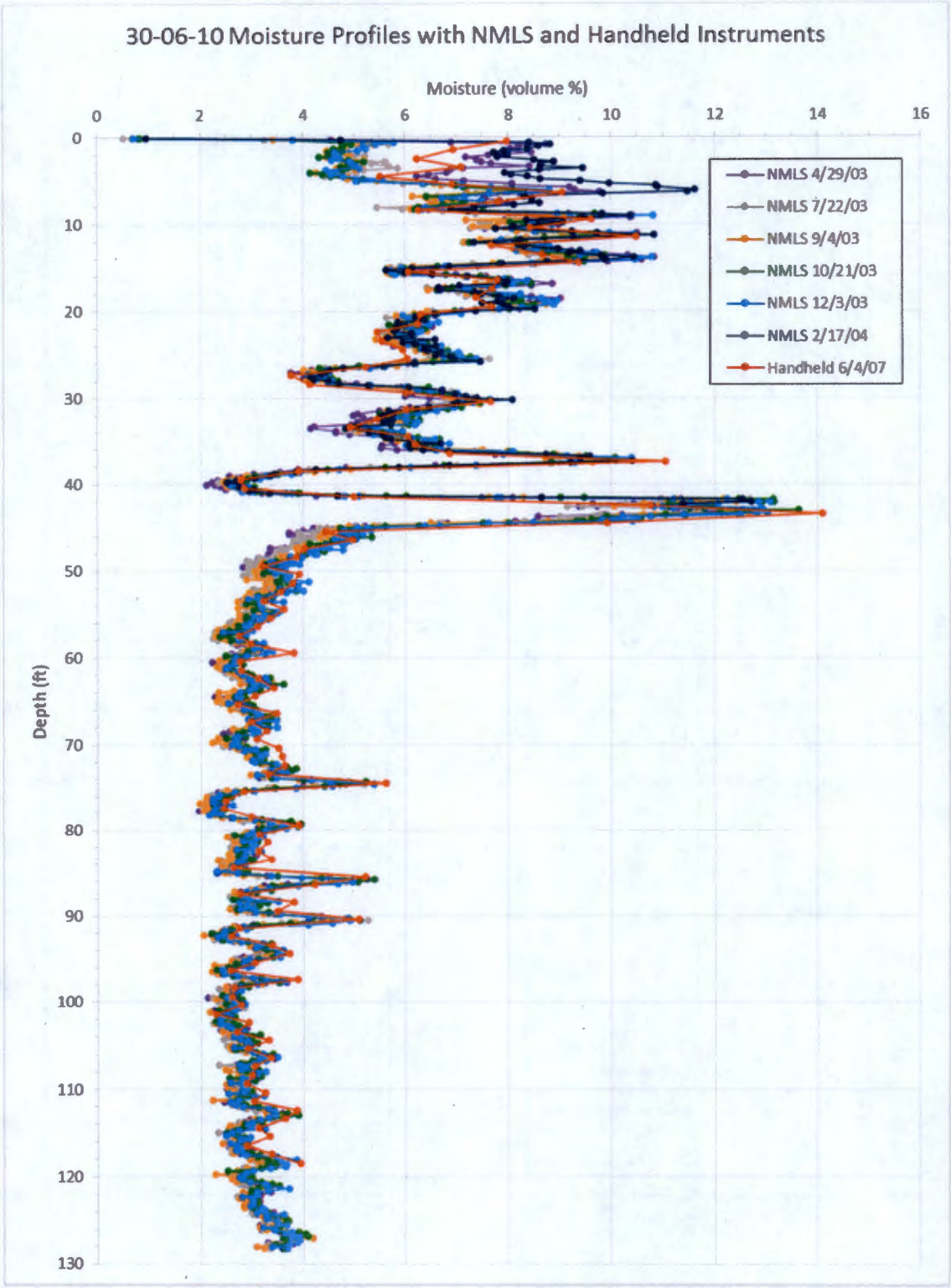

NMLS = Neutron Moisture Logging System

Figure 4-4. Comparison of Neutron Moisture Logging System and Handheld Instrument Logs of Neutron Moisture Profile in Drywell A6698 (30-06-04).

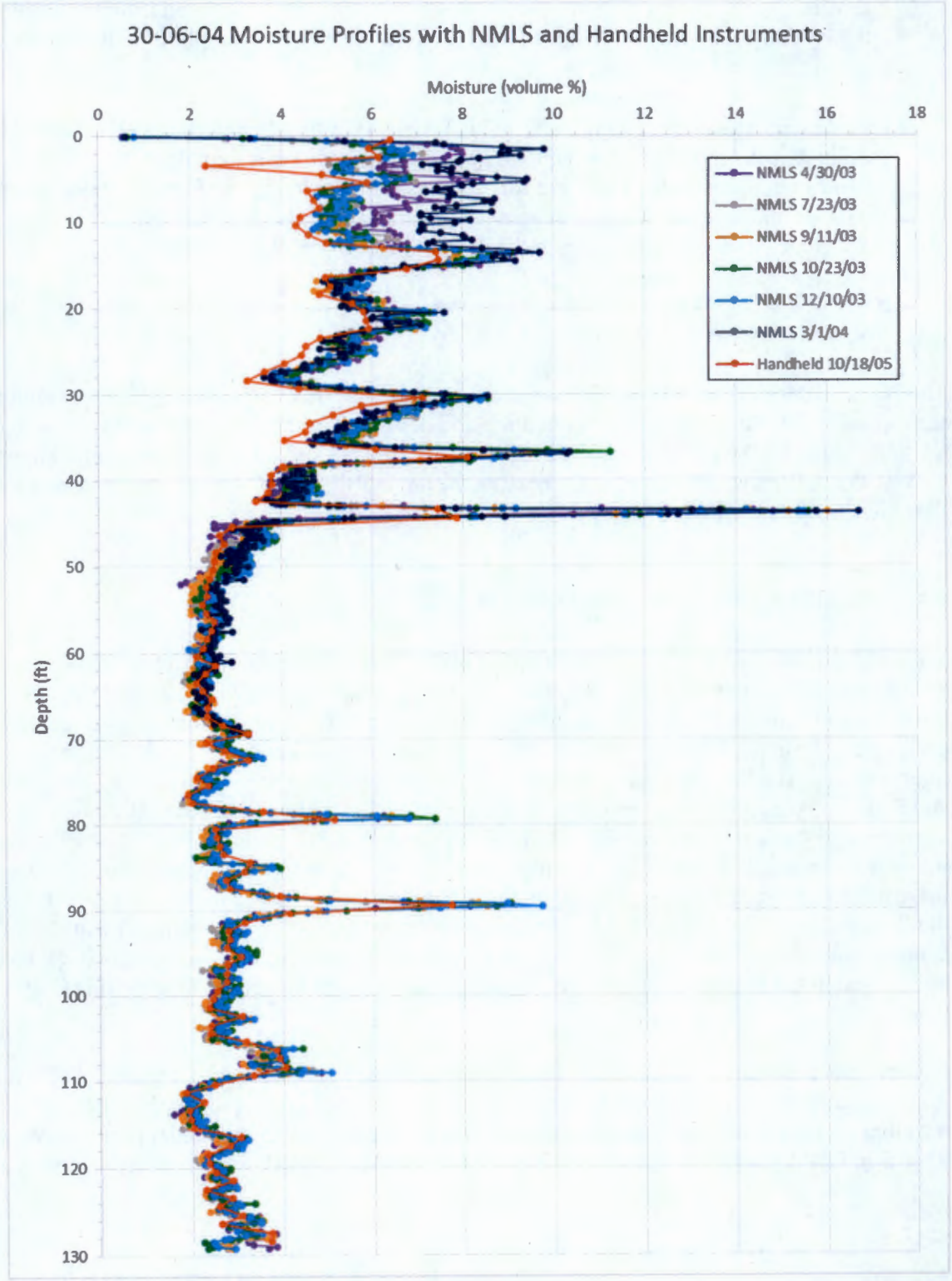

NMLS = Neutron Moisture Logging System

- Data from different instruments, operators, etc. was sufficiently comparable for interpolation. Two locations (drywells) had both handheld and NMLS profiles available to compare; the dataset justifies that NMLS and handheld neutron moisture gauge profiles are consistent (Figures 4-3 and 4-4). In these cases with data from both sources, the NMLS data were retained for interpolation due to higher sampling frequency and greater or equal depth coverage.

- A constant value for soil bulk density of 1.8 g/cm^3 in the H2 unit provided sufficiently accurate conversion of gravimetric data to a volumetric basis to make data comparable to neutron moisture data. Note that this conversion was already performed on the provided dataset, and that the soil bulk density value differs slightly from the value of about 1.7 g/cm^3 discussed elsewhere in the development of the WMA C PA model.

4.2 VARIOGRAM ANALYSES

The adjusted datasets were used for the variogram analyses. Each of the datasets is presented in the input files for the geostatistical estimation and described in the file "readme.txt". These files are archived in EMMA maintained by INTERA, Inc. and backed up to a server location managed by WRPS. A file directory in EMMA bearing the name RPP-CALC-60345 identifies that the files are associated with this EMCF.

4.3 GEOSTATISTICAL ESTIMATION

Values of moisture content were estimated for a 5 m by 5 m by 0.3048 m grid in x-, y- and z-directions, respectively, using the simple kriging algorithms provided from KT3D of GSLIB (Deutsch and Journel 1998). Because simple kriging was used, a constant mean was assumed for each dataset. Simple kriging was selected to preserve the global mean of the dataset for the interpolation. The length of the grid in the x-direction was 160.0 m, 300 m in the y-direction, and 73 m in the z-direction. The origin of the grid was 574,970 m, 136,540 m (Lambert coordinate system, NOAA Manual NOS NGS 5, "State Plane Coordinate System of 1983"), and the grid was rotated 35 degrees east of north based on the variogram analysis. The top surface of the grid was assigned elevations based on the ground surface modeled in the STOMP© model for the WMA C (see RPP-ENV-58782, "Performance Assessment of Waste Management Area C, Hanford Site, Washington"). The file, titled GridNodes.txt, specifying x-y-z locations of the grid nodes used in the moisture content estimation is archived with the model files for this EMCF in EMMA.

Each time KT3D runs, a "parameter" file that contains information such as the names of the input and output files, the variables to analyze, and the type of kriging to be performed is developed as the input file. These parameter files are archived with the model files for this EMCF in EMMA, and a description of each of the files is provided in the file "readme.txt".

4.3.1 Sensitivity Analyses

Sensitivity analyses were used to qualitatively assess uncertainties in the dataset and interpretation on the geostatistical estimation of moisture content for the study area. Model variogram ranges can affect the apparent data connections for the geospatial estimation. For the base case dataset, both shorter and longer ranges can be determined that still reasonably fit the empirical data upon visual inspection. To examine the effects on the geostatistical estimation of the interpreted base case range of the variograms, sensitivity analyses for representative endpoint minimum and maximum vertical and horizontal ranges were performed.

A subset of the combined adjusted data that removed the handheld data was used for a sensitivity analysis. Summary statistics for the component datasets showed that the handheld data tended to have lower moisture content than the rest of the database [Figures 4-5b) and 4-5c)]. The handheld data comprised the bulk of the database in the center of the domain (accounting for all but two of the drywell locations), so the difference between the handheld data and other dataset values produces a strong contrast between drier values in the center and moister values on the periphery in the base case interpolation [see, for example, Figure 4-5a)]. The sensitivity analysis was intended to elucidate whether the difference was a genuine feature of the spatial distribution of moisture at WMA C or was attributable in significant part to any differences in data collection methods (such as different vertical sampling intervals, instruments, operators, or calibrations) or quality assurance measures. New variograms were established based on the trimmed dataset and interpolation of the values to the same interpolation grid used for the base case.

A sensitivity analysis was also performed to examine impacts on spatial correlation when the data was constrained by lithologic boundaries, and the potential effects of removing the backfill. The data was cropped based on the upper and lower Hanford H2 unit contacts defined in the STOMP© model. A secondary grid for the geologic estimate with the same x and y discretization was established based on the H2 unit. The top elevation of the grid was assigned based on the Hanford H2 top contact as designated in the STOMP© model. The bottom elevations of the model grid were assigned based on the top contact of the H3 unit in the STOMP© model. The x-y-z grid node elevations are in the file "H2GridNodes.txt" archived in EMMA. The moisture content data was estimated based on the variogram ranges and other parameters derived for the base case combined dataset and the H2-only dataset.

Figure 4-5. Histograms for Moisture Content (vol %) Datasets.

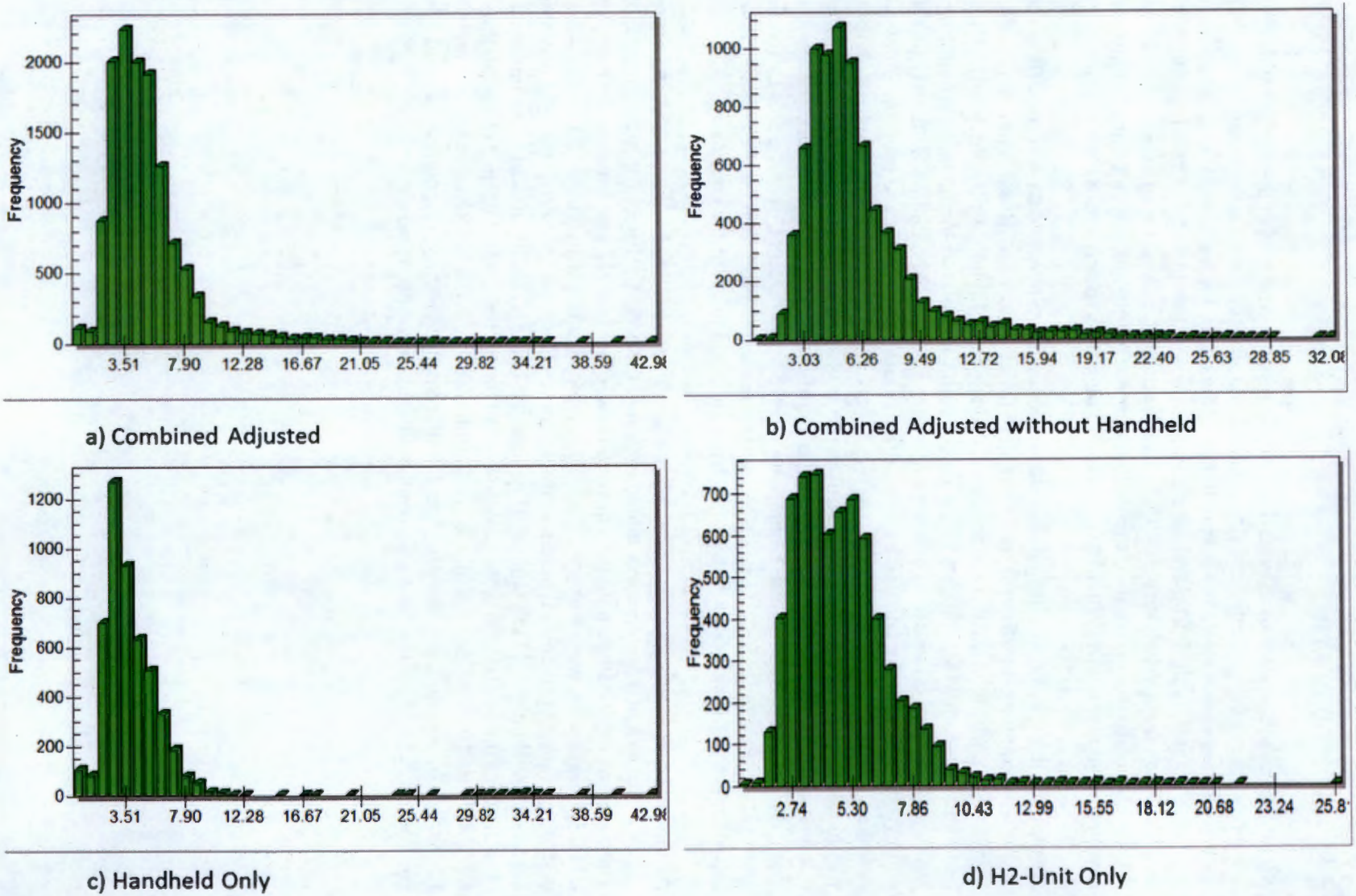

Figure 4-6. Cross-Section D-D' with Continuous Contours for Moisture Content (vol %) Interpolation.

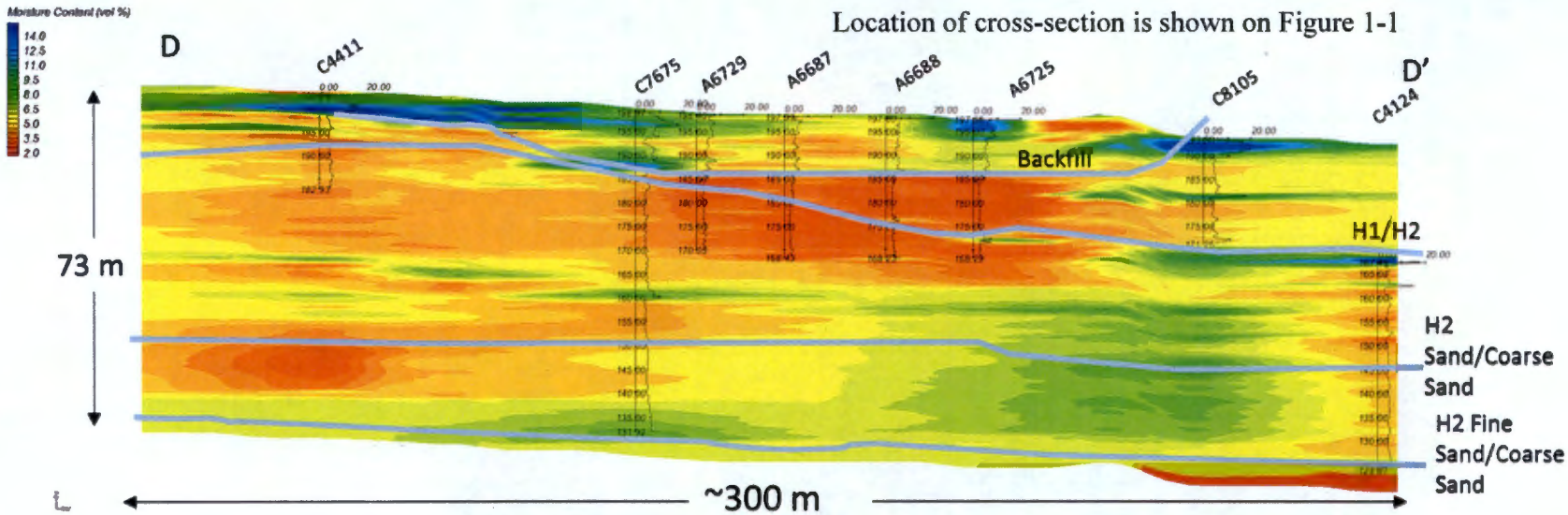

4.4 VADOSE ZONE HYDRAULIC PROPERTIES

Hydraulic properties for a range of sediments representative of the vadose zone materials at WMA C were determined from analysis of available data from investigations at nearby facilities on the Hanford Site in RPP-RPT-58949, Appendix B. These facilities include the Integrated Disposal Facility (IDF) in the 200 East Area, the 218-E-12B and 218-E-10 low-level solid waste burial grounds in 200 East Area, the Environmental Restoration Disposal Facility site located in between the 200 West and 200 East Areas, and the 241-T-106 tank site located in 200 West Area. Table 4-1 shows the vadose zone hydraulic parameters for the hydrostratigraphic units that have been used in the base case model. For the H2 unit comprising most of the stratigraphic column for the vadose zone at WMA C, the data were obtained from 44 sandy samples from IDF with the unsaturated hydraulic conductivity and moisture retention curves shown in Figure 4-7. Analyses of these IDF data provided hydraulic properties for both a composite H2 sand in the base case and for representation of multiple sediment types in the heterogeneous case. The IDF is located approximately 1 kilometer southwest of WMA C.

Table 4-1. Vadose Zone Hydraulic Properties for Waste Management Area C Hydrostratigraphic Units.

Hydrostratigraphic Unit	θ_s, Saturated Water Content	θ_r, Residual Water Content	α, van Genuchten Alpha (1/cm)	n, van Genuchten n	ℓ, Pore Size Connectivity Factor	K_s, Fitted Saturated Conductivity (cm/s)
Backfill Gravelly Unit	0.138	0.010	0.021	1.374	0.5	5.60E-04
H1 and H3 Gravelly Units	0.171	0.011	0.036	1.491	0.5	7.70E-04
H2 Sand-Dominated Unit	0.315	0.039	0.063	2.047	0.5	4.15E-03

Source: RPP-RPT-58949, "Model Package Report Flow and Contaminant Transport Numerical Model used in WMA C Performance Assessment and RCRA Closure Analysis."

Figure 4-7. Moisture Retention Curves and Unsaturated Hydraulic Conductivity Curves for 44 Integrated Disposal Facility Samples.

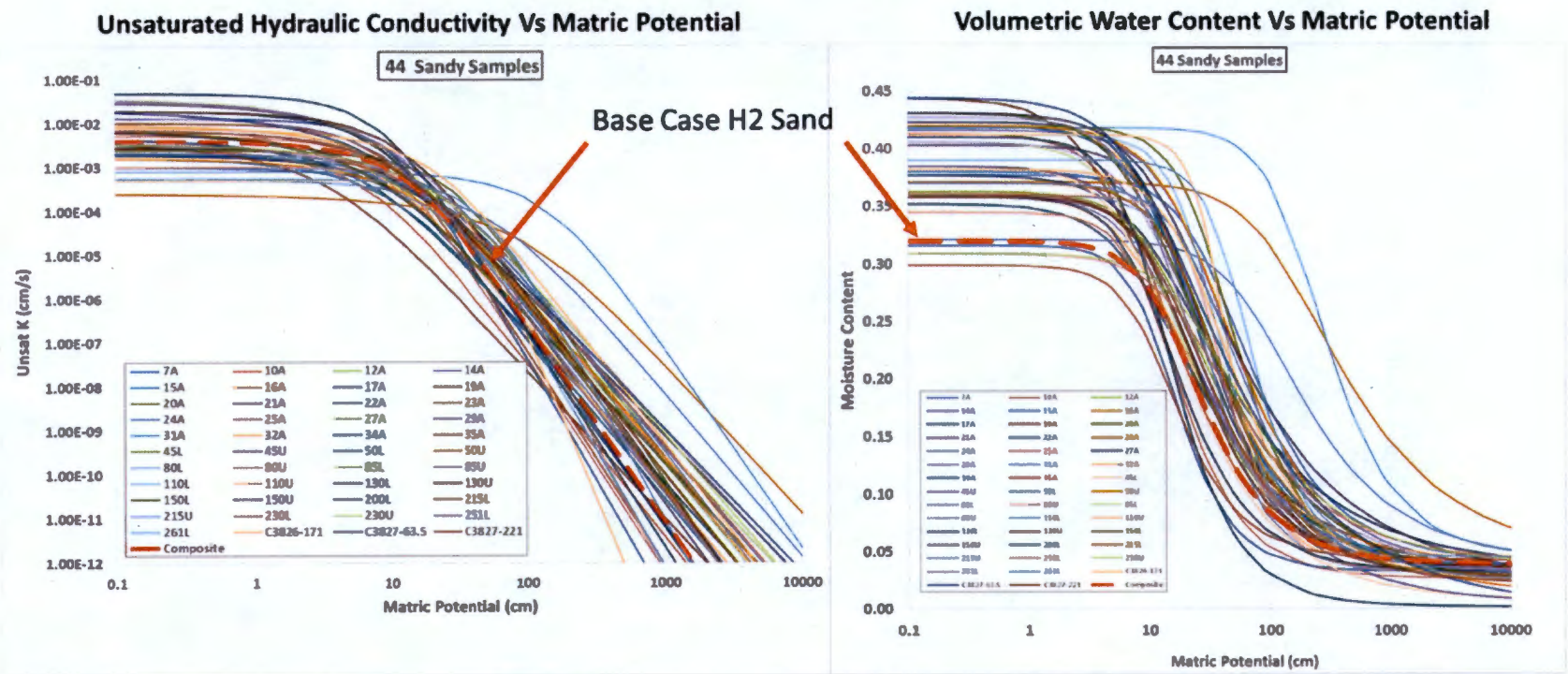

Reference: RPP-RPT-58949, "Model Package Report Flow and Contaminant Transport Numerical Model used in WMA C Performance Assessment and RCRA Closure Analysis," Appendix B.

This page intentionally left blank.

5 SOFTWARE APPLICATIONS

The software used to perform this calculation are approved, managed, and used in compliance with the CH2M HILL Plateau Remediation Company (CHPRC) requirements of PRC-PRO-IRM-309, "Controlled Software Management."

5.1 EXEMPT SOFTWARE

Microsoft Excel® and Microsoft Access® are site-licensed software used to compile moisture data, perform unit conversions, and select unique data values for the grid input to interpolation (e.g., by applying unique location names and by using maximum queries to select data among multiple dates or closely-spaced measurements). The Excel® spreadsheets and the Access® database used for these purposes are wholly incorporated into this calculation and verified during the technical review of this report, and are therefore rated as exempt software (PRC-PRO-IRM-309, Section 1.3, Exemptions).

5.2 APPROVED SOFTWARE

The moisture interpolation portion of this calculation uses the approved software KT3D from GSLIB with supporting functions in GMS 10.0[6]. The contaminant fate and transport simulations reported in this EMCF use the approved software STOMP© with supporting functions in Tecplot®[7]. The STOMP© models used are based on models reported in RPP-RPT-58949.

5.2.1 GSLIB – KT3D

KT3D from GSLIB was used for kriging soil moisture data for interpretation of the moisture distribution at WMA C to support development of the alternative heterogeneous case model tested in this EMCF.

GMS 10.0 was used in conjunction with KT3D for variogram visualization, histogram calculation, and dataset summary statistics (minimum, maximum, mean, etc.). Also, GAMV from GSLIB was used to process empirical variograms/correlograms. These uses were limited to the spreadsheet category/support software.

5.2.1.1 Description. Kriging calculations used KT3D, a subroutine of GSLIB, approved for use at the Hanford Site in accordance with the requirements of PRC-PRO-IRM-309. The installed KT3D software was tested in accordance with the procedure per CHPRC-00258, "MODFLOW and Related Codes Software Management Plan." GSLIB is incorporated into Revision 4 of CHPRC-00258 as support software. The manner in which GSLIB is used to support modeling with STOMP© is identical to the manner in which it is intended for support of MODFLOW, so procedures for STOMP© do not implement redundant management procedures for GSLIB.

---

[6] GMS 10.0 is a product of Aquaveo, LLC, Provo, Utah.

[7] Tecplot and Tecplot 360 are registered trademarks or trademarks of Tecplot, Inc. in the United States and other countries.

Software is registered on the Hanford Information System Inventory (HISI) and is identified as approved for use. The identification for the software package used in the calculation is as follows:

- Software Title: GSLIB – KT3D
- Software Version: GSLIB Version 2.0 (64-bit version of Fortran 90 executable for Windows)
- HISI Identification Number: 3851
- Workstation type and property number (from which software is run):
    - Lenovo W 540
    - Windows 8.1 Pro
    - Intel®[8] Core i7-4800MQ CPU @2.70GHz
    - RAM 8.00 GB
    - 64-bit Operating System, x64-based processor
    - AUS-Tin, AUS-Tin.intera.local.

5.2.1.2 Software Installation and Checkout. An installation and checkout process is not required for this software (CHPRC-00258).

5.2.1.3 Statement of Valid Software Application. Deutsch and Journel's (1998) GSLIB family is of geostatistical programs, including programs to compute semivariograms, compute correlograms, and to do kriging, cokriging, and kriging with a trend that include the code three-dimensional kriging program KT3D. The KT3D program can be used to analyze two-dimensional and three-dimensional data, data on a rectangular grid, and irregularly spaced data. The program is written in FORTRAN and is routinely incorporated into other software programs as a subroutine. This analysis was a valid application of KT3D within the software limitations, namely, the analysis employed simple kriging using the exponential variogram model for which use KT3D is validated and approved (Attachment 2 to CHPRC-00258).

5.2.2 Subsurface Transport Over Multiple Phases

STOMP© was used for vadose zone and groundwater contaminant fate and transport simulations. Tecplot® was used as support software in conjunction with STOMP© to visualize and map the soil moisture interpolation from KT3D to the STOMP© grid so that interpolated moisture values could subsequently be interpreted to assign rock/soil zones to the grid blocks. The linear interpolation feature of Tecplot® was used to map moisture values to the grid which had already been interpolated on a higher-resolution KT3D grid. Tecplot® was also used to visualize STOMP© output.

[8] Intel is a registered trademark of Intel Corporation.

5.2.2.1 Description. Model simulations used STOMP© Build 4, approved for use by CHPRC at the Hanford Site in accordance with the requirements of PRC-PRO-IRM-309. The installed STOMP© software was tested in accordance with the procedure per CHPRC-00176, "STOMP Software Management Plan."

Software is registered on HISI and is identified as approved for use. The identification for the software package used in the calculation is as follows:

- Software Title: STOMP©
- Software Version: CHPRC Build 4 (executable "stomp-w-cgst-chprc04l.x")
- HISI Identification Number: 2471 (Safety Software, Level C)
- Workstation type and property number (from which software is run): STOMP© was executed on the INTERA Richland GREEN Linux®[9] Cluster that is owned and managed by INTERA, Inc., a subcontractor to CHPRC. The computer property tag for the front-end node is #469 at INTERA's office in Richland, Washington. This node is a Dell™[10] PowerEdge™ R510 with two six-core Intel® Xeon®[11] X5660 processors @ 2.80GHz and 48 GB of RAM. As given by the command "uname –a", the operating system details are:
    - Linux green 3.2.0-65-generic #98-Ubuntu SMP Wed Jun 11 20:27:07 UTC 2014 x86_64 x86_64 x86_64 GNU/Linux.

5.2.2.2 Software Installation and Checkout. The Software Installation and Checkout form for STOMP© is provided in Attachment 2 to this EMCF.

5.2.2.3 Statement of Valid Software Application. DOE/RL-2011-50, Regulatory Basis and Implementation of a Graded Approach to Evaluation of Groundwater Protection contains a summary of the main model attributes and code selection criteria that serve as the basis for the demonstration of the adequacy of the STOMP© code for use in vadose zone modeling at the Hanford Site. The results of the evaluation in DOE/RL-2011-50 show that the STOMP© code is capable of meeting or exceeding the identified attributes and criteria. The comparison of the code selection criteria to the STOMP© code capabilities indicates the STOMP© code is capable of simulating all of the necessary Features, Events, and Processes, and that STOMP© meets all of the other required code selection criteria. Section 6.4.1 of DOE/RL-2011-50 addresses code selection criteria, including quality assurance documentation of verification studies for specific model attributes (e.g., unsaturated flow, solute transport, infiltration, and drainage), and includes a discussion of other code-related criteria (i.e., inter-code comparisons, hardware requirements, solution methodology, dimensionality, and output capability).

[9] Linux is a registered trademark of Linus Torvalds in the United States and in other countries.

[10] Dell™ and PowerEdge™ are trademarks of Dell Inc., Round Rock, Texas.

[11] Xeon is a registered trademark of Intel Corporation.

The results of CHPRC acceptance testing (CHPRC-00515, "STOMP Acceptance Test Report CHPRC Build 4") demonstrate that the STOMP© software is acceptable for its intended use by the CHPRC. Installations of the software are operating correctly, as demonstrated by the INTERA Linux® Cluster system producing the same results as those presented for selected problems from the STOMP© application guide (PNNL-11216, "STOMP Subsurface Transport Over Multiple Phases Application Guide") in accordance with the software test plan (CHPRC-00211, "STOMP Software Test Plan").

The methodology in this EMCF adapts STOMP© models developed in RPP-RPT-58949 to test the effect of changing the values and assignment of the hydraulic parameters to the model grid blocks within a reasonable range constrained by representative Hanford Site data. The extraction of two-dimensional models from the original three-dimensional model is done for the limited purpose of efficiently comparing effects of changes to the parameter distribution in this EMCF and is not intended as a basis by itself for further modeling; however, the two-dimensional models are a valid application subject to the usual caveats associated with two-dimensional vadose zone modeling. The validity of other aspects of the models is addressed in RPP-RPT-58949.

CHPRC-00176 requires that a "STOMP Options Analysis" be prepared and reported to identify all invoked options in a STOMP© input file and the Nuclear Quality Assurance (NQA)-1 testing status of options reported by the software vendor, Pacific Northwest National Laboratory (PNNL), to ensure that only NQA-1 qualified options of the STOMP© code are used in a quality-affecting calculation. The STOMP© Options Analysis for this EMCF is provided in Attachment 3, and indicates no unqualified options were used in this calculation.

6 CALCULATIONS

Calculations performed for the moisture content interpolation included: (a) adjustments made to the data as they were compiled for analysis, (b) statistical analysis of the compiled datasets, (c) variogram and correlogram analysis of the datasets, and (d) geostatistical estimation of moisture content to gridded node locations. Sensitivity analyses were also performed to evaluate the impact of interpreted variogram ranges and categorization of the data. The moisture content interpolation was then mapped onto the WMA C PA three-dimensional STOMP© grid and used to assign hydraulic properties to grid blocks for heterogeneous case simulations. Two-dimensional model domains were next extracted from the three-dimensional model domains. STOMP© flow and transport simulations were made for the two-dimensional cross-sections.

Simulation results were obtained and selected moisture content profiles, matric potential profiles, and contaminant breakthrough curves were compared for the heterogeneous media case and the base case models.

6.1 COMPILATION OF DATA

The moisture content data from all three sources (HEIS GPL, handheld, and the RPP-CALC-60450 datasets) were imported into tables in the Microsoft Access® 2013 database, WMAC_Moisture.accdb as listed in Attachment 1. Merging and processing of the datasets using Access® queries are described below. The table within the database titled "Moisture_Merged" represents the combined dataset prior to processing to remove replicate measurements and adjust the data for interpolation. The Excel® file 7_One_ft_Interval_Max_to_Krig.xlsx is the output of the final data processing query and the input data for the interpolation analysis. Data was copied from this file into text files formatted for use with the KT3D routine of GSLIB as specified in the user's guide (Deutsch and Journel 1998). These files are archived in EMMA along with the summary file "readme.txt".

6.1.1 Data Reduction and Conditioning

Microsoft Access® queries were used to efficiently process the datasets and are stored in the attached Access® 2013 database. The individual operations performed by the queries are routine calculator-type operations that benefit from, but do not depend on, use of Access® and that could be reproduced by other means by following the procedures described. As an alternative to inspecting the saved queries, one could verify the outcome of the operations by comparing the progressive tables in the attached spreadsheets. In this case the EMCF checker opted to check the Access® queries. The queries are named beginning with integers to help identify their place in the sequence of operations.

The first step was to calculate each measurement's nominal depth in order to handle any replicate measurements (for repeatedly-measured or closely-spaced depths). The nominal depth (taken as the nearest regular 3-in. increment) was obtained using an Access® query to multiply the depth in feet by 4, round to the nearest integer, and divide back by 4. A separate query was

used for each dataset due to differences in formatting in the source data. At the same time each query determines nominal depths, it also matches each location to the appropriate WELL_ID and other required information in the Locations table such as the reference (e.g., ground surface) elevation. Feet were converted to meters by multiplying by 0.3048. Nominal elevations were calculated by subtracting nominal depths from reference elevations. All elevations are on the NAVD88 datum. In order to calculate nominal depths for angled boreholes in the RPP-CALC-60450 dataset, vertical depths were first determined from data elevations and reference elevations. This left one data point with a negative depth, so that point was rejected in a subsequent query.

Having used the initial Access® queries to obtain nominal elevations and consistent formatting for each dataset, a second set of queries was used to create the table Moisture_Merged, excluding handheld moisture gauge data for the two drywells with NMLS data. The corresponding Excel® file is named Moisture_Merged.xlsx.

This table represents the compiled dataset prior to use of any statistics for data reduction.

A subsequent query of the table Moisture_Merged grouped data by WELL_ID, easting, northing, and nominal elevation and selected maximum values among any replicates. The next query repeats the operation except that it averages the easting values and averages the northing values for each nominal elevation and WELL_ID, because some angled boreholes had many measurements closely-spaced in a vertical sense due to shallow dip. The step is divided into two queries as a matter of good practice in the event that different data were added to the database or a revised calculation relied on something other than maximum values to handle replicates.

A final sequence of queries takes the maximum moisture for each 1-ft (0.3048-m) vertical interval for kriging and attributes the measurement to the vertical center of the interval. Four nominal depths are attributed to each 1-ft vertical interval for each WELL_ID using the Int() function in Access® (essentially equivalent to the floor operation in many programming languages) and adding 0.5 ft. A maximum is taken of the four measurements, and the center elevation of the interval is obtained by subtracting the center depth from the reference elevation. Averaging of easting and northing is repeated for angled boreholes to obtain the interval center in the x- and y- dimensions. The Excel® file 7_One_ft_Interval_Max_to_Krig.xlsx is the output of the final data processing query and the basis for the input data for the interpolation analysis.

6.2 DATASET STATISTICS

The statistics for each data set are presented in Table 6-1. The base case data set that includes the combined adjusted data has a mean of 5.55% (vol) and a median 4.90 % (vol) moisture content. The H2-Only dataset exhibits a much smaller range than the other datasets [25.64% (vol) compared to the base case range of 43.85% (vol)] but has similar mean and median values. The Handheld Only data exhibits the same range as the base case (the data are included in the base case dataset); however, the mean (4.33% vol) and the median (3.75% vol)

values for the handheld data indicate "more dry" conditions as compared to the mean (6.30% vol) and median (5.51% vol) of the dataset that excludes this data.

Table 6-1. Summary Statistics for the Moisture Content (volume %) Dataset at Waste Management Area C.

Dataset	Combined Adjusted	Combined Adjusted Dataset without Handheld	Handheld Only	H2 Unit Only
Number Samples	12,926	7,983	4,943	6,715
Minimum	0.0067	0.45	0.0067	0.68
Maximum	43.86	32.73	43.86	26.32
Range	43.85	32.28	43.85	25.64
Mean	5.55	6.30	4.33	5.08
Median	4.90	5.51	3.75	4.81
Standard Deviation	3.34	3.37	2.89	2.12

Note: See explanation within text for various datasets designated in first row.

Histograms for each dataset described in Table 6-1 are shown in Figure 4-5. A text file containing each individual dataset is archived with the model files for this EMCF in EMMA and is described in the file "readme.txt".

6.3 VARIOGRAM/CORRELOGRAM ANALYSIS

Directional variograms were constructed for each of the datasets based on Equations 2 and 3 (Figure 6-1). The parameters used for the each of the datasets are presented in Table 6-2. Relative stationarity in the empirical variograms was observed (i.e., the variograms reached a sill). Vertical anisotropy was observed within this range.

The longest range represents the primary direction of the anisotropy. For the base case interpolation, the direction of anisotropy in the horizontal direction is 35° east of north, with a dip of 1°. Note this anisotropy is observed from correlation in the soil moisture data alone. All of the vertical variograms exhibited similar sills (variances) but shorter ranges, meaning that the moisture content data show continued correlation over longer maximum distances in the horizontal direction than in the vertical direction. Such behavior is reflective of the depositional history for the sedimentary units.

Directional correlograms for each of the datasets are shown in Figure 6-2. The correlation lengths as defined for the exponential model by Freeze et al. (1990), i.e., the distances over which the autocorrelation functions decay to a value of e^{-1} (or approximately 0.37), were estimated by linearly interpolating between the two points bracketing the value of 0.37 on each correlogram. These correlation lengths are presented in Table 6-3.

Model variograms were visually fit to the empirical variograms. In the empirical variograms for the combined-adjusted dataset, the horizontal range was observed to be 85 m and the vertical range was 15 m, and these values were used for the base case. An exponential model variogram was used for both the horizontal and vertical variograms. A description of the variograms is given in Table 6-4 below.

6.4 GEOSTATISTICAL ESTIMATION

Each of the datasets was used to estimate moisture content values for the gridded nodes. Example selections of the output for the base case results using horizontal and vertical ranges of 85 m and 15 m, respectively, are drawn on cross-sections presented in Figures 6-3 through 6-10. The location of each line of section is shown on the base map (Figure 1-1) for reference. The output was also contoured using binned values that represent the range of moisture content by volume for representative sediment type moisture characteristic curves (WHC-EP-0883, "Variability and Scaling of Hydraulic Properties for 200 Area Soils, Hanford Site"). The base case output using these binned contours is also shown on the figures. For comparison and review, each of the cross-sections shows the approximate elevations of the lithologic units represented in the STOMP© model (RPP-RPT-58949) including the backfill, Hanford H1, and Hanford H2. Figure 6-10 shows the three-dimensional intersection of these surfaces with the cross-section selected from the kriging grid. The output was contoured using a continuous contour from 2.0 to 15.0 % moisture content by volume to observe the range of heterogeneity of the kriged values.

6.5 SENSITIVITY ANALYSES

Following the base case estimates, sensitivity analyses were performed using representative variogram range endpoints (see Table 6-4), and selected subsets of the data that excluded the handheld data measurements or confined the data used to the H2 unit. Figure 6-11 shows a picture "grid" of the contours of a selected cross-section from the kriging to compare with the base case the effects of selecting minimum and maximum ranges on the moisture content interpolation. Similarly, Figure 6-12 shows the range of endpoint minimum, maximum, and base case range combinations of estimated moisture contents with the binned contour intervals based on the soil moisture characteristics for comparison.

A sensitivity analysis for the handheld data showed the variability in properties when compared to the complete (Combined Adjusted) dataset. Figure 4-5 shows the histogram for the handheld data, and the dataset without the handheld data. Similarly, Table 6-1 shows a comparison of the dataset statistics for both the handheld data and the dataset without the handheld data to the original base case (Combined Adjusted) dataset. A comparison to the base case of the interpolations performed without the handheld data is shown in Figure 6-13. Two different interpolations were performed; one based on the variogram ranges established for the combined adjusted dataset and one based on the ranges estimated from the trimmed dataset without the handheld data (see the variograms in Figure 6-1).

Figure 6-1. Horizontal and Vertical Variograms for Moisture Content Datasets with Model Variograms Fit to Empirical Variograms Using Indicated Values of Range.

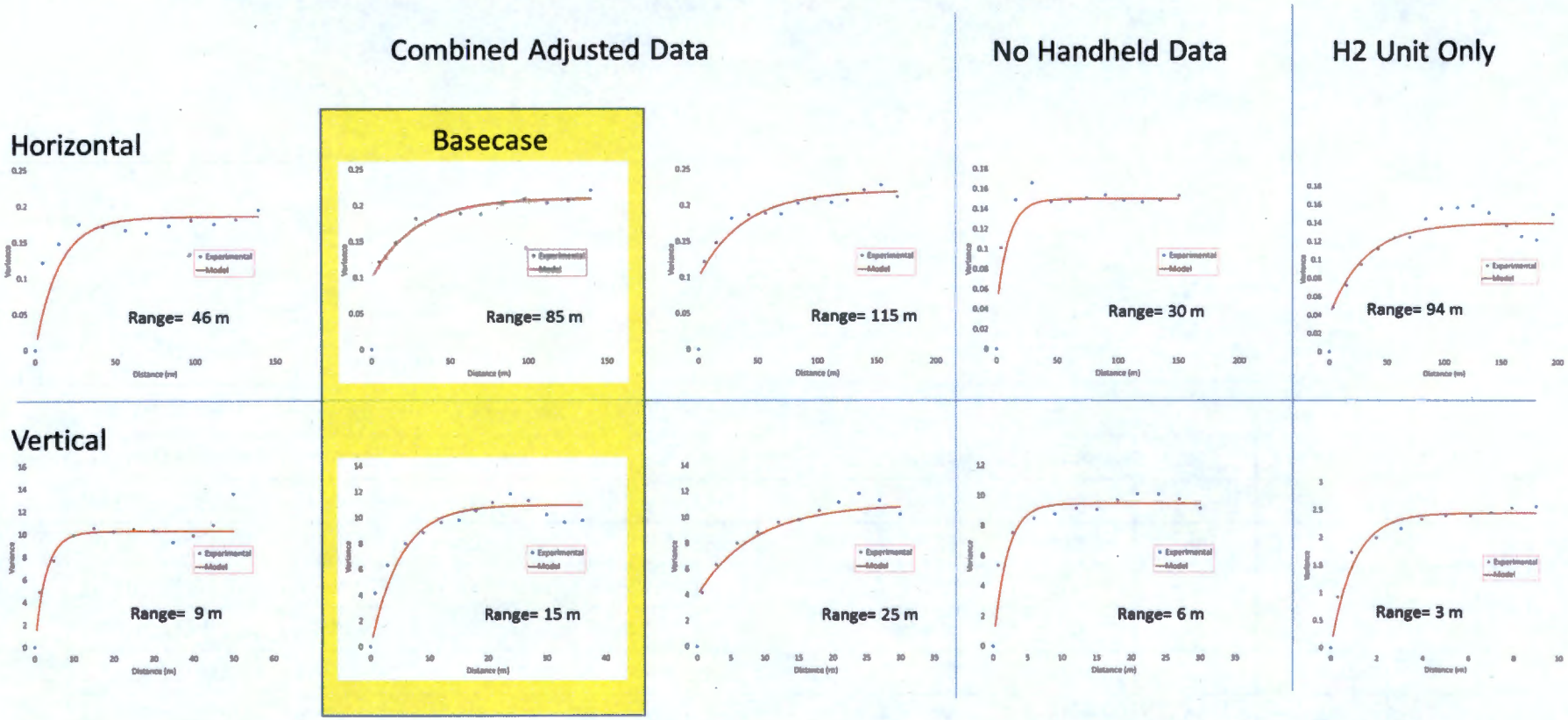

Table 6-2. Empirical Variogram Parameters for Different Datasets.

Dataset	Variogram Type	Lag Distance (m)	Lag Tolerance (m)	Number of Lags	Azimuth Angle (degrees)	Azimuth Tolerance (degrees)	Azimuth Bandwith (m)	Dip Angle (degrees)	Dip Tolerance (degrees)	Dip Bandwidth (m)
Combined Dataset	Horizontal	14	7	12	35	60	1000	1	30	30
Combined Dataset	Vertical	3	1.5	12	35	60	1000	90	30	10
Handheld Data Only	Horizontal	10	5	10	35	60	1000	0	30	10
Handheld Data Only	Vertical	2	1	10	35	30	10	90	30	10
No Handheld Data	Horizontal	15	7.5	10	35	60	1000	1	90	50
No Handheld Data	Vertical	3	1.5	10	0	30	10	90	30	10
H2 Data Only	Horizontal	14	7	14	35	60	90	1	90	90
H2 Data Only	Vertical	1	0.5	9	35	60	90	90	10	15

Note: See explanation within text for various datasets designated in first column.

Sensitivity analyses for only the moisture content of the H2 unit were also performed. Points from the Combined Adjusted were excluded based on H2 upper and lower contact elevations as defined in the STOMP© model. The z-discretization of the model grid was also adjusted based on these contact elevations. New variography was developed for the trimmed dataset (Figure 6-1), and the resulting model variograms were used to perform additional kriging to the adjusted model grid. Cross-sections comparing the interpolation results of the H2-only results to the base case results are shown in Figure 6-14.

6.6 DEVELOPMENT OF TWO-DIMENSIONAL SUBSURFACE TRANSPORT OVER MULTIPLE PHASES MODELS

6.6.1 Base Case Two-Dimensional Models

From the WMA C PA base case three-dimensional model, two-dimensional STOMP© models were extracted for three different cross-sections. Figure 6-15 presents the locations of the selected cross-sections and the compiled moisture content data locations in a plan view of the WMA C PA model domain. The WMA C PA model domain is larger than the tank farm vicinity where interpolation was supported by moisture content data. The cross-sections were selected to be in similar locations to cross-section B-B' and cross-section C-C' of the moisture content interpolation (Figure 1-1). Two directions were chosen to be parallel or orthogonal to groundwater flow. Cross-Section 1 passes near the general location of tank 241-C-105 (C-105) and it intercepts the borehole C4297, whereas Cross-Section 2 is outside the tank area and intercepts the general location of UPR-86 near its intersection with Cross-Section 3. Cross-Section 3 is orthogonal to the other cross-sections (to examine heterogeneity in an orthogonal dimension) and it also passes near the general location of tank C-105 and intercepts the general location of UPR-86.

The two-dimensional models representing the base case were developed by the following steps.

1. The three-dimensional STOMP© model grid was exported into Tecplot 360®.

2. For Cross-Section 1, J = 46 (Y direction node index for STOMP© model) was selected to create an X-Z model grid. The geologic properties and the flow and transport properties were kept the same as in the original three-dimensional model.

3. Similarly for Cross-Section 2, J = 33 was selected to create an X-Z model grid, keeping the geologic properties and flow and transport properties the same as in the original three-dimensional model.

4. Similarly for Cross-Section 3, I = 46 (X direction node index for STOMP© model) was selected to create a Y-Z model grid, keeping the geologic properties and flow and transport properties the same as in the original three-dimensional model.

Figure 6-2. Horizontal and Vertical Correlograms for Waste Management Area C Moisture Content Datasets.

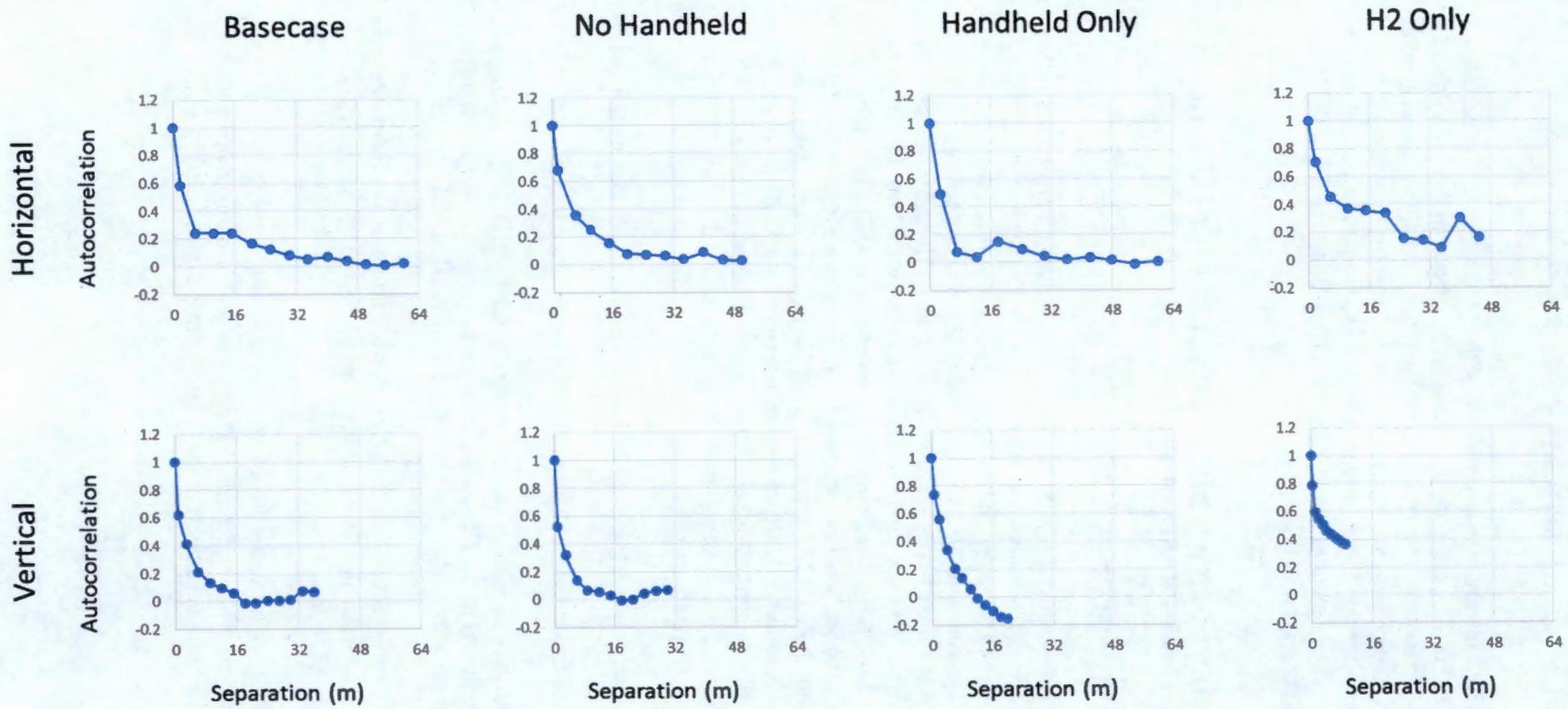

Table 6-3. Correlation Lengths for Different Moisture Content Datasets.

Dataset	Correlogram Type	Lag Distance (m)	Correlation Length (m)
Combined Dataset	Horizontal	5	4.2
Combined Dataset	Vertical	3	3.6
Handheld Data Only	Horizontal	6	4.0
Handheld Data Only	Vertical	2	3.7
No Handheld Data	Horizontal	5	5.9
No Handheld Data	Vertical	3	2.4
H2 Data Only	Horizontal	1	10.0
H2 Data Only	Vertical	1	8.7

Note: See explanation within text for various datasets designated in first column.

Table 6-4. Model Variogram Parameters for Different Moisture Datasets.

Dataset	Horizontal Sill	Horizontal Range (m)	Vertical Sill	Vertical Range (m)
Combined Adjusted (Base Case Parameters)	11.0	85.0	11.0	15
Combined Adjusted (Minimum Ranges)	11.0	45.0	11.0	9.0
Combined Adjusted (Maximum Ranges)	11.0	115.0	11.0	25.0
No Handheld Data	9.5	30.0	9.5	6.0
H2 Data Only	4.5	94.0	2.45	3.0

Notes:
See explanation within text for various datasets designated in first column.
The horizontal sills (variances) have been converted from the relative values depicted on the pairwise relative semivariograms shown in Figure 6-1.

Figure 6-3. Cross-Section A-A' with Continuous Contours for Moisture Content (vol %) Interpolation.

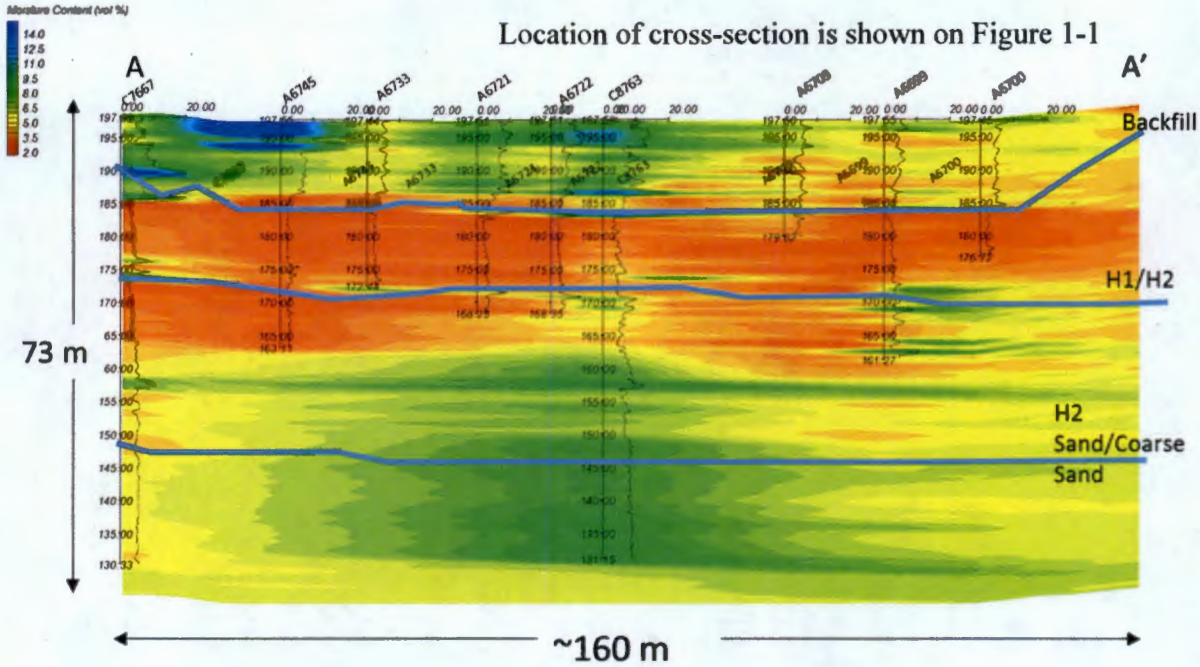

Figure 6-4. Cross-Section A-A' with Binned Contours for Moisture Content (vol %) Interpolation.

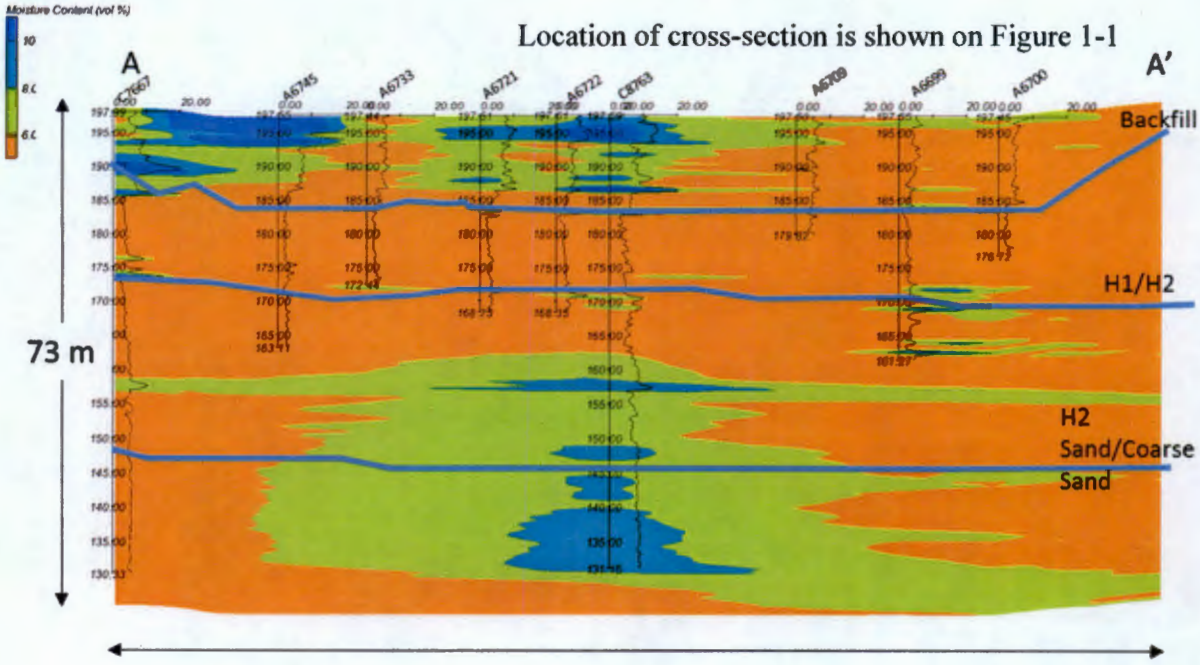

Figure 6-5. Cross-Section B-B' with Continuous Contours for Moisture Content (vol %) Interpolation.

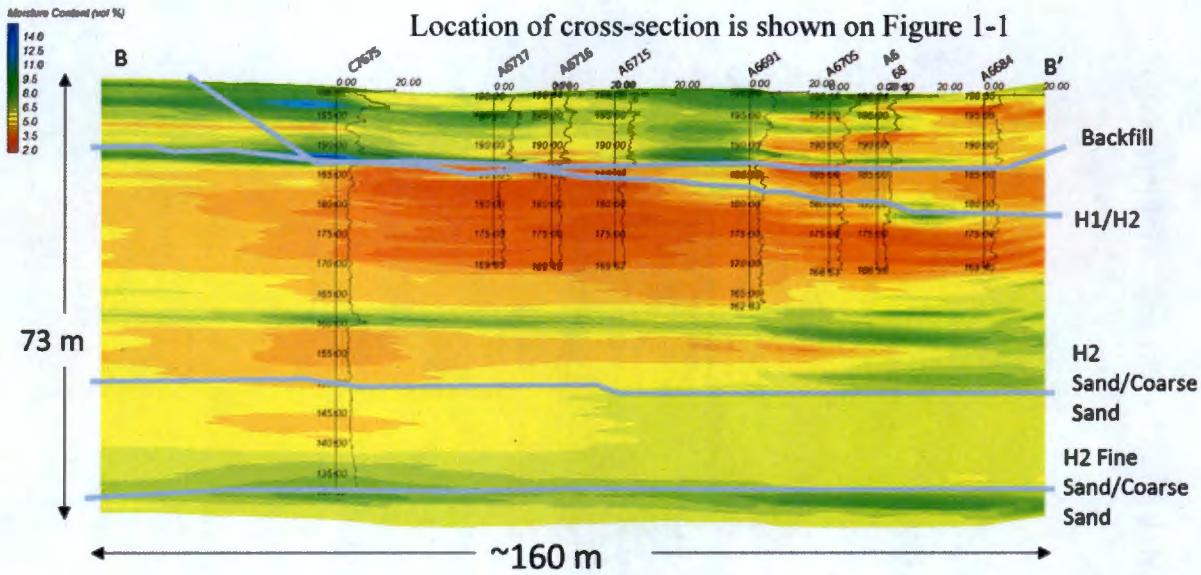

Figure 6-6. Cross-Section B-B' with Binned Contours for Moisture Content (vol %) Interpolation.

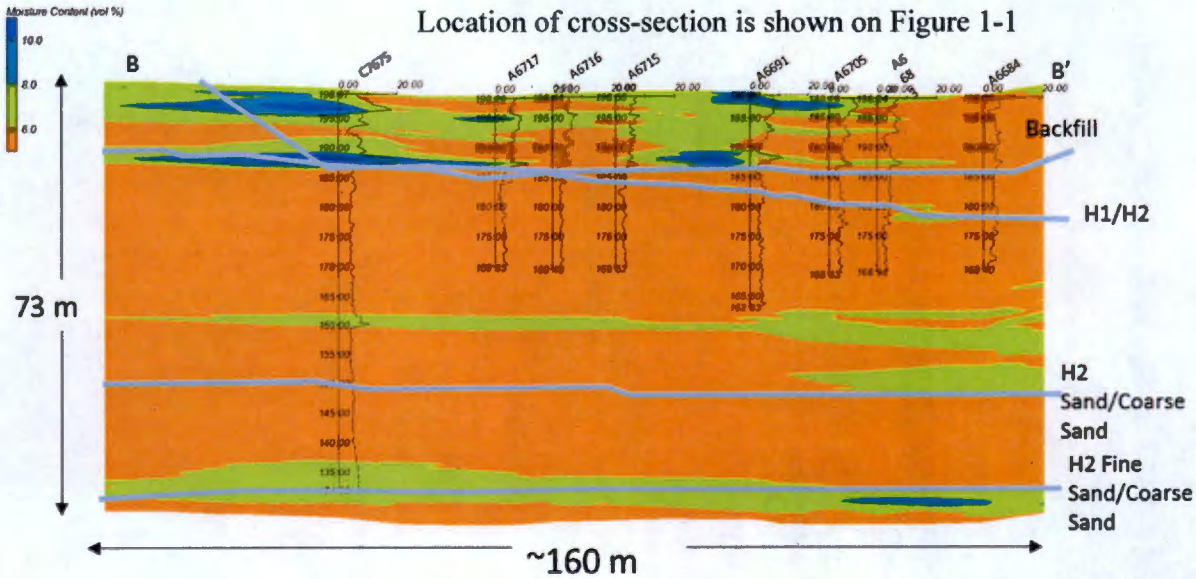

Figure 6-7. Cross-Section C-C' with Continuous Contours for Moisture Content (vol %) Interpolation.

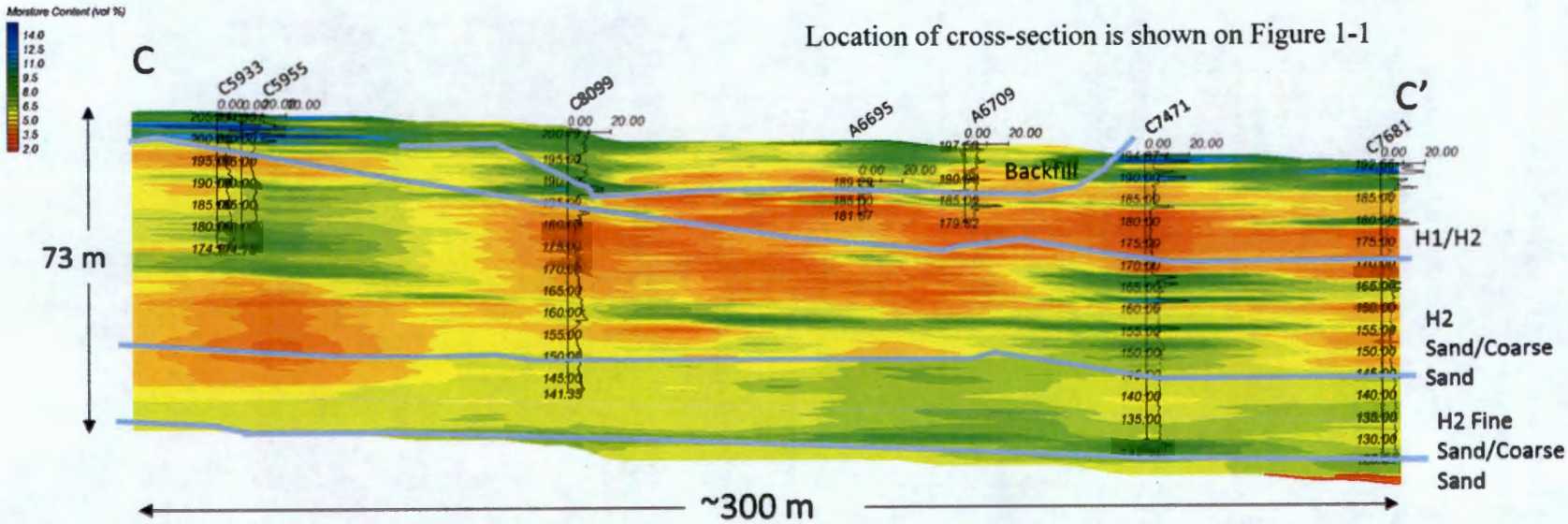

Figure 6-8. Cross-Section C-C' with Binned Contours for Moisture Content (vol %) Interpolation.

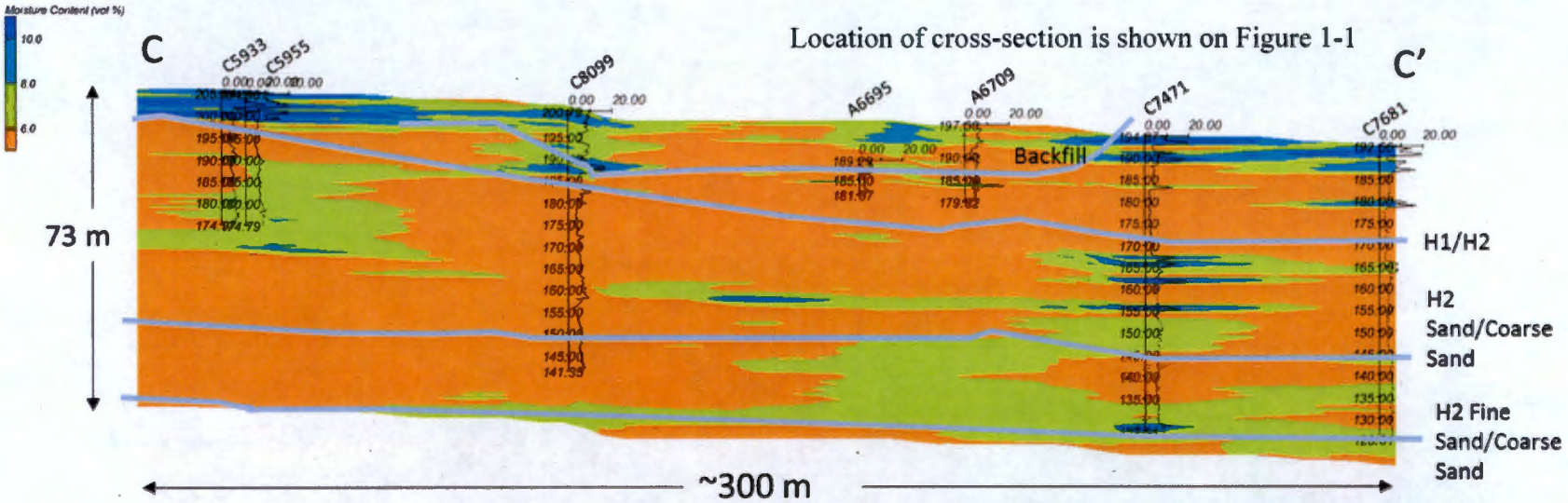

Figure 6-9. Cross-Section D-D' with Binned Contours for Moisture Content (vol %) Interpolation.

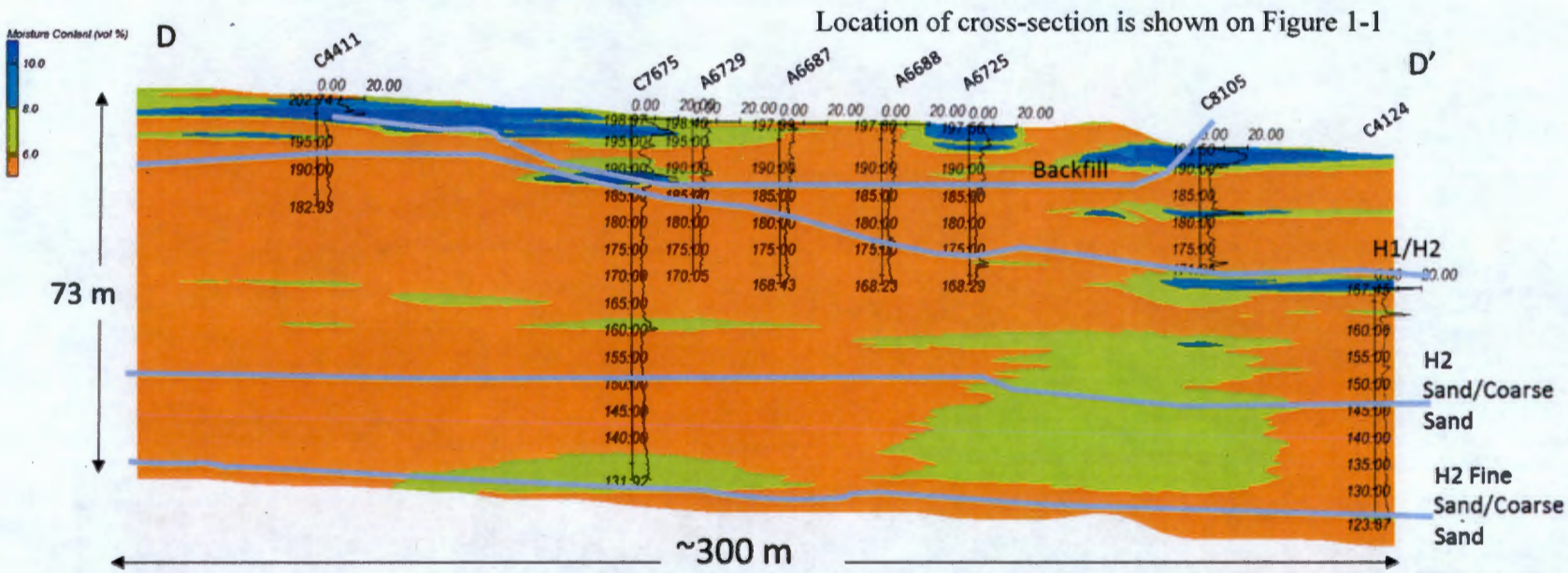

Figure 6-10. Fence Diagram with Moisture Content (vol %) Data Interpolation Showing Approximate Elevations of Hydrogeologic Contacts.

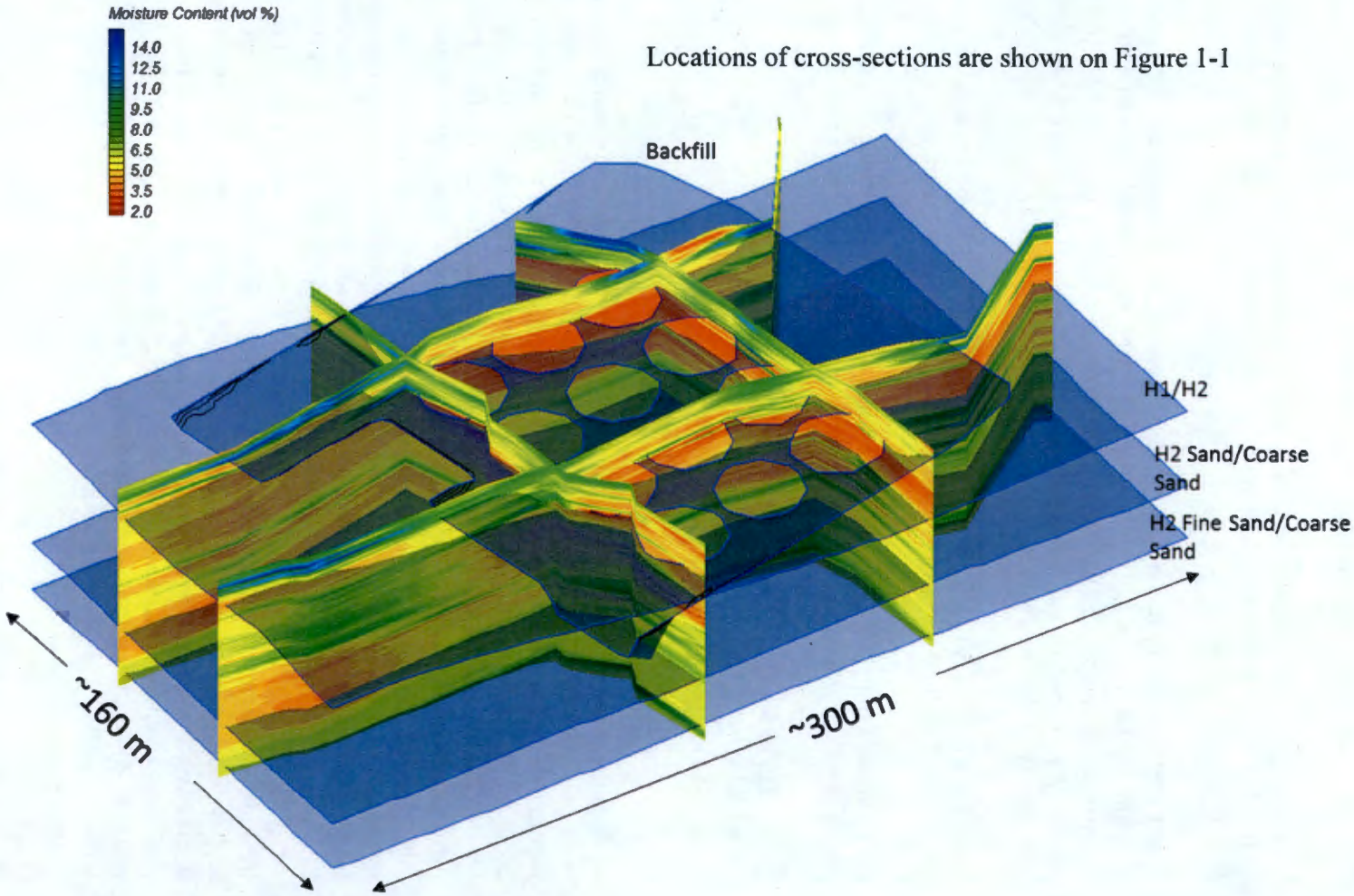

6.6.2 Heterogeneous Case Two-Dimensional Models

For each cross-section, a heterogeneous case two-dimensional STOMP© model was developed using interpolated moisture values to assign one of four new sets of hydraulic properties to each grid node as described below.

1. Using the linear interpolation technique in Tecplot®, the moisture content values from the moisture model were mapped to the three-dimensional STOMP© model grid. A satisfactory mapping of the moisture content interpolation onto the STOMP© grids was ascertained by visually comparing the moisture content distributions before and after mapping as well as by checking values for random locations.

2. The STOMP© rock/soil zonation number for each grid block on each of the two-dimensional cross-sections was printed out along with the moisture content value.

3. Four bands of moisture values were specified to group the continuous range of interpolated moisture values into a discrete set used to declare new rock/soil zones:

   - 2% to 6% (vol.) moisture content zone
   - 6% to 8% (vol.) moisture content zone
   - 8% to 10% (vol.) moisture content zone
   - >10% (vol.) moisture content zone.

   Hydraulic parameters for the new moisture content-based rock/soil zones were selected from four samples out of the 44 IDF samples described in Section 4 (Table 6-5 and Figure 6-16). The four samples were selected such that under a unit hydraulic gradient condition the sample hydraulic parameters yield moisture contents within the specified bands. The WMA C PA base case model uses a recharge rate of 3.5 mm/yr for the natural background condition and long-term recharge rates and applies annual average rates of up to 63 mm/yr during the site operational period for areas in WMA C where the natural ground surface and vegetation were disturbed and/or anthropogenic discharges of water occurred (RPP-RPT-58949). These rates provide bounds on the unsaturated hydraulic conductivity for each sample under a unit gradient condition, which in turn constrains the matric potential to a small enough range so as to select samples that match the moisture content bands. Figure 6-16 shows the unsaturated hydraulic conductivity and moisture retention curves for the four selected samples. Table 6-5 summarizes the hydraulic properties of the samples used for the new rock/soil zones. Whereas moisture-dependent anisotropy (RPP-RPT-58949, Appendix B) was invoked for the base case two-dimensional simulations, it was not applied for the heterogeneous case models since the geologic layers were discretized at a much finer scale compared with the much coarser representation of the base case EHM model.

   Base case values for the H2 unit of 200 cm for longitudinal dispersivity and 20 cm for transverse dispersivity were assumed in each of the new moisture content-based rock/soil zones.

Figure 6-11. Moisture Content (vol %) Interpolations Using Base Case Ranges (Middle Figures) Compared to Minimum (Upper Figures) and Maximum (Lower Figures) Ranges (Cross-Section C-C').

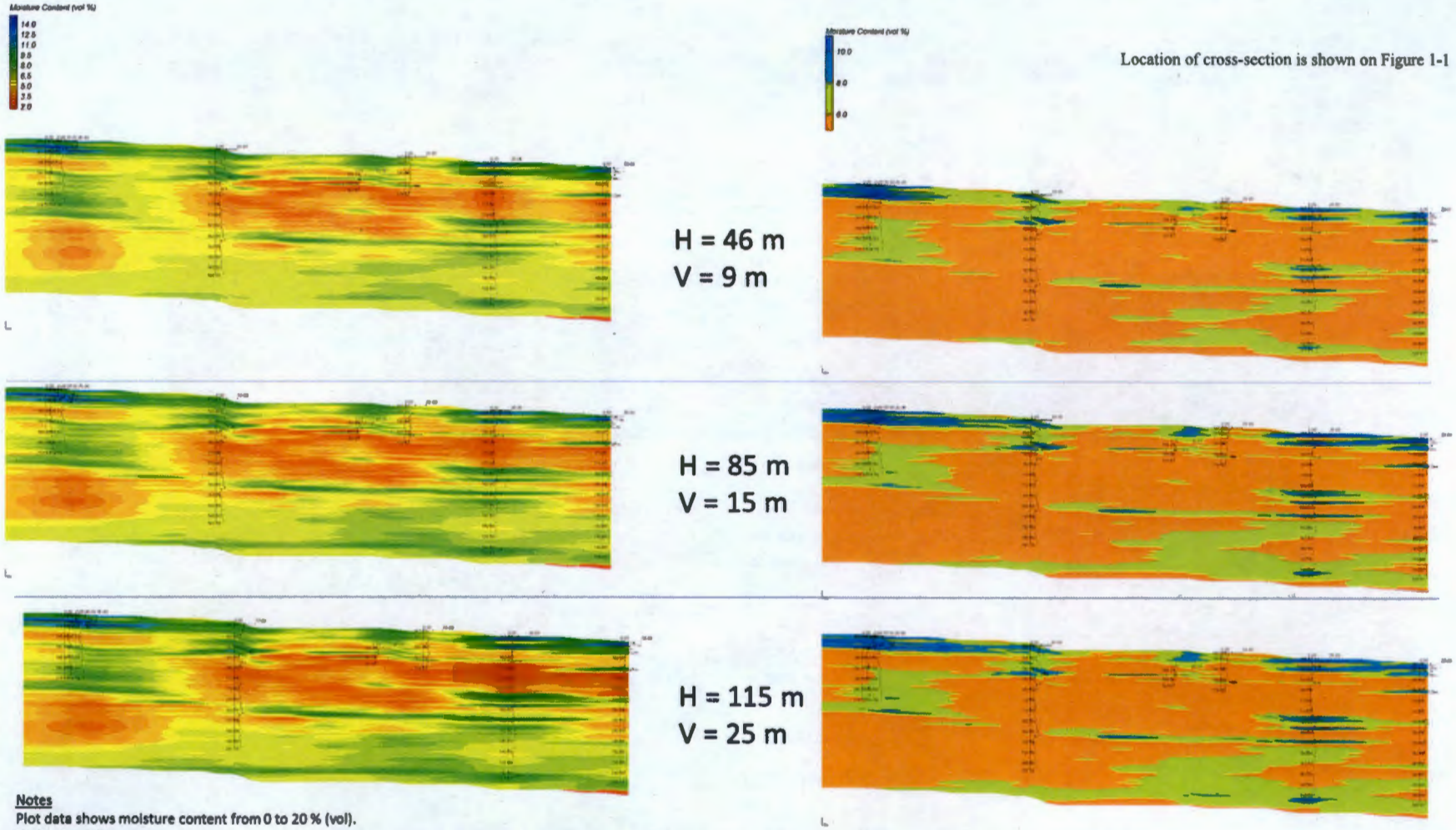

Notes
Plot data shows moisture content from 0 to 20 % (vol).
H: Horizontal range
V: Vertical range

Figure 6-12. Moisture Content (vol %) Interpolations Showing Sensitivity to Range (Cross-Section A-A').

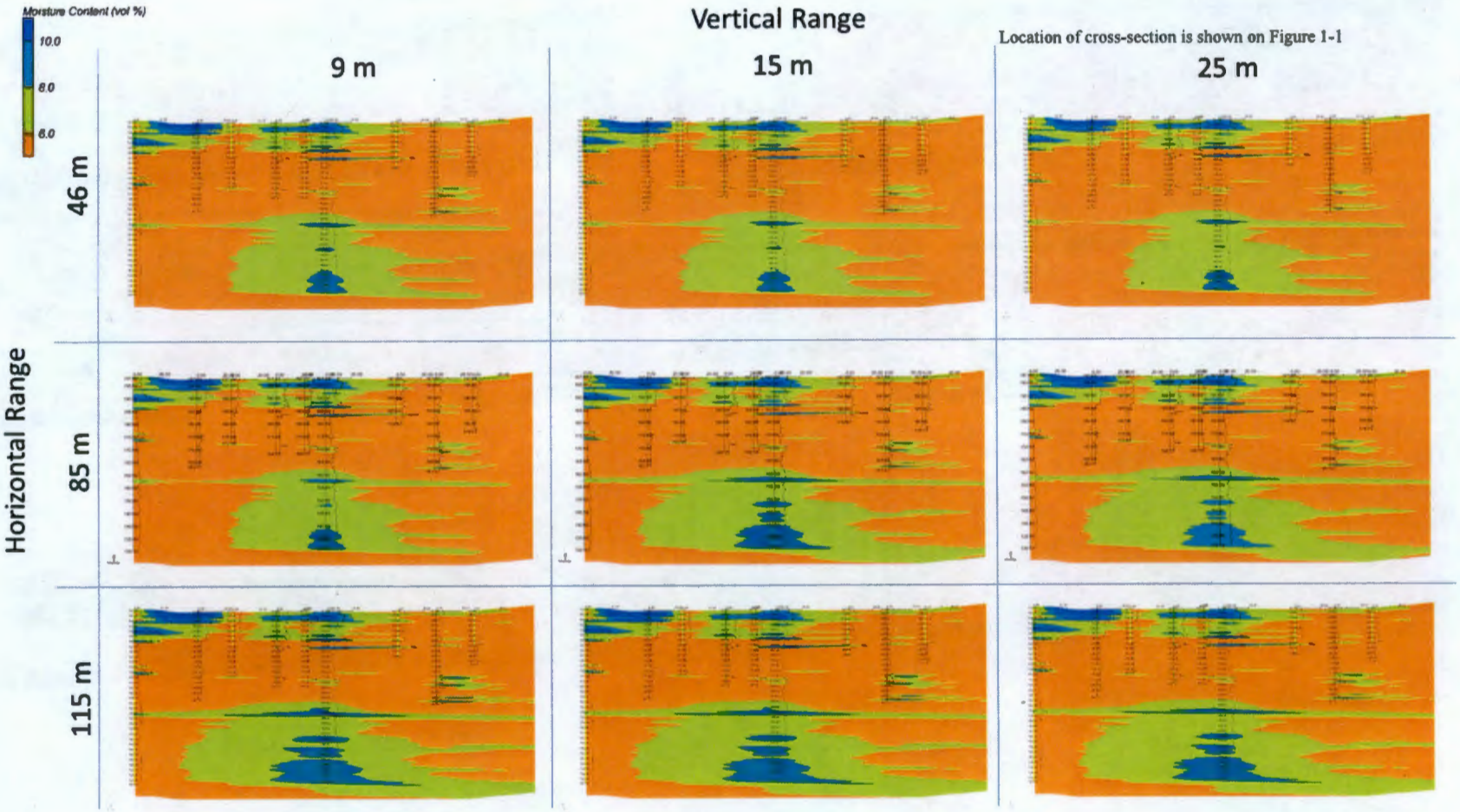

Location of cross-section is shown on Figure 1-1

Notes
Plot data shows moisture content from 0 to 20 % (vol).
H: Horizontal range
V: Vertical range

Figure 6-13. Base Case versus Exclusion of Handheld Data (Cross-Section C-C').

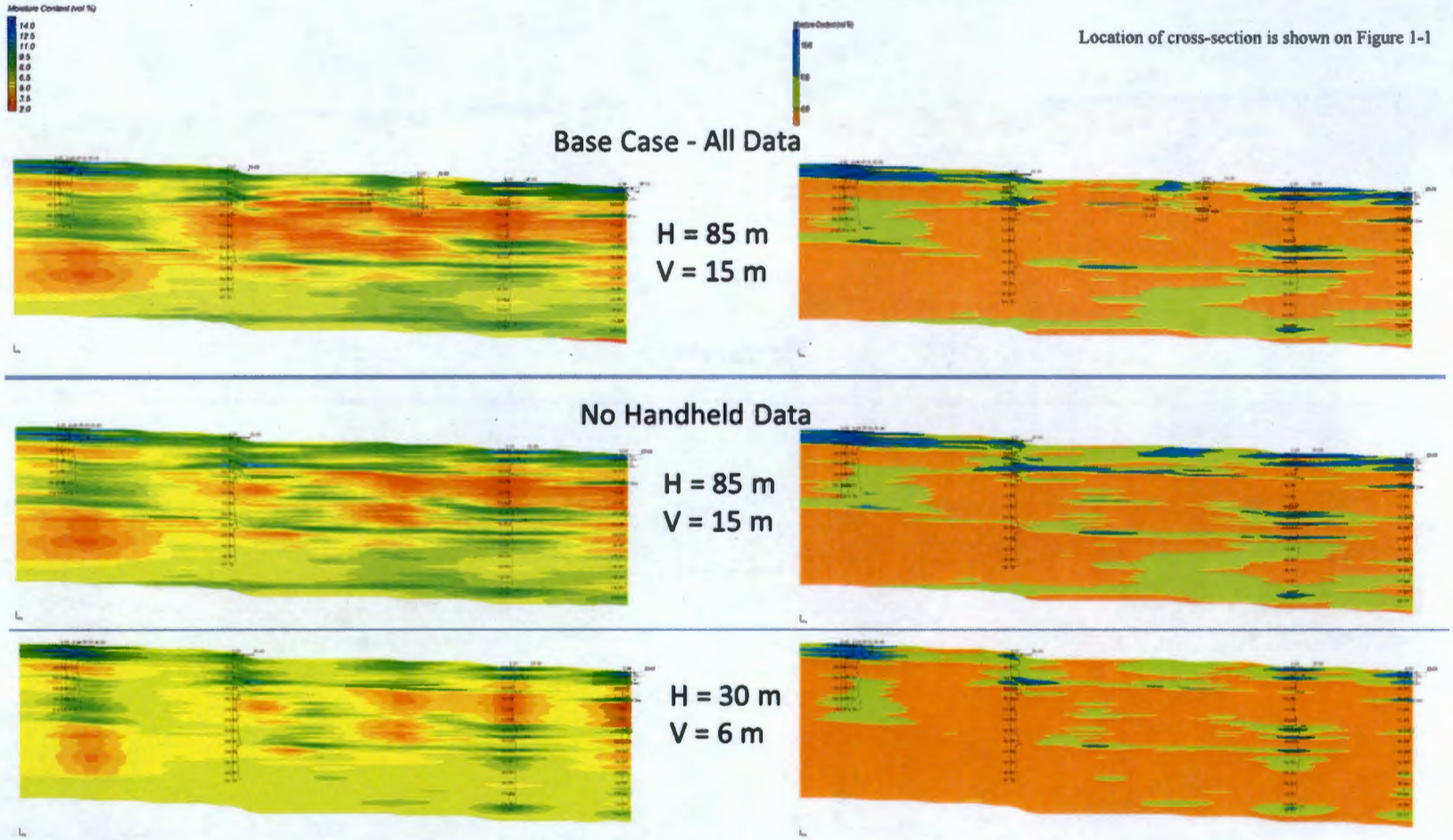

Notes
Plot data shows moisture content from 0 to 20 % (vol).
H: Horizontal range
V: Vertical range

Figure 6-14. Base Case versus Samples from H2 Interval Only (Cross-Section C-C').

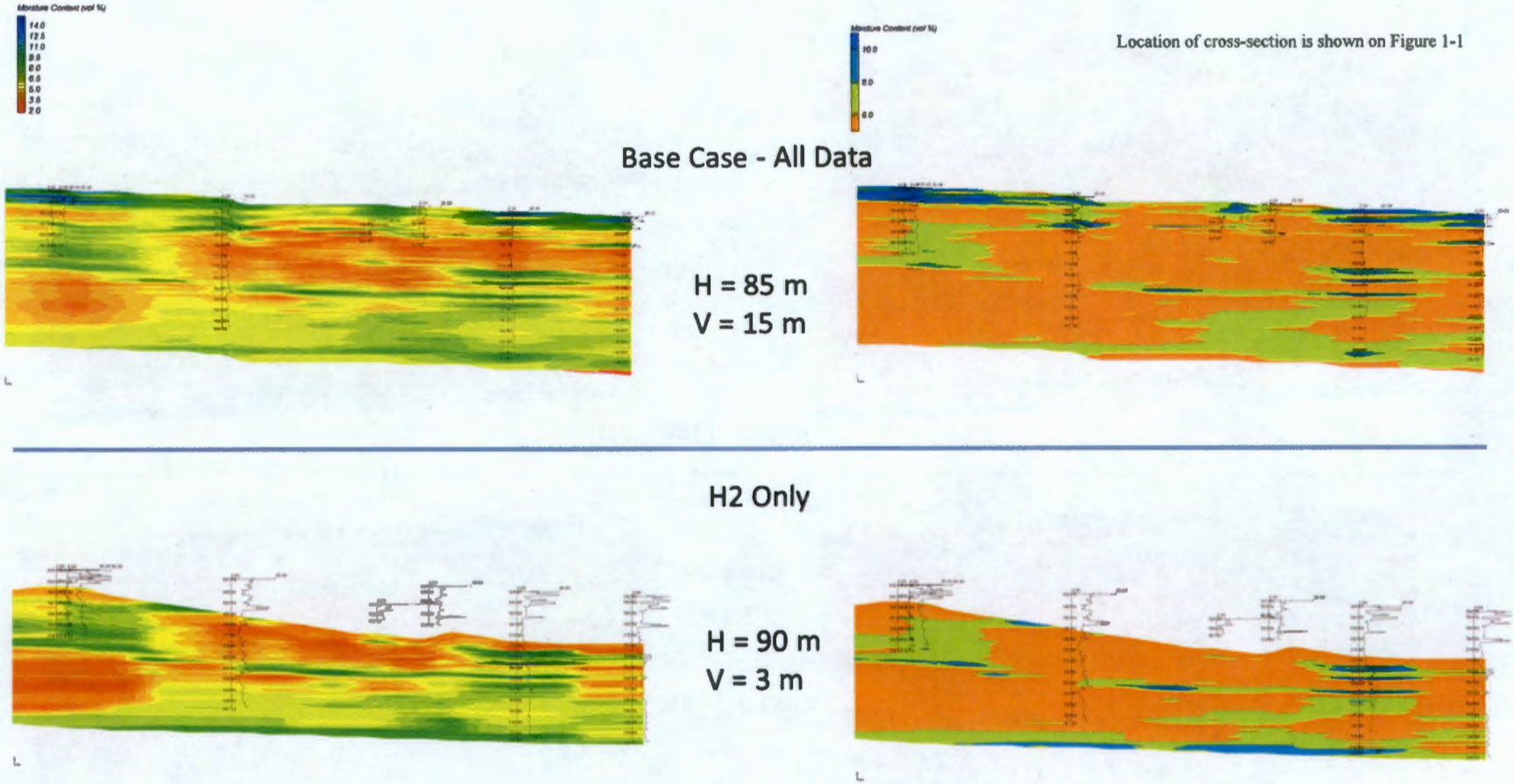

Notes
Plot data shows moisture content from 0 to 20 % (vol).
H: Horizontal range
V: Vertical range

Figure 6-15. Location of Selected Cross-Sections for the Two-Dimensional Models.

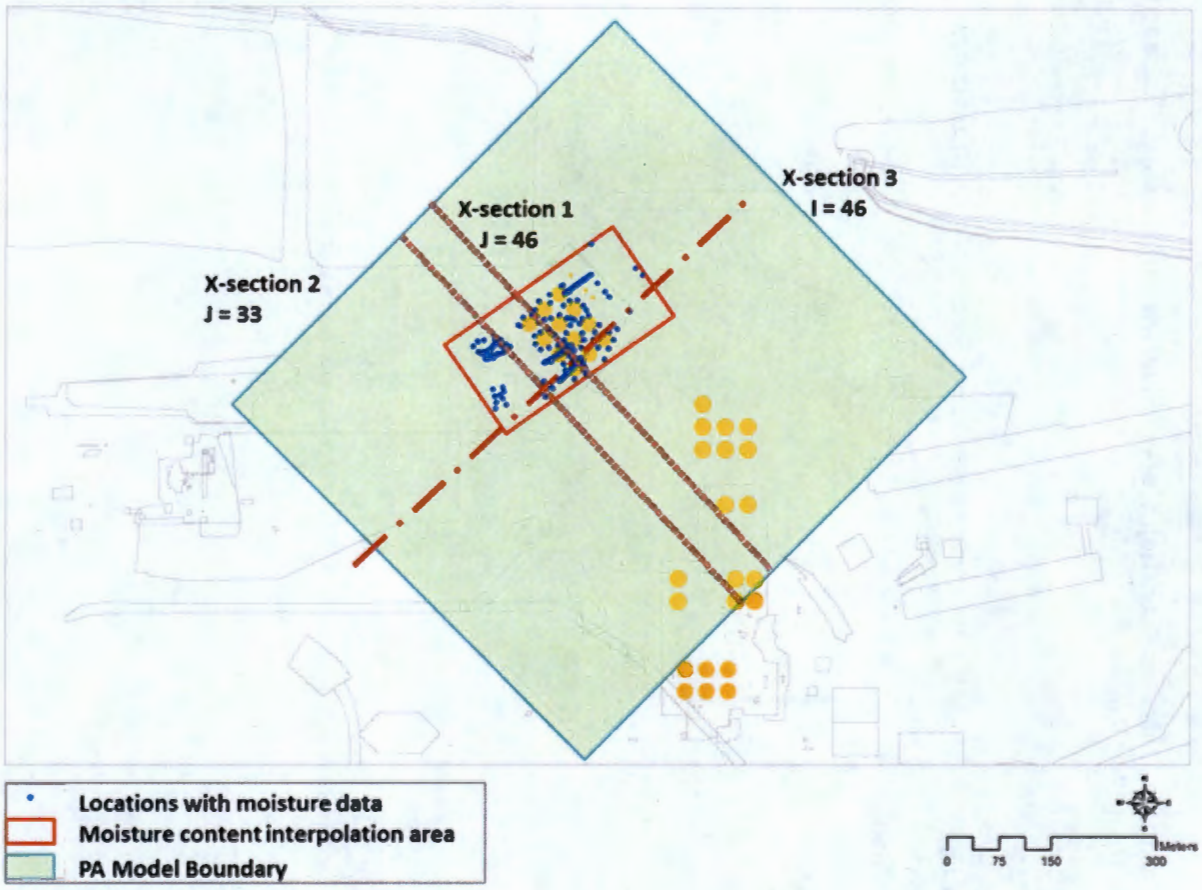

PA = performance assessment

Table 6-5. Vadose Zone Hydraulic Properties for Moisture Content-Based Rock/Soil Zones.

Sample ID (Moisture Content-Based Rock/Soil Zone)	θ_s, Saturated Water Content	θ_r, Residual Water Content	α, van Genuchten Alpha (1/cm)	n, van Genuchten n	ℓ, Pore Connectivity Factor	K_s, Fitted Saturated Conductivity (cm/s)
25A (2%-6%)	0.345	0.0267	0.0842	2.158	0.5	5.40E-03
45U (6%-8%)	0.385	0.0050	0.0880	1.664	0.5	3.24E-02
261L (8%-10%)	0.390	0.0450	0.0191	2.485	0.5	5.54E-04
31A (>10%)	0.418	0.0444	0.0058	2.012	0.5	8.21E-04

Source: RPP-RPT-58949, "Model Package Report Flow and Contaminant Transport Numerical Model used in WMA C Performance Assessment and RCRA Closure Analysis," Appendix B.
Note: First column lists individual sample ID followed by rock/soil zone based on moisture content bands in units of percent on a volumetric basis.

Figure 6-16. (a) Unsaturated Hydraulic Conductivity and (b) Moisture Retention Curves Selected for Moisture Content-Based Rock/Soil Zones.

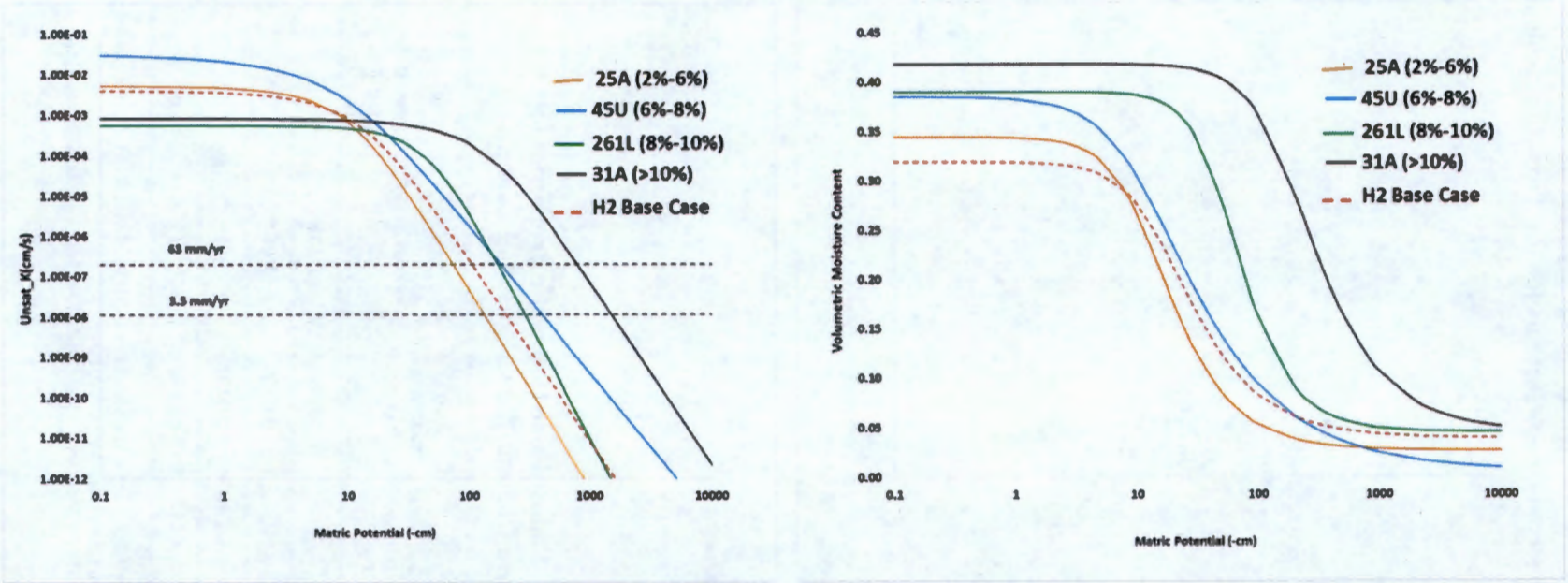

(a) (b)

Note: Individual sample numbers are indicated preceding the moisture cutoff ranges.
Source: RPP-RPT-58949, "Model Package Report Flow and Contaminant Transport Numerical Model used in WMA C Performance Assessment and RCRA Closure Analysis," Appendix B.

4. For the heterogeneous case, new rock/soil zonation assignments were overwritten for grid blocks according to their interpolated moisture values. Base case rock/soil zonation assignments were retained outside the region of the moisture interpolation, so the heterogeneous case models have 9 different rock/soil zones:

    - 2% to 6% (vol.) moisture content zone
    - 6% to 8% (vol.) moisture content zone
    - 8% to 10% (vol.) moisture content zone
    - >10% (vol.) moisture content zone
    - Backfill
    - H1 Unit
    - H2 Unit
    - H3 Unit
    - Aquifer.

Figures 6-17, 6-18 and 6-19 show the geologic representation of the EHM-based base case model and moisture content-based heterogeneous case model for the selected cross sections.

6.6.3 Boundary and Initial Conditions

For both the base case and heterogeneous case simulations for each two-dimensional cross-section model, a 3.5 mm/yr recharge rate, corresponding to the long-term rate for the WMA C PA three-dimensional base case model throughout the majority of the 10,000-year post-closure analysis period, was applied throughout the simulation duration. For Cross-Sections 1 and 2, aquifer boundary conditions were taken directly from the appropriate nodes of the WMA C PA three-dimensional base case model to simulate groundwater fluxes consistent with the PA base case. Cross-Sections 1 and 2 are aligned parallel to groundwater flow, and Cross-Section 3 is aligned orthogonal to real-world groundwater flow. For Cross-Section 3, boundary conditions were selected to match the aquifer flux of the other cross-sections (the purpose of this simulation is to test the effect of vadose zone heterogeneity in the orthogonal dimension). Initial conditions for the forward simulations were established as in the WMA C PA three-dimensional base case model by running the model for a 3,000-year historical simulation period until calendar year 1945.5, then running the cross-sectional models with base case or heterogeneous case properties until calendar year 2020. No contaminants are simulated to be present in the historical simulation period or at the beginning of the forward simulations; as noted in Section 6.6.4, the simulations in this EMCF compare results of the base case and heterogeneous case for a hypothetical source and are not intended to quantify impacts for actual sources at WMA C.

6.6.4 Contaminant Source and Model Output Point of Calculation

For both the base case and heterogeneous case, simulations for each two-dimensional cross-section model, a hypothetical source with a concentration (in bulk volume) of 1,000 pCi/m^3 of ^{99}Tc was instantly injected at calendar year 2020 along a line of nodes with a total length of 22.8 m. The simulations lasted until calendar year 3020. The nodes had 1 m height, so for each 1 m in the direction normal to the plane of the cross-section, the hypothetical

source injection was equivalent to a total of 22,800 pCi over a 22.8 m^2 area. Because the objective was to compare the heterogeneous case and base case, the magnitude of the initial injected concentration is not important. As in the PA simulations in RPP-RPT-58949, the input properties of ^{99}Tc included a half-life of 213,000 years, a distribution coefficient (K_d) of zero for all geologic media, and a diffusion coefficient of 2.5×10^{-5} cm^2/s.

Figure 6-20 shows the location of the source and the point of calculation for Cross-Section 1. The horizontal location of the source within Cross-Section 1 is arbitrarily chosen to be in the center of the area that had interpolated moisture data, which approximately corresponds to tank C-105. In the heterogeneous case, the source location overlies one of the more prominent heterogeneities within the H2 sand. The vertical location of the contaminant mass is positioned 68 m above the water table, which corresponds to the base of the tank farm excavation. The simulated concentrations were recorded at a point of calculation 100 m downgradient from the source location. The same rules were applied for Cross-Sections 2 and 3, with an arbitrary horizontal location of the source within the cross-section, and with flow artificially aligned to the cross-section for Cross-Section 3 as stated in Section 6.6.3. Again, the arbitrary horizontal locations were in the center of the area that had interpolated moisture data. Similar to Cross-Section 1, Cross-Section 3 had a source location that was near tank C-105 and overlying multiple heterogeneities (which occurred to a greater degree in the dimension orthogonal to groundwater flow). The source location in Cross-Section 2 was near UPR-86 overlying a relatively homogeneous region of the vadose zone, although some heterogeneities occurred above the source and to the side of it in deeper soils. Thus, the simulations for all the cross-sections as a group cover a range of conditions by which to explore the effects of heterogeneities underlying sources as well as heterogeneities that affect the flow field around releases over relatively homogeneous coarse soils. Results for a given cross-section would differ somewhat if different source locations were assumed.

Figure 6-17. Cross-Section 1 (Northwest to Southeast).

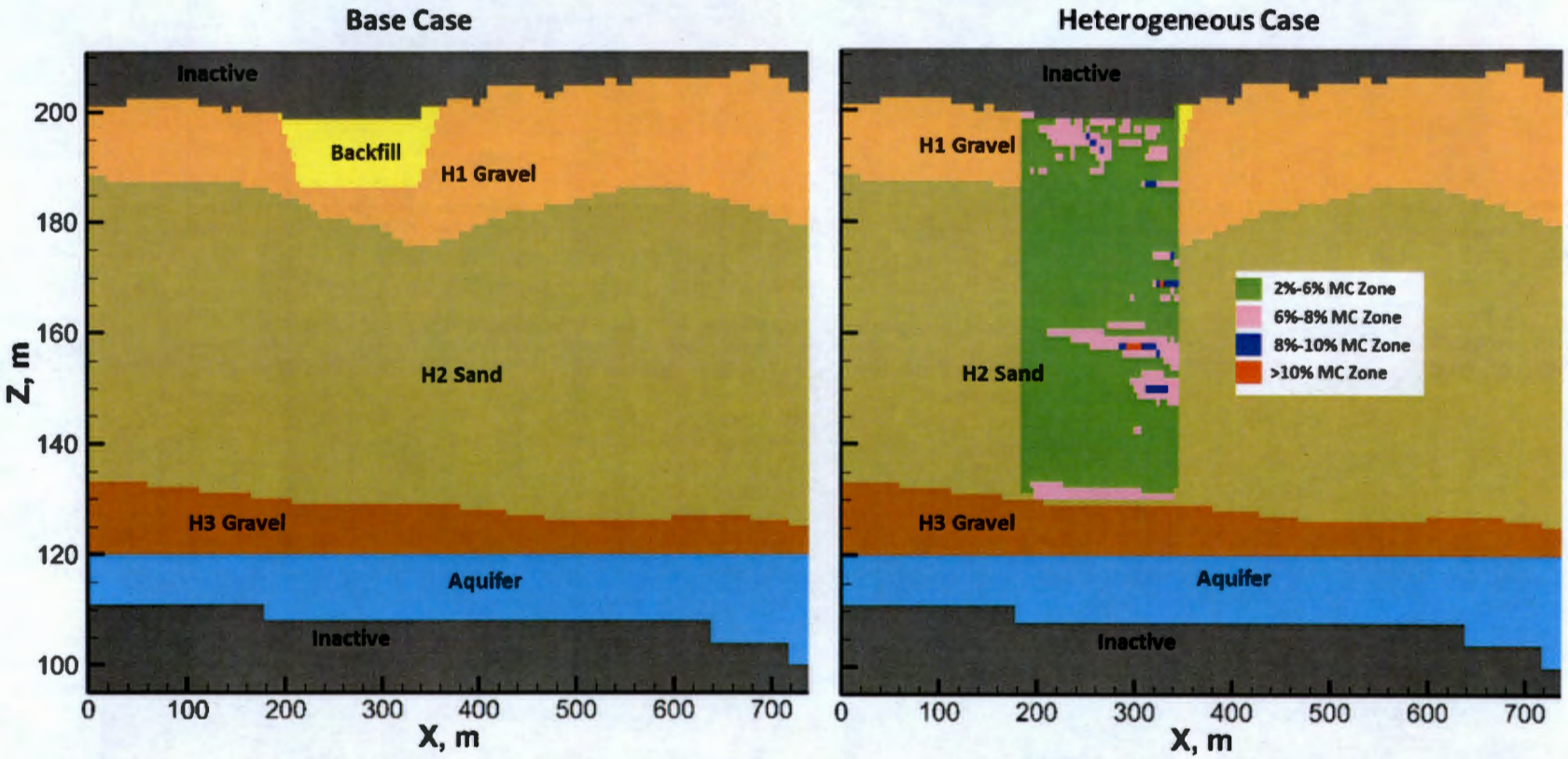

Figure 6-18. Cross-Section 2 (Northwest to Southeast).

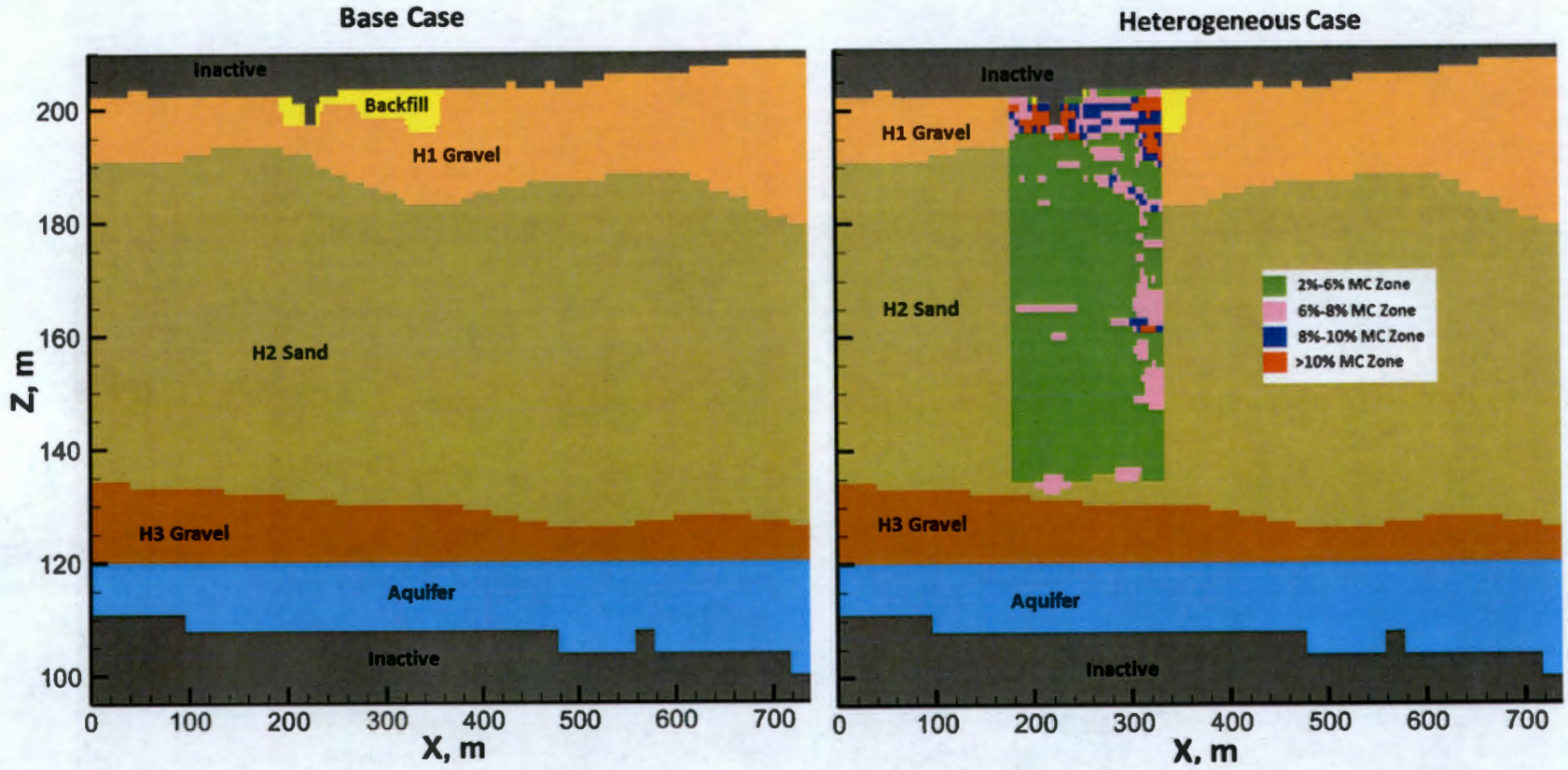

Figure 6-19. Cross-Section 3 (Southwest to Northeast).

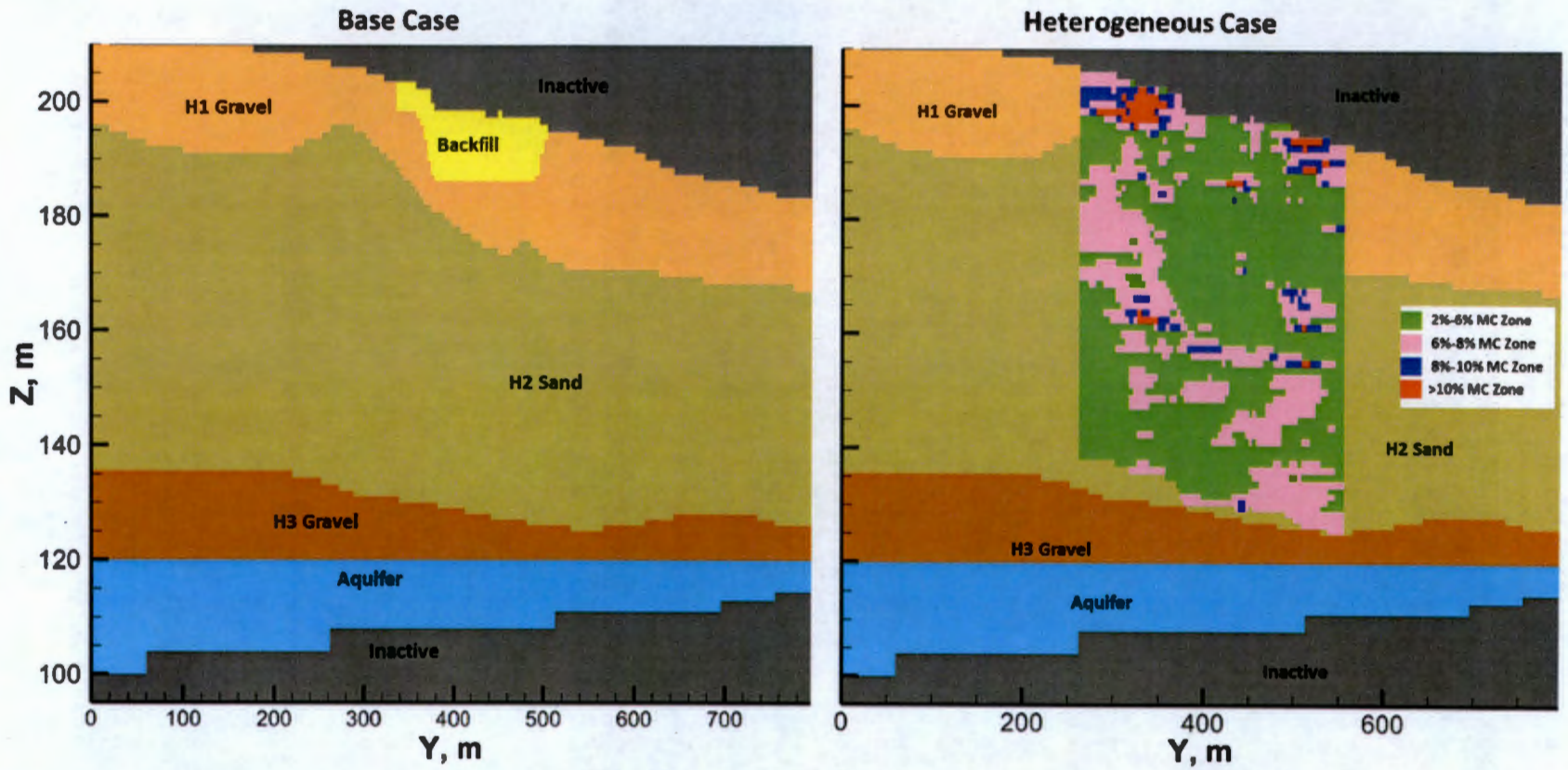

Figure 6-20. Location of Contaminant Source and Point of Calculation.

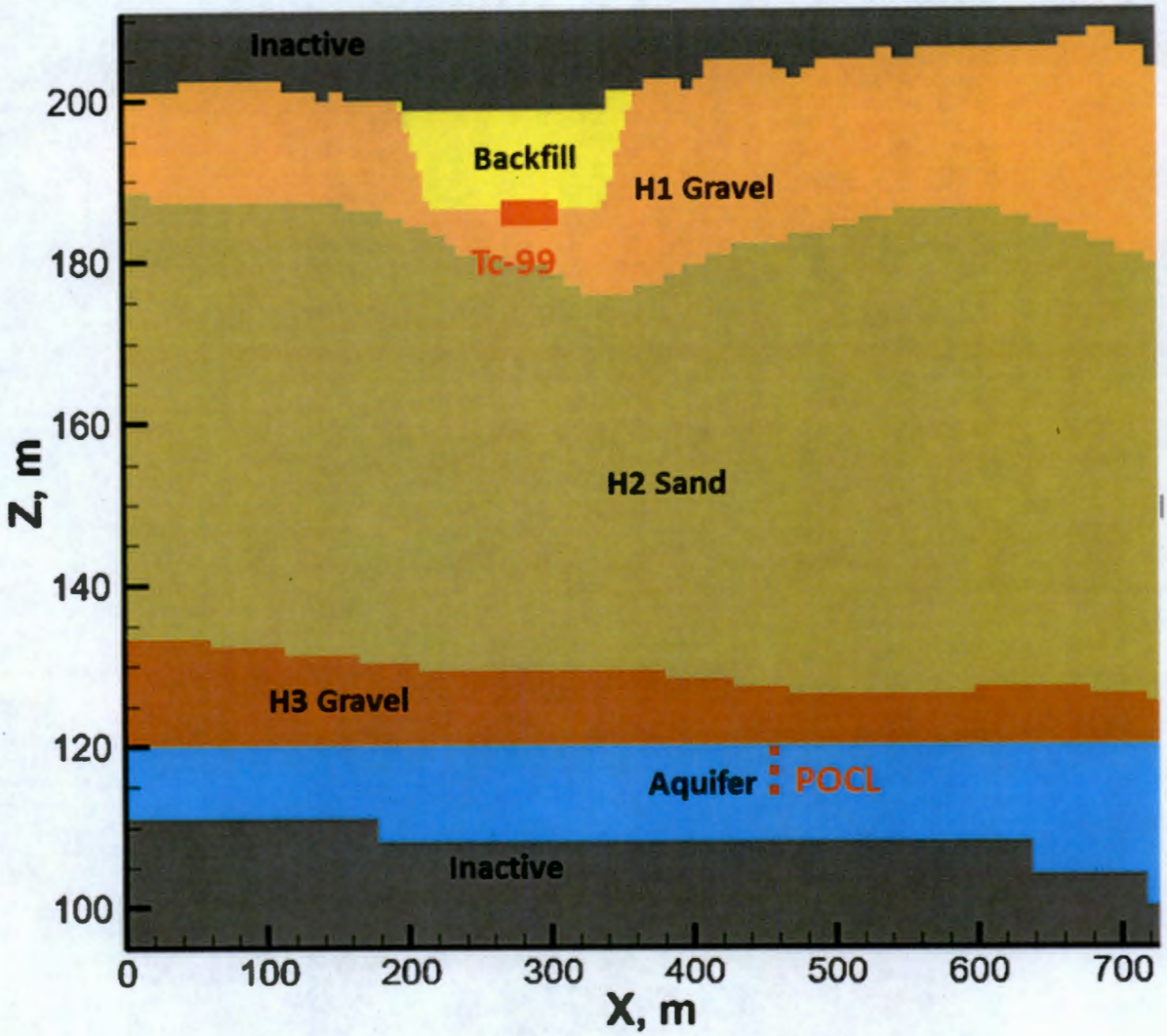

7 RESULTS AND DISCUSSION

Section 7.1 discusses the summary statistics for the moisture content datasets as compared to other Hanford Site datasets. Section 7.2 discusses results of the moisture content interpolation including the base case interpolation and sensitivity cases. Sections 7.3 through 7.5 present and compare results of the model simulations for the two-dimensional STOMP© base case and heterogeneous case cross-section models. Comparisons are made for simulated moisture contents (Section 7.3), matric potentials (Section 7.4), and contaminant breakthrough curves (Section 7.5).

7.1 SUMMARY STATISTICS FOR MOISTURE CONTENT DATASETS

Prior to processing to remove replicate measurements and adjust the data for interpolation, the compiled dataset contained over 46,000 soil moisture measurements. The adjustment included reduction of data by re-sampling the compiled dataset at 1-ft (0.3048-m) vertical intervals, which was done mostly for practical reasons but has the desirable effect of reducing sampling bias relative to the nominal 3-in. (0.0762-m) vertical intervals common in dataset. After processing, the combined adjusted dataset included 12,926 measurements with which to support statistical description of the sample population and to perform interpolation.

Summary statistics for the compiled dataset and subsets are presented in Section 6.2, in Table 6-1, and in Figure 4-5. The central tendency values (mean and median) are consistently between about 4% (vol) and 6% (vol) for the base case (combined adjusted) dataset and the subsets examined, but the subsets have differences in the extreme values of the range. The central tendency values are consistent with experience at WMA C and with Hanford Site vadose zone moisture contents commonly around 5% vol (e.g., PNL-10801, "Calibration Models for Measuring Moisture in Unsaturated Formations by Neutron Logging"). Minimum values are less than 1% (vol) for all subsets, and differences in minimum values between subsets are of minor practical importance since values less than about 2% are uncommon (Figure 4-5). Differences in maximum values are more important to understand in order to describe sediment heterogeneities, and these differences are traceable to anomalies occurring at relatively shallow depths in regions of limited extent. In particular, the H2-Only dataset exhibits a much smaller range than the other datasets [25.64% (vol) compared to the base case range of 43.85% (vol)] though it has similar mean and median values.

The maximum values measured at depths shallower than the H2 are higher than observed in other Hanford Site data for similar sediment textures (e.g., PNL-10801 reports a range of 4% vol to 40% vol for 3,600 gravimetric analyses of unsaturated Hanford formation sediments) and likely include outliers. Potential reasons for outlying values may include any combination of measurement error, regions of unusually high moisture retention, and transient recharge effects (including anthropogenic effects). RPP-22393 Section 4.2.1.1 implies that calibration functions for most of the dataset were developed using standards with 25% (vol) moisture content or less, so it is possible that measurement error increases at higher values. In this work, the potential impact of such error on interpolation is considered tolerable, because most of the domain and the dataset are within the sand-dominated H2 unit, where measurements are within the intended

calibration range, and, for purposes of this EMCF, it is not necessary to predict precise moisture contents above a threshold value that is well within that range. As is more clearly illustrated by the interpolation discussed in Section 7.2, the anomalously high moisture measurements occur in discrete regions of relatively shallow depth—some inside the backfill and some within undisturbed horizons. These regions may be evidence of unusually high moisture retention, transient recharge effects, or both; furthermore, because of the calibration functions, the effect of measurement error may be more apparent where such physical anomalies occur. Thus, a combination of differences in soil texture and factors unrelated to soil texture could be causing shallow moisture content anomalies. However, where the cause of anomalies is ambiguous, the extent of the regions is limited, and tenuous conclusions driven by extreme measurements can be avoided by treating interpolated values above a threshold value as a single textural group rather than a continuous distribution.

Transient recharge effects are also observed to be more significant at shallower depths consistent with the backfill horizon (with moisture content varying roughly 1 to 2% vol) based on repeatedly logged moisture profiles in drywells within the tank farm (Figures 4-1 through 4-4). It may be that compaction of sediments near the base of the tank farm excavation occurred during construction and contributes to slower drainage within the backfill relative to underlying sediments. Within the tank farm, there may also have been some focused recharge caused by the slope of impervious surfaces or grading, and similarly there may have been continuing small anthropogenic releases of water at discrete locations in volumes too small to cause observable moisture content changes below a certain depth.

Another relevant source of detailed soil characterization for comparison purposes is the Sisson and Lu (S&L) field injection site in the 200 East Area. In general, the inference of discrete regions of sediments with elevated moisture retention from interpolated moisture content at WMA C is consistent with the approach of Ye and Khaleel (2008) for the S&L site, although the moisture dataset for the S&L site had a higher mean between about 8% vol and 10% vol and a narrower range with most values less than about 20% ("Stochastic analysis of moisture plume dynamics of a field injection experiment" [Ye et al. 2005]; Ye and Khaleel [2008]) (the summary statistics for the WMA C subset from the H2 unit only are more similar to those for the H2 unit from other locations such as the S&L site [Ye et al. 2005]). Ye and Khaleel (2008) considered a combined dataset of soil textural classes determined from particle size distribution measurements on 93 samples from the S&L site in which coarse sand dominated but a minority of samples were loamy sand or rarely sandy loam. Consideration of the S&L moisture content database led to predictions of more extensive regions of fine-textured horizons than the core sampling population would suggest, thus providing a better fit to simulated data for the S&L injection experiments. Fitted van Genuchten parameters for the S&L samples included saturated moisture contents of 35% for sandy loam and 39.5% for loamy sand, which provide an upper bound estimate for moisture contents that could possibly be measured locally, for example, shortly after rainfall or an anthropogenic discharge of water. Similar to other past characterization of Hanford formation sediments (PNL-10801), the S&L samples suggest the higher portion of the range of reported moisture contents at WMA C exceeds that expected for unsaturated site sediments of similar texture, possible reasons for which are stated in the preceding paragraph, while at the same time the S&L samples demonstrate a potential limitation to the ability of discrete sampling to capture the full range of variability. Again, these observations favor the approach of

interpreting the available data based on a discrete number of textural groups as opposed to inferring a continuous distribution of textures from outlying values or undertaking an attempt to identify and reject outliers without a clearly objective basis.

The base case dataset was retained for interpolation with the understanding that interpretations of textural heterogeneity would consider the major spatial trends in the moisture interpolation rather than rely literally on moisture content values that become problematic at the extremes of the distribution.

7.2 MOISTURE CONTENT INTERPOLATION

To evaluate the site-wide distribution of moisture content at WMA C, geostatistical estimation was used to interpolate sampled moisture content data to un-sampled locations across the site. Variography was used to determine spatial correlations within the dataset that were used for the interpolation. Directional correlations derived from the variogram analysis are consistent with prior interpretations of the geologic conditions (Ye et al. 2005). Base case estimates of the variogram range and the data variance (sill) in the horizontal and vertical direction were established from empirical variograms. An exponential model variogram was visually fitted to the empirical variograms. The parameters developed from the dataset were then used to interpolate the data to a three-dimensional grid using the kriging algorithms provided by the KT3D package in GSLIB. The kriging results provide a detailed estimation of moisture content across the modeled area of WMA C.

The base case interpolation provides a reasonable fit to the observed data (in Figure 4-6 and Figures 6-3 through 6-9, changes in the colored interpolation contours correspond to changes in observed vertical moisture profiles plotted as black lines). Spatial trends in moisture content are apparent with changes occurring near hydrostratigraphic contacts (e.g., the backfill/H1 and H1/H2 contacts); elevated moisture at relatively shallow depths, especially outside the backfill region (Figures 6-5 and 6-6); a relatively dry region underlying the tank farm backfill (Figures 4-6 and 6-9); and an elevated moisture region midway through the H2 sand subunit (e.g., Figures 6-3 and 6-4).

A high moisture anomaly was observed at depth in the northeast region of the domain (Cross-Section D-D' in Figures 4-6 and 6-9). Boreholes C8763, C8765, C8766, and C8767 each had moisture measurements greater than 8 vol. % over long segments in the lower half of the borehole at elevations within the H2 unit at which such high values are relatively uncommon and not usually so continuous. Hypotheses to explain these measurements include locally elevated moisture due to heterogeneous lithology, locally elevated moisture due to site operations (which could complicate indirect interpretation of lithology based on moisture, at least locally), or differences in data quality between the anomalous measurements and the rest of the dataset. The data were retained since there were not readily identifiable site operations that would have led to this moisture distribution including the more typical observations at shallower depths, nor were there obvious data quality differences. For example, the profiles in borehole C8763 and drywell A6722 appear to be well correlated over the segment where they overlap (Cross-Section A-A' in Figures 6-3 and 6-4). Boreholes 8763, 8765, and 8766 were collected by

TRS using the "N-2" detector. The contractor and individual detector differed from other locations, but the neutron moisture instrument was similar to those used elsewhere and was operated by similar procedures, such as the nominal 3-in. depth sampling interval and the 15-second count time typically used with mounted instruments by all the contractors. The feature is not easily attributable to any interpolation artifact because it persisted over a range of sensitivity cases.

Data reserved for validation support the base case interpolation at locations between included data points. For example, Figures 6-5 and 6-6 indicate a change in moisture content below the maximum observed depth in drywell A6691 (30-04-08) as part of a continuous region of moisture content in the 6 vol. % to 8 vol. % band throughout the cross-section in between regions with less than 6 vol. % moisture content. Only one borehole directly on the cross-section has data at a comparable depth. Additional data that were not in the HEIS GPL dataset were collected in 2003 from drywell A6691 (30-04-08) with the NMLS through the depth of the elevated moisture region and were plotted on a figure titled "C Farm Data Acquired to Support Drilling of Exploration Borehole" in Appendix D of GJO-2004-554-TAC, "Hanford Tank Farms Vadose Zone Monitoring Project, Annual Monitoring Report for Fiscal Year 2003." The NMLS data indicate a distinct peak of elevated moisture content up to approximately 9 vol. % in drywell A6691 (30-04-08) at the same depth. In this example, the interpolation correctly predicted the continuity of the spatial trend with a slight under-prediction of the magnitude of the change observed in the reserved data.

Sensitivity analyses were performed both on the correlation parameters and the dataset construction. Sensitivity analyses in this context measure sensitivity of the moisture interpolation to different inputs in order to characterize the confidence of the interpolation used to develop the heterogeneous case models; they were performed apart from other sensitivity analyses around the WMA C PA base case. Variations in the model variogram range could affect the "connectedness" of elevated moisture content regions. To probe the sensitivity to the dataset range, endpoints were determined by varying the ranges of the model variograms while maintaining visual fit to the empirical data. The interpolation results showed some sensitivity to the horizontal range; however, sensitivity to changes in the vertical range are minimal because of data spacing (control) in the vertical direction.

The data from handheld detectors was potentially different from other data sources (generally drier measurements from handheld instruments may have been tool-related or site-related as explained in Section 4.3.1). To evaluate the impact of the handheld data on the overall dataset and the interpolation of the data to the model grid, a dataset was developed without the handheld locations for analyses. The handheld data was also reviewed independent of the complete dataset. This handheld-only dataset showed a wider range and slightly lower mean (drier) for the moisture content values. Evaluation of the dataset correlation showed a sensitivity to the removal of the handheld dataset because it was primarily located in the center of the interpolation space (at the drywells around the tanks). Removal of the handheld dataset reduced the overall variogram range since it left longer distances between measured boreholes and a weaker correlation among more distant data. However, the same spatial trends that are seen in the full dataset are apparent (at reduced intensity) with removal of the handheld dataset, especially if the range of the model variogram is held constant (Figure 6-13). Figures 4-3 and

4-4 show that where both NMLS and handheld data were available, both were consistent even if collected years apart, and the small differences were not systematically lower or higher for one instrument. Figures 6-3 and 6-4, depicting both observed data and the interpolation using the full base case dataset, show that the handheld instrument measurements in drywells allow high moisture anomalies detected near the backfill/H1 and H1/H2 contacts to be traced approximately halfway across the 160-m-long Cross-Section A-A'. The visible trend in the observed data thus supports the range of 85 m determined from the variogram for the base case dataset, a conclusion not possible to reach with as much confidence if the handheld dataset is excluded. Therefore, there does not appear to be a basis to exclude handheld instrument data, and the base case dataset benefits from greater resolution by including it.

Sensitivity analyses for the Combined Adjusted dataset that excluded data not within the Hanford H2 unit as defined by lithologic contact elevations assigned from the STOMP© model show variability in the vertical variogram range of the data compared to the base case dataset, but little difference in the horizontal variogram range. The reduced vertical range reflects the structure of heterogeneities of the moisture content distribution within the H2 (sand-dominated) unit, whereas the longer vertical range of the base case dataset is representative of the structure of the overall Hanford formation which includes the gravel-dominated H1 and H3 units, in addition to the sand-dominated H2 unit. The appropriate dataset for vertical interpolation to identify heterogeneities thus depends on the size of the domain under consideration. The minimal difference between horizontal variogram ranges suggests that the inclusion in the base case of some shallow data from different units with potential texture differences, such as the backfill and the H1 unit, does not unduly influence the overall interpolation for the larger domain including the Hanford H2 unit.

Based on these findings, the development of the heterogeneous case models (Section 6.6) adopted the base case moisture content interpolation (discussed in Sections 6.3 and 6.4).

7.3 SIMULATION OF MOISTURE CONTENT

Simulated moisture content values in calendar year 2020 from the column of grid blocks in Cross-Section 1 closest to borehole C4297 were output as a point of comparison between the base case and heterogeneous cases models. The borehole C4297 is in close proximity to Cross-Section 1 and to tank C-105 (Figures 6-14 and 6-20). The simulated vertical moisture profile was also plotted against the gravimetric data from boreholes C4297 (Figure 7-1) and 299-E27-22 (Figure 7-2) for illustrative purposes. Gravimetric data were converted to volumetric moisture content using an assumed sediment bulk density of 1.7 g/cm^3 (this value is slightly different than the 1.8 g/cm^3 assumed in the RPP-CALC-60450 dataset in order to be consistent with the data treatment elsewhere in the WMA C PA, i.e., RPP-RPT-58949). Gravimetric data from both boreholes within the H2 unit were used in the moisture content interpolation underlying the heterogeneous case model development, but these data points were not used to directly calibrate the models, so the comparison has at least some limited utility.

Comparing the blue lines in the left-hand and right-hand plots of Figure 7-1, the heterogeneous case predicts typically lower moisture contents through the vadose zone relative to the base case

(lower mode), with the addition of several small vertical intervals where moisture content is elevated to varying degrees, yielding essentially the same mean (see also Table 7-1). This pattern is as expected given the moisture retention curves selected for the H2 unit in the base case and the moisture-based rock/soil zones in the heterogeneous case, in which the dominant material type had a generally drier curve and the three material types representing heterogeneities had generally wetter curves relative to the base case representing an EHM (Figure 6-16).

Figure 7-1. Comparison of Measured (C4297) and Simulated Moisture Contents for Base Case and Heterogeneous Case for Cross-Section 1.

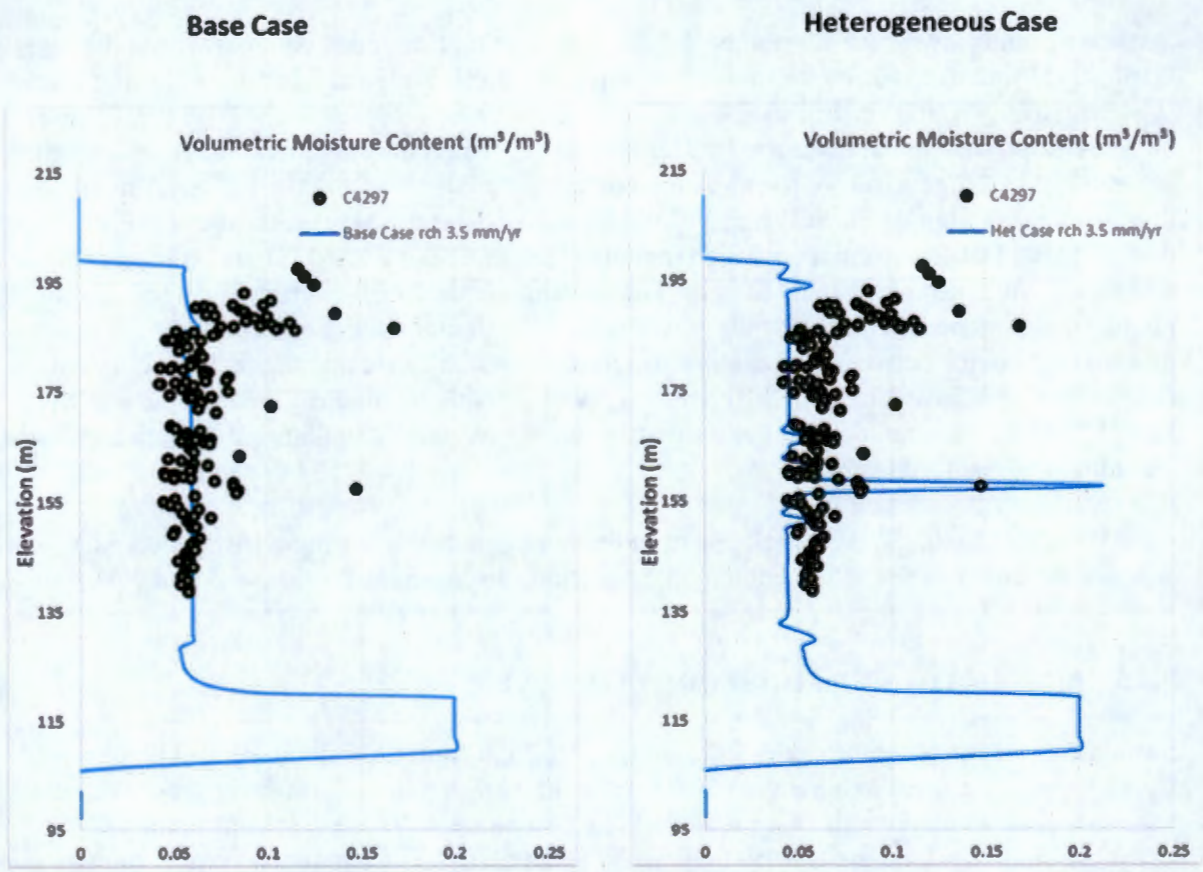

For a recharge rate of 3.5 mm/yr, the simulated moisture content profile (blue line) for Cross-Section 1 compares well with the field measurements (black circles) for both the EHM-based base case and the heterogeneous case (Figure 7-1). The simulated profile in the base case is comparable to the mean measured moisture content from C4297. In the heterogeneous case, the simulated profile predicts a baseline moisture content similar to the minimum measured moisture content as well as peaks similar to some of the elevated moisture measurements. Using the same simulated moisture profile as Figure 7-1 as a common reference, Figure 7-2 demonstrates the drier mean moisture content from the other borehole with gravimetric data, even as compared to the moisture profile below the tank farm where drywell data indicated a relatively dry regime.

Figure 7-2. Comparison of Measured Moisture Contents at 299-E27-22 and Simulated Moisture Contents near C4297 for Base Case and Heterogeneous Case for Cross-Section 1.

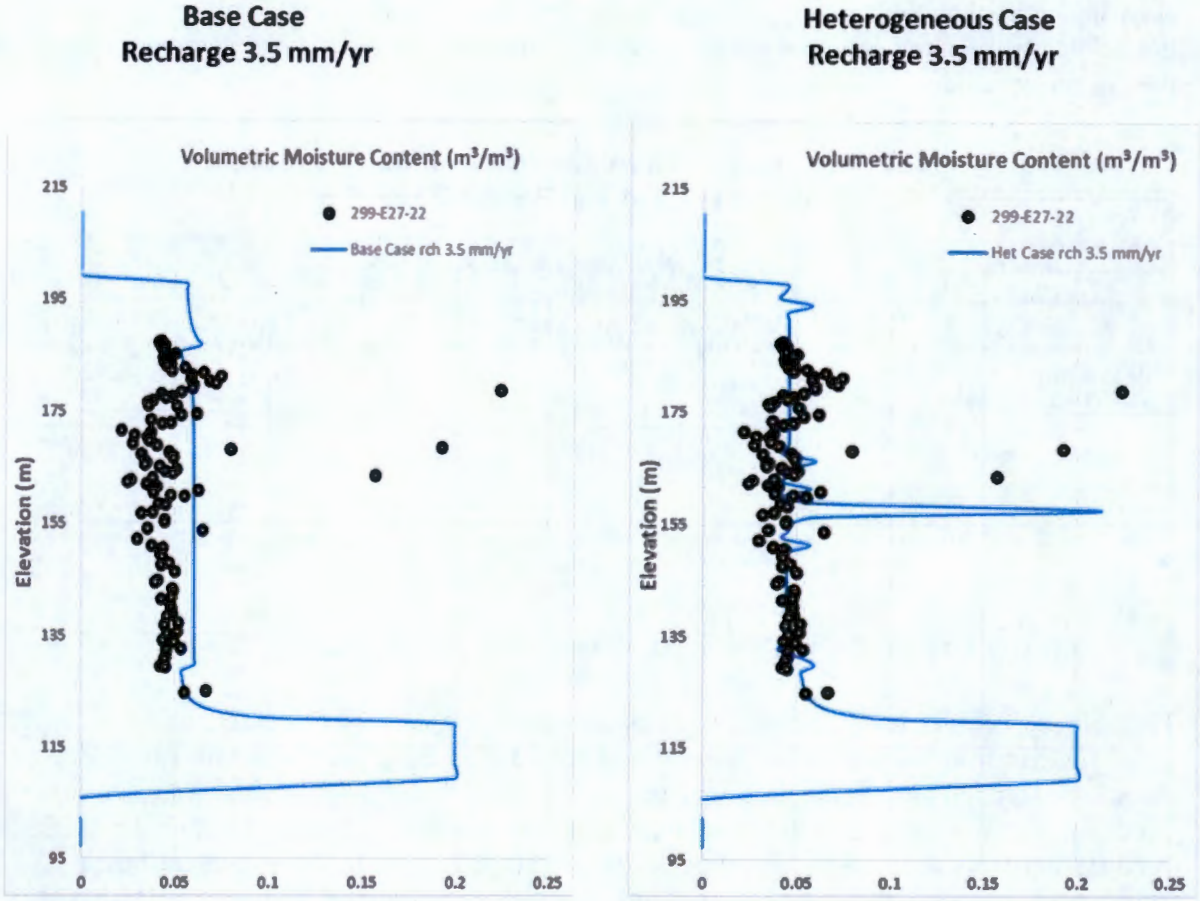

7.4 SIMULATION OF MATRIC POTENTIAL

Table 7-1 summarizes the mean moisture content and the mean filter paper matric potential measurements for samples from the two boreholes C4297 and 299-E27-22 (Figure 7-3) and the model-predicted average moisture content and matric potential values for both the base case and the heterogeneous case. As indicated, the simulated steady-state moisture contents between 0.06 and 0.07 for the H2 unit for both model cases compare well with field-measured moisture contents (Table 7-1). However, compared to the measured matric potential results, simulated matric potentials between -150 cm and -200 cm for the H2 unit were much less negative for both model cases. The EHM approximation (base case) essentially results in a smoothing of the model estimates. In contrast, the filter-paper-based soil matric potentials are point measurements, and are not consistent with the smoothing resulting from the use of averaged upscaled or effective properties for the large grid blocks used in PA simulations. Therefore, the variability of filter-paper-based point measurements is inherently larger in comparison to that based on PA simulations using homogenized upscaled properties. In addition, the error bar for filter paper measurements is rather large (0.1 to 0.2 MPa or ~1,000 to ~2,000 cm). Similar

arguments apply to the heterogeneous case. Soil moisture measurements are typically more accurate than matric potential measurements, and the matric potential variability is typically larger than the soil moisture variability. Nonetheless, the overall characterization data are consistent with the relatively dry moisture regime predicted by the PA simulations. The deviation in soil matric potential values is due to a mismatch between the modeling scale and the measurement scale.

Table 7-1. Mean Moisture Content and Matric Potential from Simulations and Borehole Samples.

Result	Base Case Model Predicted Value	Heterogeneous Case Model Predicted Value	Borehole C4297 (inside tank farm)	Borehole 299-E27-22 (outside tank farm)
Mean moisture content (% volume)	0.068	0.069	0.060	0.046
Mean matric potential (-cm)	190	148	498	1,616

Note: Gravimetric data were converted to volumetric moisture contents using an assumed sediment bulk density of 1.7 g/cm^3.

7.5 SIMULATION OF TECHNETIUM-99 CONCENTRATION

Breakthrough curves for ^{99}Tc concentrations simulated at the point of calculation 100 m downgradient from the source location for both the base case and heterogeneous case for the three cross-section models are presented in Figures 7-4, 7-5, and 7-6. Table 7-2 summarizes the ^{99}Tc transport simulation results. In all three cross-section models, the EHM-based base case predicts similar but somewhat higher peak concentration than the moisture content-based heterogeneous case model, a finding that adds credibility and support for use of EHM-based modeling for the WMA C PA.

The absolute magnitudes of ^{99}Tc concentrations simulated in this EMCF have no meaning, and comparison of them to regulatory objectives or standards is not appropriate. Bear in mind the arbitrary source term used for each cross-section for purposes of comparing the base case and heterogeneous case representations of the vadose zone, and note the artificial boundary conditions used in Cross-Section 3. Interpretations are based on the relative magnitude of simulated ^{99}Tc concentrations in different cases (with emphasis on peak concentrations and the time of initial breakthrough). Although the locations of the source terms and points of calculation have some relationship to real-world features, the locations were chosen mainly for convenience of testing the effects of heterogeneity at multiple locations and in multiple directions.

Heterogeneities induced by variability in sediment texture and moisture content lead to smearing of the contaminant distribution and result in slightly lower peak concentrations for the heterogeneous flow domain versus an EHM model-based flow domain. Breakthrough times and peak concentration times were similar overall between the base case and heterogeneous case,

with some small differences predicted in opposite directions depending on the cross-section and its particular distribution of heterogeneities between the source and the point of calculation. The breakthrough curves for Cross-Section 1 were similar in breakthrough time, peak time, and peak concentration for both cases. The base case simulation for Cross-Section 2 did not fully reach the peak ^{99}Tc concentration within the 3,000-year simulation period, but the concentration was sufficiently past the inflection point in the breakthrough curve to approximately describe the peak to make a comparison. The heterogeneous case had somewhat earlier breakthrough and peak times than the base case for Cross-Section 2. Conversely, the heterogeneous case had somewhat later breakthrough and peak times than the base case for Cross-Section 3. Cross-Section 3 had the greatest difference in the peak ^{99}Tc concentrations between cases, with the heterogeneous case predicting a peak concentration less than the base case by about a factor of 3 because of more heterogeneity in the dimension orthogonal to groundwater flow than in the dimension parallel to flow as in Cross-Sections 1 and 2.

Figure 7-3. Location of Well C4297 and 299-E27-22.

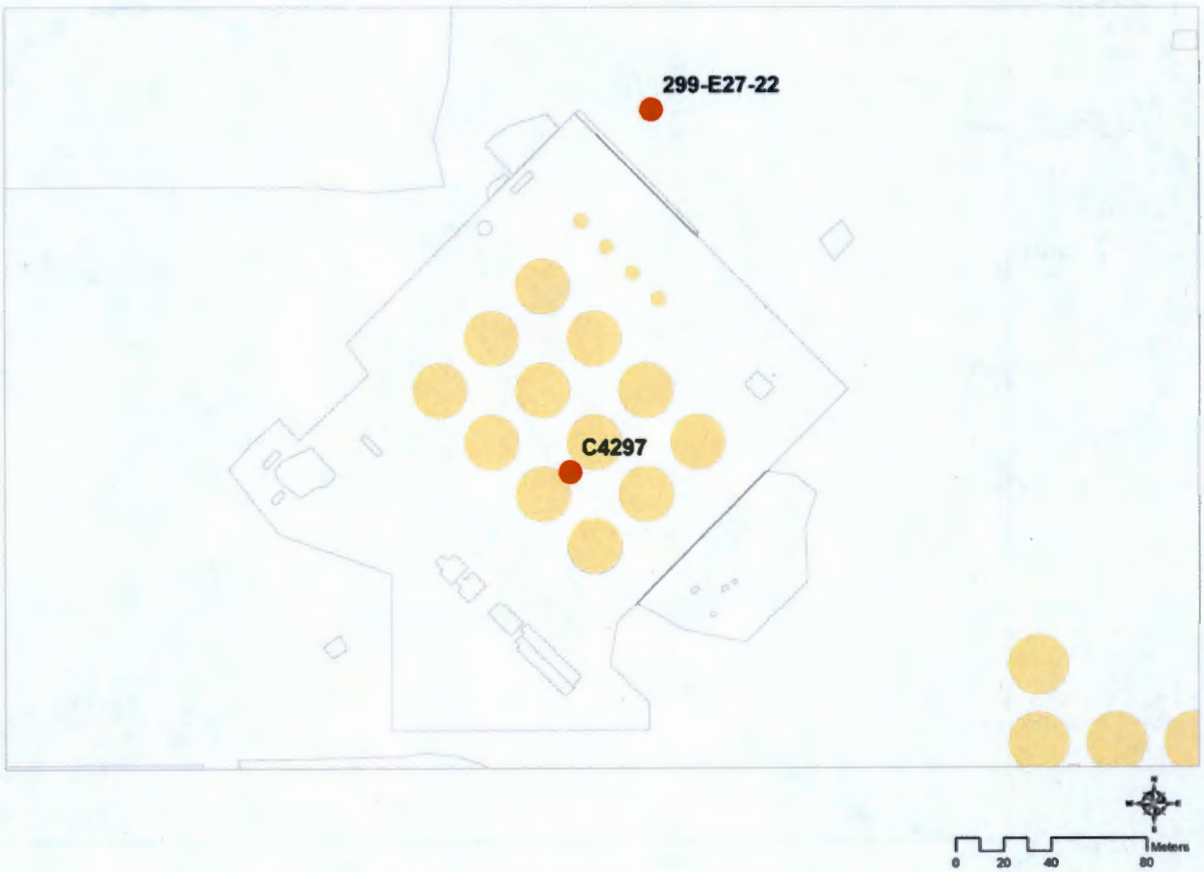

The results are compatible with independent modeling results for the S&L field injection site (RPP-RPT-58949 Appendix B; Ye and Khaleel 2008). As discussed in RPP-RPT-58949 Appendix B, the S&L site database provided a framework for testing a variety of upscaling modeling approaches (e.g., combining soft data such as the initial moisture content and hard data such as the vadose zone soil hydraulic properties). Although the use of both soft and hard data

for the S&L injection test site modeling was valuable in representing the detailed moisture plume (i.e., the splitting of the moisture plume sandwiched within the coarse media between two fine layers), the observed and simulated spatial moments (first and second) were not significantly different from those using the EHM model. With the WMA C PA simulations being conducted over a large flow domain and over a long time frame, this is an important finding because, as the field data from controlled as well as uncontrolled past discharges suggest, the relatively thick Central Plateau vadose zone is effective in dispersing the impact of small-scale heterogeneities over time and space (WCH-520, "Performance Assessment for the Environmental Restoration Disposal Facility, Hanford Site, Washington").

Figure 7-4. Technetium-99 Breakthrough Curves for Cross-Section 1 for Arbitrary Source Term.

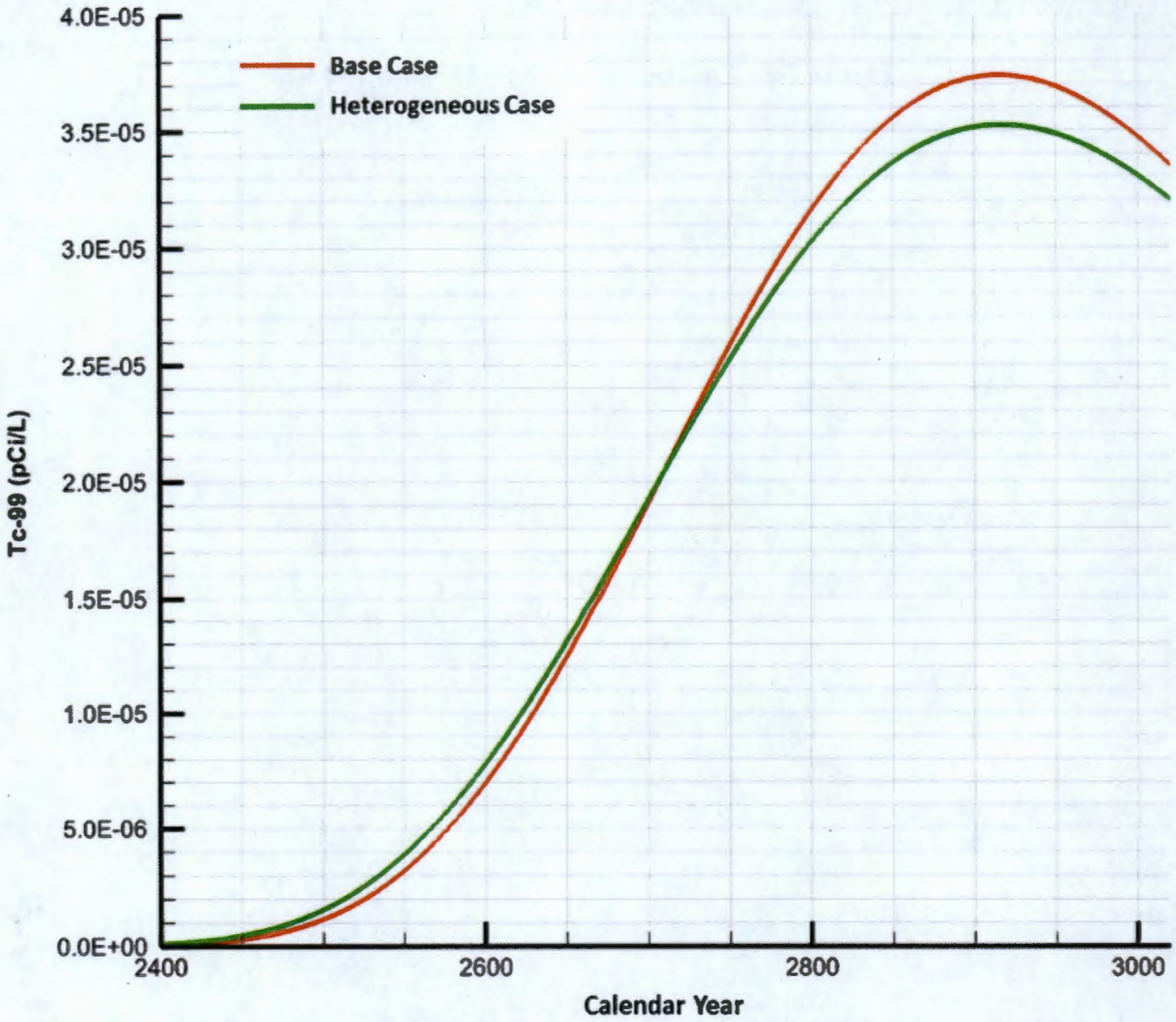

Consistent with independent modeling results, the results of this EMCF indicate that for the evaluation of long-term impacts from residual waste in the WMA C PA, where peak groundwater concentration is the key metric, an EHM approximation is sufficient for the PA

objectives. This EMCF compared a heterogeneous model to the EHM-based hydrostratigraphic model of Alternative Geologic Model I in the WMA C PA. This exercise does not evaluate whether that particular hydrostratigraphic model is optimal; rather, it demonstrates that the heterogeneous model does not provide a critical improvement relative to Alternative Geologic Model I.

Figure 7-5. Technetium-99 Breakthrough Curves for Cross-Section 2 for Arbitrary Source Term.

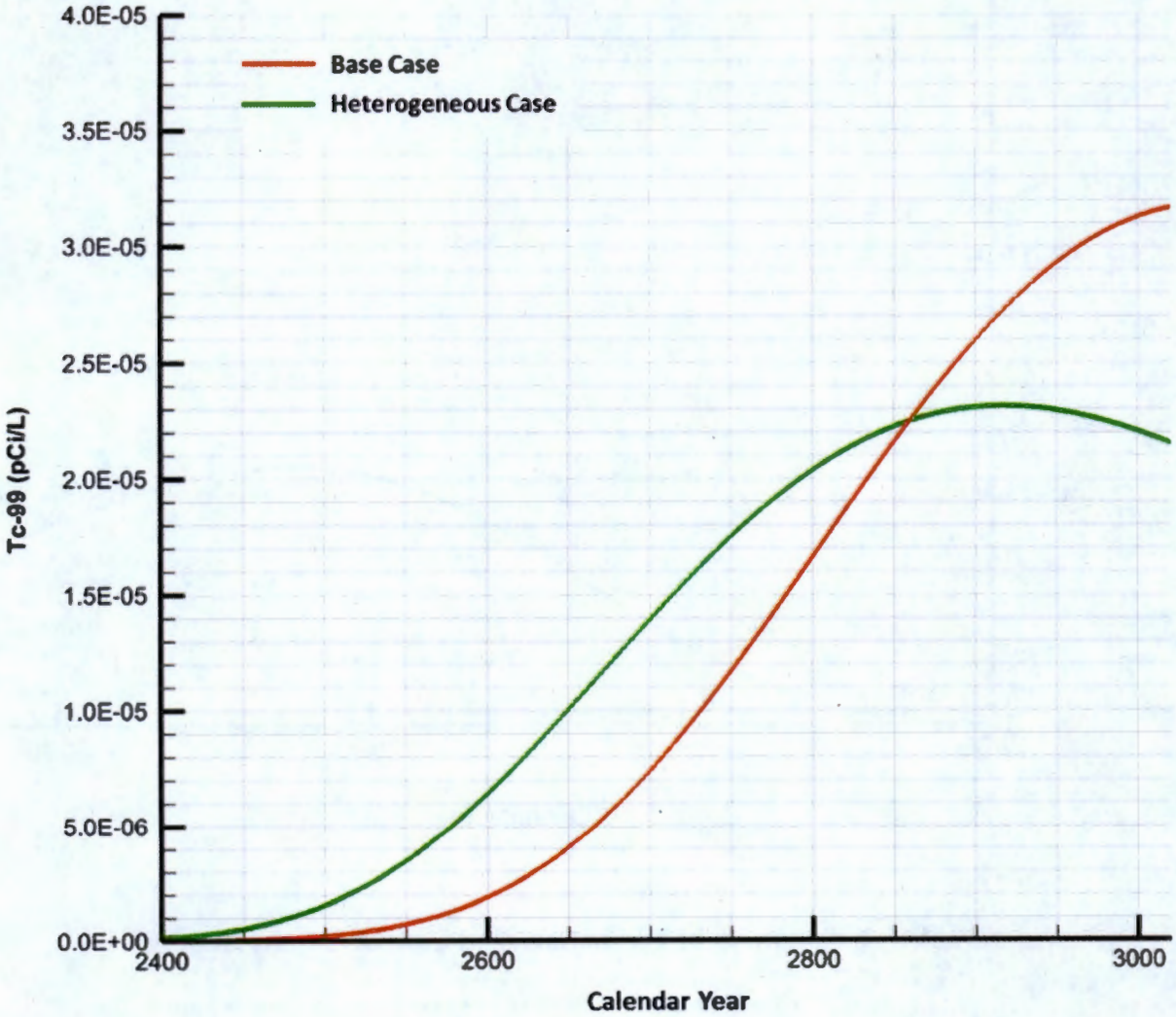

Figure 7-6. Technetium-99 Breakthrough Curves for Cross-Section 3 for Arbitrary Source Term.

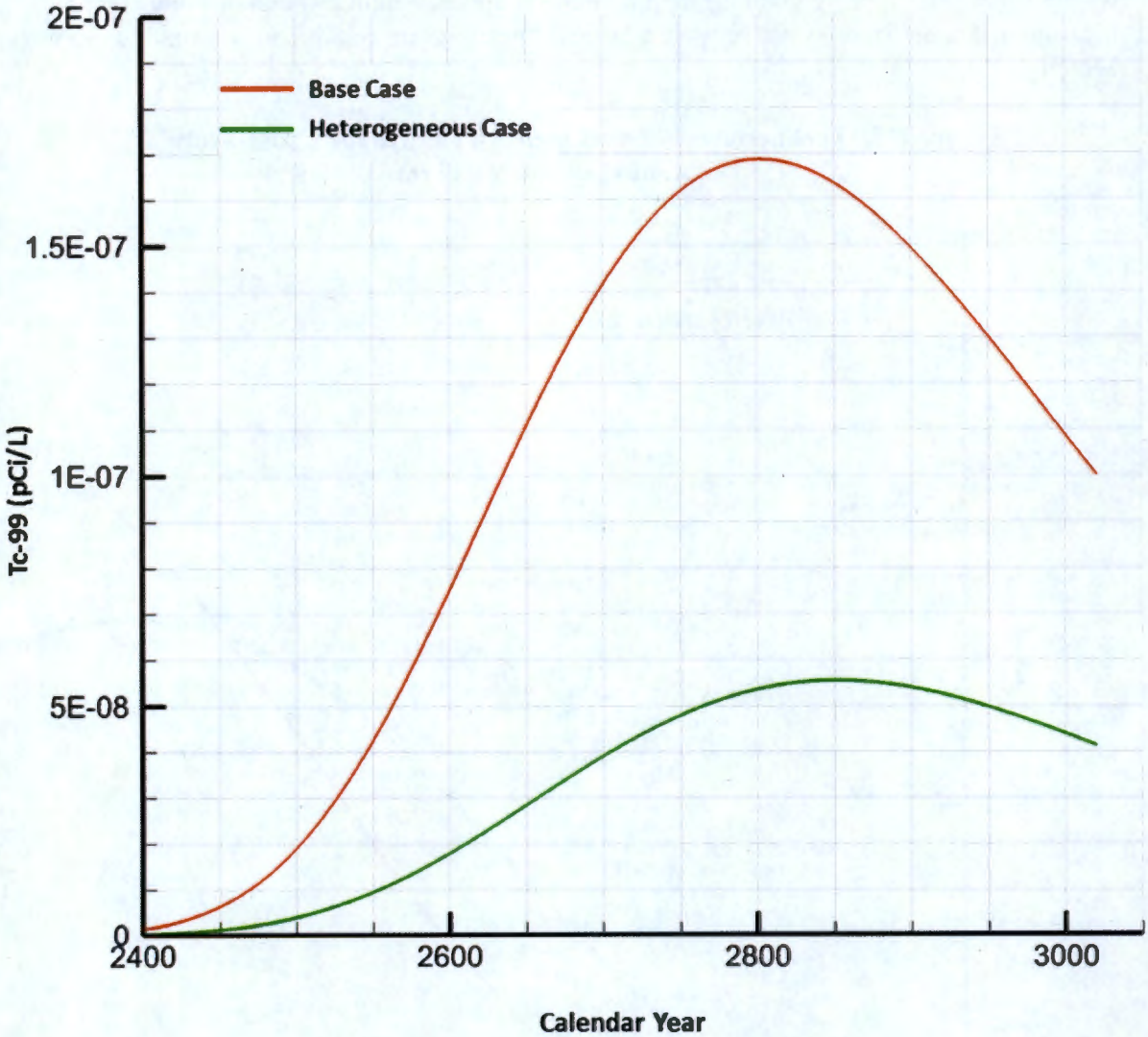

Table 7-2. Summary of Technetium-99 Transport Model Results.

Cross-Section	Time of Breakthrough (Calendar Year)		Time of Peak (Calendar Year)		Peak Concentration (pCi/L)	
	Base Case	Heterogeneous Case	Base Case	Heterogeneous Case	Base Case	Heterogeneous Case
1	2226	2210	2916	2916	3.73E-5	3.52E-5
2	2253	2205	>3000	2918	>3.16E-5	2.31E-5
3	2212	2232	2798	2843	1.69E-7	5.44E-8

8 SUMMARY AND CONCLUSIONS

For heterogeneous media such as that those existing at WMA C, in the absence of transient effects such as from anthropogenic recharge, the natural moisture content distribution can be used as an indicator of sediment texture. Field-measured moisture contents can then be used as indirect data from which estimates of soil hydraulic properties can be inferred. Also, in the absence of transient recharge effects, the field-measured moisture contents can be assumed to be in equilibrium with natural recharge. This important set of inferences as well as the results of geostatistical analysis of the moisture content database were used to identify and select the hydraulic properties data used in the WMA C PA heterogeneous media model.

The extensive set of moisture data for WMA C was developed from neutron moisture logging done at both direct push characterization locations and in drywell boreholes. A statistical and geostatistical analysis of the moisture content data was performed for the compiled dataset as well as subsets, including the subset of data from the Hanford H2 sand-dominated unit. The analysis yielded statistical characteristics of the moisture content distribution which are generally consistent with those reported for the Hanford H2 sand-dominated unit at the nearby S&L field injection site. Subsequent kriging yielded a heterogeneous moisture distribution, which, unlike the EHM approximation, captures the spatial variability of moisture content distribution and the subsequent variability in hydraulic properties.

Four cut-off values of moisture were chosen and hydraulic properties were identified and mapped onto the heterogeneous media model developed in STOMP©. Model runs were made and contaminant breakthrough curves generated for the heterogeneous model, and results compared to those based on the base case model. The heterogeneous media models do not invoke the EHM approximation. Peak contaminant concentrations for the heterogeneous model and the base case model were similar. In fact, heterogeneities induced by sediment texture and variability in moisture content lead to increased dispersion, resulting in a lower peak concentration for the heterogeneous model versus the base case model. The net effect on unsaturated hydraulic conductivity of the interaction of sediment textures and moisture contents in various model conditions is not straightforward, but essentially the heterogeneous representation causes lower effective unsaturated hydraulic conductivity than the EHM for the same data at comparable matric potentials, because splitting out higher than average values for the heterogeneities requires lower than average values for the dominant texture as a matter of course. The fact that the models compare well, with the base case model producing slightly higher results, enhances the credibility of use of an EHM modeling approach for the WMA C PA. With the WMA C PA simulations being conducted over a large flow domain and over a long time frame, this is an important finding because, as the field data from the S&L site as well as past discharges in the Central Plateau suggest, the relatively thick vadose zone is effective in dispersing the impact of small-scale heterogeneities over time and space (WCH-520).

This page intentionally left blank.

9 REFERENCES

CHPRC-00176, 2011, "STOMP Software Management Plan," Rev. 2, CH2M HILL Plateau Remediation Company, Richland, Washington.

CHPRC-00211, 2014, "STOMP Software Test Plan," Rev. 2, CH2M HILL Plateau Remediation Company, Richland, Washington.

CHPRC-00258, 2015, "MODFLOW and Related Codes Software Management Plan," Rev. 4, CH2M HILL Plateau Remediation Company, Richland, Washington.

CHPRC-00515, 2013, "STOMP Acceptance Test Report CHPRC Build 4," Rev. 3, CH2M HILL Plateau Remediation Company, Richland, Washington.

Deutsch, C. V., and A. G. Journel, 1998, GSLIB: Geostatistical Software Library and User's Guide, Second Edition, Oxford University Press, New York, New York.

DOE M 435.1-1, 2007, Radioactive Waste Management Manual, U.S. Department of Energy, Washington, D.C.

DOE O 435.1, 2001, Radioactive Waste Management, U.S. Department of Energy, Washington, D.C.

DOE O 5400.1, 1990, General Environmental Protection Program, U.S. Department of Energy, Washington, D.C.

DOE O 5400.5, 1993, Radiation Protection of the Public and the Environment, U.S. Department of Energy, Washington, D.C.

DOE/RL-2011-50, 2012, Regulatory Basis and Implementation of a Graded Approach to Evaluation of Groundwater Protection, Rev. 1, U.S. Department of Energy, Richland Operations Office, Richland, Washington.

Ecology, EPA, and DOE, 1989, Hanford Federal Facility Agreement and Consent Order – Tri-Party Agreement, 2 vols., as amended, State of Washington Department of Ecology, U.S. Environmental Protection Agency, and U.S. Department of Energy, Olympia, Washington.

EMDT-OB-0009, 2015, "WMA C Vadose Zone Moisture Content from Handheld Neutron Moisture Gauges," Rev. 0, Washington River Protection Solutions, LLC, Richland, Washington.

Freeze, R. A., J. Massmann, L. Smith, T. Sperling, and B. James, 1990, "Hydrogeological Decision Analysis: 1. A Framework," Ground Water, Vol. 28, No. 5, pp. 738–766.

GJO-2004-554-TAC, 2004, "Hanford Tank Farms Vadose Zone Monitoring Project, Annual Monitoring Report for Fiscal Year 2003," S.M. Stoller Corporation, Grand Junction, Colorado.

Goovaerts, P., 1997, Geostatistics for Natural Resource Evaluation, Oxford University Press, New York, New York.

NAVD88, 1988, "North American Vertical Datum of 1988," National Geodetic Survey, U.S. Department of Commerce, National Oceanic and Atmospheric Administration, Silver Spring, Maryland.

NOAA Manual NOS NGS 5, 1990, "State Plane Coordinate System of 1983," National Geodetic Survey, U.S. Department of Commerce, National Oceanic and Atmospheric Administration, Rockville, Maryland.

PNL-10801, 1995, "Calibration Models for Measuring Moisture in Unsaturated Formations by Neutron Logging," Pacific Northwest Laboratory, Richland, Washington.

PNNL-11216, 1997, "STOMP Subsurface Transport Over Multiple Phases Application Guide," Pacific Northwest National Laboratory, Richland, Washington.

PNNL-15503, 2008, "Characterization of Vadose Zone Sediments Below the C Tank Farm: Borehole C4297 and RCRA Borehole 299-E27-22," Rev. 1, Pacific Northwest National Laboratory, Richland, Washington.

PNNL-15782, 2006, "STOMP Subsurface Transport Over Multiple Phases Version 4.0 User's Guide," Pacific Northwest National Laboratory, Richland, Washington.

PRC-PRO-IRM-309, "Controlled Software Management," CH2M HILL Plateau Remediation Company, Richland, Washington.

Rockhold M. L., C. J. Murray, and M. J. Fayer, 1999, "Conditional simulation and upscaling of soil hydraulic properties," in Characterization and Measurement of the Hydraulic Properties of Unsaturated Porous Media, vol. 2, ed. M. Th. van Genuchten, F. J. Leij, and L. Wu, pp. 1391–1401, University of California Press, Riverside, California.

RPP-22393, 2013, "241-C-102, 241-C-104, 241-C-107, 241-C-108 and 241-C-112 Tanks Waste Retrieval Work Plan," Rev. 7, Washington River Protection Solutions, LLC, Richland, Washington.

RPP-23748, 2006, "Geology, Hydrogeology, Geochemistry, and Mineralogy Data Package for the Single-Shell Tank Waste Management Areas at the Hanford Site," Rev. 0, CH2M HILL Hanford Group, Inc., Richland, Washington.

RPP-32130, 2008, "Summary of Direct Push Exploration at 241-C-152 Diversion Box in 241-C Tank Farm," Rev. 0, Energy Solutions Federal Services, Inc., Richland, Washington.

RPP-CALC-60450, in process, "Process for Determining the Volumetric Moisture Content for the Vadose Zone Geologic Units Underlying Waste Management Area C," Draft B, Washington River Protection Solutions, LLC, Richland, Washington.

RPP-ENV-58782, in process, "Performance Assessment of Waste Management Area C, Hanford Site, Washington," Rev. B DRAFT, Washington River Protection Solutions, LLC, Richland, Washington.

RPP-RPT-49956, 2011, "Completion Report for the 241-C Tank Farm, C-104 Angle Direct Push Characterization," Rev. 0, Washington River Protection Solutions, LLC, Richland, Washington.

RPP-RPT-50581, 2011, "Completion Report for the 241-C Tank Farm, C-101 Angle Direct Push Characterization," Rev. 0, Washington River Protection Solutions, LLC, Richland, Washington.

RPP-RPT-51384, 2013, "Completion Report for the 241-C Tank Farm C-203 Angle Direct Push Characterization," Rev. 1A, Washington River Protection Solutions, LLC, Richland, Washington.

RPP-RPT-58949, in process, "Model Package Report Flow and Contaminant Transport Numerical Model used in WMA C Performance Assessment and RCRA Closure Analysis," Rev. Draft A, Washington River Protection Solutions, LLC, Richland, Washington.

Stoller, 2006, "Hanford Geophysical Logging Project DOE-RL Annual Report for FY 2005," S.M. Stoller Corporation for U.S. Department of Energy, Richland, Washington.

TO-320-022, "Operate Model 503DR Ml HP-2 or Ml HP-3 Hydroprobe Neutron Moisture Gauge," Washington River Protection Solutions LLC (WRPS) Tank Farms, Richland, Washington.

TO-320-060, "Operate Model 503DR Ml HP-4 Hydroprobe Neutron Moisture Gauge," Washington River Protection Solutions LLC (WRPS) Tank Farms, Richland, Washington.

WCH-520, 2013, "Performance Assessment for the Environmental Restoration Disposal Facility, Hanford Site, Washington," Rev. 1, Washington Closure Hanford, Richland, Washington.

WHC-EP-0883, 1995, "Variability and Scaling of Hydraulic Properties for 200 Area Soils, Hanford Site," Westinghouse Hanford Company, Richland, Washington.

Ye, M. and R. Khaleel, 2008, "A Markov chain model for characterizing medium heterogeneity and sediment layering structure," Water Resources Research, Vol. 44, Issue 9, W09427.

Ye, M., R. Khaleel, and T.-C. J. Yeh, 2005, "Stochastic analysis of moisture plume dynamics of a field injection experiment," Water Resources Research, Vol. 41, W03013.

This page intentionally left blank.

ATTACHMENT 1

LISTING OF MICROSOFT ACCESS® AND EXCEL® FILES CONTAINING MOISTURE CONTENT DATA ANALYZED IN THIS ENVIRONMENTAL MODEL CALCULATION FILE

This page intentionally left blank.

The moisture content data from Hanford Environmental Information System geophysical logs (HEIS GPL), handheld neutron moisture instruments, and RPP-CALC-60450, "Process for Determining the Volumetric Moisture Content for the Vadose Zone Geologic Units Underlying Waste Management Area C" evaluated in this environmental model calculation file (EMCF) were imported into tables used in a Microsoft Access®[1] 2013 database named WMAC_Moisture.accdb that has been archived in the Environmental Model Management Archive (EMMA). Copies of the tables are also archived in EMMA as Microsoft Excel® 2013 format (extension .xlsx). A listing of these files and their descriptions are provided below.

WMAC_Moisture.accdb is a Microsoft Access® 2013 database containing moisture content data from three sources (HEIS GPL, handheld, and Freestone) as discussed in this EMCF. All moisture data are on a percent volume basis.

The .xlsx files listed below are Microsoft Excel® 2013 spreadsheet copies of tables in WMAC_Moisture.accdb provided for the convenience of users who are not able or prefer not to open the Access® file.

The Access® database table named "Locations" (or Excel® file named Locations.xlsx) includes the surface coordinates of locations from all datasets and the multiple names used for each location by different sources.

The Access® database table "Angled_boreholes" (or Excel® file named Angled_boreholes.xlsx) summarizes directional borehole data as applicable.

The Access® database table "Freestone_data" (or Excel® file named Freestone_data.xlsx) includes moisture measurements with x-, y-, and z-coordinates as provided in the RPP-CALC-60450 dataset for the angled boreholes and the other selected locations.

The Access® database table "HEIS_GPL_data" (or Excel® file named HEIS_GPL_data.xlsx) contains moisture measurements imported from the HEIS GPL dataset (selected fields).

The Access® database table "HandheldDataCorrected" (or Excel® file named HandheldDataCorrected.xlsx) contains moisture measurements imported from the "handheld" dataset documented in EMDT-OB-0009, "WMA C Vadose Zone Moisture Content from Handheld Neutron Moisture Gauges" in EMMA.

The Access® database queries accomplish merging and processing of the datasets within the Access® file as discussed in this EMCF. Queries are numbered in the sequence they were called.

The number 2 queries should not be executed again; they are "create" and "append" type queries which will attempt to create new tables or add data to existing tables if called. They may be reviewed in "Design View."

[1] Access® and Excel® are registered trademarks of Microsoft Corporation in the U.S. and other countries.

All other queries are "select" type queries that may be safely executed to view results in "Datasheet View", and they may also be reviewed in "Design View."

The Access® database table "Moisture_Merged" (or Excel® file named Moisture_Merged.xlsx) represents the combined dataset (created by the number 2 queries) prior to processing to remove replicate measurements and adjust the data for interpolation.

The Excel® file named 7_One_ft_Interval_Max_to_Krig.xlsx is the output of the final data processing query and the input data for the KT3D interpolation analysis presented in this EMCF.

REFERENCES

EMDT-OB-0009, 2015, "WMA C Vadose Zone Moisture Content from Handheld Neutron Moisture Gauges," Rev. 0, Washington River Protection Solutions, LLC, Richland, Washington.

RPP-CALC-60450, in process, "Process for Determining the Volumetric Moisture Content for the Vadose Zone Geologic Units Underlying Waste Management Area C," Draft B, Washington River Protection Solutions, LLC, Richland, Washington.

ATTACHMENT 2

SOFTWARE INSTALLATION AND CHECKOUT

This page intentionally left blank.

1

CHPRC SOFTWARE INSTALLATION AND CHECKOUT FORM

Software Owner Instructions:

Complete Fields 1-13, then run test cases in Field 14. Compare test case results listed in Field 15 to corresponding Test Report outputs. If results are the same, sign and date Field 19. If not, resolve differences and repeat above steps.

Software Subject Matter Expert Instructions:

Assign test personnel. Approve the installation of the code by signing and dating Field 21, then maintain form as part of the software support documentation.

GENERAL INFORMATION:

1. Software Name: STOMP (Subsurface Transport Over Multiple Phases) Software Version No.: Bld 4

EXECUTABLE INFORMATION:

2. Executable Name [redacted]

All executable files installed [redacted]

MD5 File Signature	Executable File Name
6536b8e12d8c5b83dca76f2c947b6153	stomp-wae-bcg-chprc04i.x
e0cdf04bc1a2f6c55c5a1b499939f663	stomp-wae-bcg-chprc04l.x
6e72340bb39f6056e232fe5ff241c4d4	stomp-wae-bd-chprc04i.x
3f837a0fb8d9f47dbcada686f542d7fc	stomp-wae-bd-chprc04l.x
7e5b4cc36a8991b3d5a8ea2ed155ce47	stomp-wae-cgsq-chprc04i.x
00a898c0c3ec06817485781ad1c9ec46	stomp-wae-cgsq-chprc04l.x
f18ff5ab5667065d8ab12657344fb6a0	stomp-wae-cgst-chprc04i.x
061af86cf21ad8435b046d0efabe971b	stomp-wae-cgst-chprc04l.x
3c8111a9855dc0e430bf3c8a7abcf37e	stomp-w-bcg-chprc04i.x
20436d615a94955a2ce8eecdb8cba546	stomp-w-bcg-chprc04l.x
8b3df29df21d040189c3e2a50ef823bb	stomp-w-bd-chprc04i.x
066a289a75aedb933eb2536da5d7d1ff	stomp-w-bd-chprc04l.x
c8e62ad7a0d9b6fca39d8a8952ef5d8e	stomp-w-cgsq-chprc04i.x
28ad16806e1307aca51fd7bf89793e75	stomp-w-cgsq-chprc04l.x
6c25051016db2fe1f883a7caaaab1e97	stomp-w-cgst-chprc04i.x
ff9ff6f29b3469419ffaece87d7e772b	stomp-w-cgst-chprc04l.x
0c3e3fba40f5b93e71bcf9586432fd27	stomp-w-r-bcg-chprc04i.x
78492aee80a8c2d0a4e82aabf4a9c213	stomp-w-r-bcg-chprc04l.x
84b129786aba9c4be884e15e45a67389	stomp-w-r-bd-chprc04i.x
e990f1566c8099a8d54508de3da9cd88	stomp-w-r-bd-chprc04l.x
18a589a2b55aab2db290efea19b39351	stomp-w-r-cgsq-chprc04i.x
6569959476772a137df35ce874821889	stomp-w-r-cgsq-chprc04l.x

3. Executable Size (bytes): MD5 signatures above uniquely identify each executable file

COMPILATION INFORMATION:

4. Hardware System (i.e., property number or ID):

Tellus Subsurface Modeling Platform

5. Operating System (include version number):

Linux tellusmgmt.rl.gov 2.6.18-308.4.1.el5 #1 SMP Tue Apr 17 17:08:00 EDT 2012 x86_64 x86 64 x86 64 GNU/Linux

INSTALLATION AND CHECKOUT INFORMATION:

6. Hardware System (i.e., property number or ID):

Green Linux Cluster

7. Operating System (include version number):

Linux green 3.2.0-35-generic #55-Ubuntu SMP Wed Dec 5 17:42:16 UTC 2012 x86_64 x86_64 x86 64 GNU/Linux

2

Page 1 of 2 A-6005-149 (REV 0)

3

1

CHPRC SOFTWARE INSTALLATION AND CHECKOUT FORM (continued)

1. Software Name: STOMP (Subsurface Transport Over Multiple Phases) Software Version No.: Bld 4

8. Open Problem Report? ◉ No ○ Yes PR/CR No.

TEST CASE INFORMATION:

[redacted]

10. Procedure(s):

CHPRC-00211 Rev 1, STOMP Software Test Plan

11. Libraries:

N/A (static linking)

12. Input Files:

Input files for ITC-STOMP-1, ITC-STOMP-2, and ITC-STOMP-2
(Baseline for comparison are results files from ATC-STOMP-1, ATC-STOMP-2, and ATC-STOMP-3 prepared on Tellus during acceptance testing)

13. Output Files:

plot.* files produced by STOMP in testing

14. Test Cases:

ITC-STOMP-1, ITC-STOMP-2, and ITC-STOMP-3

15. Test Case Results:

Pass for all executable files listed above.

16. Test Performed By: WE Nichols

17. Test Results: ◉ Satisfactory, Accepted for Use ○ Unsatisfactory

18. Disposition (include HISI update):

Accepted; Installation noted in HISI for users TJ Budge, N Hasan, A Mayenna, WJ McMahon, WE Nichols, S Mehta, H Rashid.

Prepared By:

19. [signature] Software Owner (Signature)	WE Nichols Print	25 APRIL 2013 Date

20. Test Personnel:

[signature] Sign	WE Nichols Print	25 APRIL 2013 Date
Sign	Print	Date
Sign	Print	Date

Approved By:

21. Software SME (Signature)	N/R (per CHPRC-00211 Rev 1) Print	Date

2
3

Page 2 of 2 A-6005-149 (REV 0)

ATTACHMENT 3

STOMP OPTIONS ANALYSIS

This page intentionally left blank.

STOMP Option NQA-1 Status Check				
Input File: "input_ss_rch00_vad00_sat00" (McMahon; Water Only Steady State Approximation Initialization Input File)				
Option status check by: WJ McMahon, 04/26/2016				
Input Card	**Input Parameter**	**Input Option**	**NQA-1 Tested?**	**Comment**
Simulation Title	Simulation Title	—	Yes	
Simulation Title	Simulation Documentation Information	—	Yes	
Solution Control	Execution Mode Option	Normal	Yes	
Solution Control	Operational Mode Options	Water	Yes	
Solution Control	Interfacial Averaging Options	Default (all)	Yes	
Grid	Method of Grid Input	(Non-uniform) Cartesian	Yes	
Grid	Grid Spacing Specification Option	Count and Cell size	Yes	
Rock/Soil Zonation	Method of Zonation	External File	Yes	
Inactive Nodes	Declaration of Inactive Nodes	External File	Yes	
Mechanical Properties	Compressibility Option	Pore Compressibility	Yes	
Mechanical Properties	Tortuosity Function	Millington and Quirk	Yes	
Hydraulic Properties	Method of Hydraulic Property Input	Hydraulic Conductivity	Yes	

Saturation Function	Saturation Function Option	Nonhysteretic van Genuchten	Yes	"Nonhysteretic" is no longer a recognized keyword and is ignored according to the output files. The description the van Genuchten (1980) retention function presented on the STOMP User Guide page is nonhysteretic.
Aqueous Relative Permeability	Relative Permeability Option	Mualem with Polmann	Yes	
Initial Conditions	Initial Aqueous Pressure	Aqueous Pressure-Gas Pressure	Yes	
Initial Conditions	Method of Initial Condition Input	External File	Yes	
Boundary Conditions	Method of Boundary Node Identification	External File	N/A	Neither method of Boundary Node Identification, Explicit or External File, is identified as NQA-1 tested, although the boundary condition types, Neumann and Dirichlet Outflow, are.
Boundary Conditions	Aqueous Boundary Condition Options	Neumann	Yes	
Boundary Conditions	Aqueous Boundary Condition Options	Outflow	Yes	Dirichlet-Outflow is described on the User Guide Page, but Dirichlet is not required as a keyword according to the output files.
Output Control	Reference Node Output	Aqueous Saturation	Yes	
Output Control	Reference Node Output	Aqueous Pressure	Yes	
Output Control	Reference Node Output	Aqueous Moisture Content	Yes	

Output Control	Reference Node Output	XNC Aqueous Volumetric Flux	Yes	
Output Control	Reference Node Output	ZNC Aqueous Volumetric Flux	Yes	
Output Control	Plot File Output	Final Restart	N/A	Final Restart is not included in the list of variables. Final Restart is not a variable but a flag indicating that a restart file is only created at the end of the simulation. All other specified variables are identified as NQA-1 tested.
Output Control	Plot File Output	Rock/Soil type	Yes	
Output Control	Plot File Output	Aqueous Saturation	Yes	
Output Control	Plot File Output	Aqueous Pressure	Yes	
Output Control	Plot File Output	Aqueous Moisture Content	Yes	
Output Control	Plot File Output	XNC Aqueous Volumetric Flux	Yes	
Output Control	Plot File Output	YNC Aqueous Volumetric Flux	Yes	
Output Control	Plot File Output	ZNC Aqueous Volumetric Flux	Yes	
Surface Flux	Surface Output File Options	Multiple Surface Output Files	Yes	
Surface Flux	Defining Surfaces for the Output Fluxes	Range of Node Indices	Yes	
Surface Flux	Surface Output Flux Types	Aqueous Volumetric Flux	Yes	

STOMP Option NQA-1 Status Check				
Input File: "input_op_rch00_vad00_sat00" (McMahon; Water Only Transient Operations Period Input File)				
Option status check by: WJ McMahon, 04/26/2016				
Input Card	**Input Parameter**	**Input Option**	**NQA-1 Tested?**	**Comment**
Simulation Title	Simulation Title	—	Yes	
Simulation Title	Simulation Documentation Information	—	Yes	
Solution Control	Execution Mode Option	Restart	Yes	
Solution Control	Operational Mode Options	Water	Yes	
Solution Control	Interfacial Averaging Options	Default (all)	Yes	
Grid	Method of Grid Input	(Non-uniform) Cartesian	Yes	
Grid	Grid Spacing Specification Option	Count and Cell Size	Yes	
Rock/Soil Zonation	Method of Zonation	External File	Yes	
Inactive Nodes	Declaration of Inactive Nodes	External File	Yes	
Mechanical Properties	Compressibility Option	Pore Compressibility	Yes	
Mechanical Properties	Tortuosity Function	Millington and Quirk	Yes	
Hydraulic Properties	Method of Hydraulic Property Input	Hydraulic Conductivity	Yes	

Saturation Function	Saturation Function Option	Nonhysteretic van Genuchten	Yes	"Nonhysteretic" is no longer a recognized keyword and is ignored according to the output files. The description the van Genuchten (1980) retention function presented on the STOMP User Guide page is nonhysteretic.
Aqueous Relative Permeability	Relative Permeability Option	Mualem with Polmann	Yes	
Initial Conditions	Initial Aqueous Pressure	Aqueous Pressure-Gas Pressure	Yes	No initial conditions are included in this input file.
Initial Conditions	Method of Initial Condition Input	Restart	Yes	
Boundary Conditions	Method of Boundary Node Identification	External File	N/A	Neither method of Boundary Node Identification, Explicit or External File, is identified as NQA-1 tested, although the boundary condition types, Neumann and Dirichlet Outflow, are.
Boundary Conditions	Aqueous Boundary Condition Options	Neumann	Yes	
Boundary Conditions	Aqueous Boundary Condition Options	Outflow	Yes	Dirichlet-Outflow is described on the User Guide Page, but Dirichlet is not required as a keyword according to the output files.
Output Control	Reference Node Output	Aqueous Saturation	Yes	
Output Control	Reference Node Output	Aqueous Pressure	Yes	
Output Control	Reference Node Output	Aqueous Moisture Content	Yes	

Output Control	Reference Node Output	XNC Aqueous Volumetric Flux	Yes	
Output Control	Reference Node Output	ZNC Aqueous Volumetric Flux	Yes	
Output Control	Plot File Output	Final Restart	N/A	Final Restart is not included in the list of variables. Final Restart is not a variable but a flag indicating that a restart file is only created at the end of the simulation. All other specified variables are identified as NQA-1 tested.
Output Control	Plot File Output	Rock/Soil type	Yes	
Output Control	Plot File Output	Aqueous Saturation	Yes	
Output Control	Plot File Output	Aqueous Pressure	Yes	
Output Control	Plot File Output	Aqueous Moisture Content	Yes	
Output Control	Plot File Output	XNC Aqueous Volumetric Flux	Yes	
Output Control	Plot File Output	YNC Aqueous Volumetric Flux	Yes	
Output Control	Plot File Output	ZNC Aqueous Volumetric Flux	Yes	
Surface Flux	Surface Output File Options	Multiple Surface Output Files	Yes	
Surface Flux	Defining Surfaces for the Output Fluxes	Range of Node Indices	Yes	
Surface Flux	Surface Output Flux Types	Aqueous Volumetric Flux	Yes	

STOMP Option NQA-1 Status Check				
Input File: "input_pc_rch00_vad00_sat00_tc99_inv01_rls01_group_a" (McMahon; Water with Transport Transient Post-Closure Period Input File)				
Option status check by: WJ McMahon, 04/26/2016				
Input Card	**Input Parameter**	**Input Option**	**NQA-1 Tested?**	**Comment**
Simulation Title	Simulation Title	—	Yes	
Simulation Title	Simulation Documentation Information	—	Yes	
Solution Control	Execution Mode Option	Restart	Yes	
Solution Control	Operational Mode Options	Water with Transport and Vadose Courant	Yes	
Solution Control	Interfacial Averaging Options	Default (all)	Yes	
Grid	Method of Grid Input	(Non-uniform) Cartesian	Yes	
Grid	Grid Spacing Specification Option	Count and Cell Size	Yes	
Rock/Soil Zonation	Method of Zonation	External File	Yes	
Inactive Nodes	Declaration of Inactive Nodes	External File	Yes	
Mechanical Properties	Compressibility Option	Pore Compressibility	Yes	
Mechanical Properties	Tortuosity Function	Millington and Quirk	Yes	
Hydraulic Properties	Method of Hydraulic Property Input	Hydraulic Conductivity	Yes	

Saturation Function	Saturation Function Option	Nonhysteretic van Genuchten	Yes	"Nonhysteretic" is no longer a recognized keyword and is ignored according to the output files. The description the van Genuchten (1980) retention function presented on the STOMP User Guide page is nonhysteretic.
Aqueous Relative Permeability	Relative Permeability Option	Mualem with Polmann	Yes	
Initial Conditions	Initial Aqueous Pressure	Aqueous Saturation-Aqueous Pressure	N/A	No initial conditions are included in this input file.
Initial Conditions	Method of Initial Condition Input	Restart	Yes	
Boundary Conditions	Method of Boundary Node Identification	External File	N/A	Neither method of Boundary Node Identification, Explicit or External File, is identified as NQA-1 tested, although the boundary condition types, Neumann and Dirichlet Outflow, are.
Boundary Conditions	Aqueous Boundary Condition Options	Neumann	Yes	
Boundary Conditions	Solute Boundary Condition Options	Zero Flux	Yes	
Boundary Conditions	Solute Boundary Condition Options	Outflow	Yes	Dirichlet-Outflow is described on the User Guide Page, but Dirichlet is not required as a keyword according to the output files.
Solute/Fluid Interactions	Effective Diffusion Options	Conventional	Yes	
Solute/Fluid Interactions	Solid/Aqueous Partition Options	Continuous	Yes	

Solute/Fluid Interactions	Reaction Options	Radioactive Decay	Yes	
Solute/Porous Media Interactions	Dispersivity/ Partitioning Coefficient	Explicit	Yes	
Output Control	Plot File Output	Rock/Soil Type	Yes	
Output Control	Reference Node Output	Aqueous Saturation	Yes	
Output Control	Reference Node Output	Aqueous Pressure	Yes	
Output Control	Reference Node Output	Aqueous Moisture Content	Yes	
Output Control	Reference Node Output	XNC Aqueous Volumetric Flux	Yes	
Output Control	Reference Node Output	ZNC Aqueous Volumetric Flux	Yes	
Output Control	Reference Node Output	Solute Integrated Mass	Yes	
Output Control	Reference Node Output	Solute Aqueous Concentration	Yes	
Output Control	Plot File Output	Rock/Soil type	Yes	
Output Control	Plot File Output	Aqueous Saturation	Yes	
Output Control	Plot File Output	Aqueous Pressure	Yes	
Output Control	Plot File Output	Aqueous Moisture Content	Yes	
Output Control	Plot File Output	XNC Aqueous Volumetric Flux	Yes	
Output Control	Plot File Output	ZNC Aqueous Volumetric Flux	Yes	
Output Control	Plot File Output	Solute Aqueous Concentration	Yes	
Output Control	Plot File Output	Solute Volumetric Concentration	Yes	

Output Control	Plot File Output	Final Restart	N/A	Final Restart is not included in the list of variables. Final Restart is not a variable but a flag indicating that a restart file is only created at the end of the simulation. All other specified variables are identified as NQA-1 tested.
Surface Flux	Surface Output File Options	Multiple Surface Output Files	Yes	
Surface Flux	Defining Surfaces for the Output Fluxes	Range of Node Indices	Yes	
Surface Flux	Surface Output Flux Types	Aqueous Volumetric Flux	Yes	
Surface Flux	Surface Output Flux Types	Solute Flux	Yes	